# Specification of horizontal basal cell fate during olfactory epithelium regeneration

A thesis submitted by

Jonathan D. Louie

in partial fulfillment of the requirements for the degree of

PhD

in

Neuroscience

Tufts University

Graduate School of Biomedical Sciences

August 2022

Advisor: James E. Schwob, MD, PhD

**Abstract**

Despite lineage-tracing experiments demonstrating that horizontal basal cells (HBCs) serve as resident stem cells capable of regenerating the olfactory epithelium (OE), the intervening interval in which HBCs mount their response to severe tissue injury remains a relative black box. Few mechanisms that govern HBCs and their ability to mediate OE regeneration have been elucidated, especially those that hinge on cell-cell interactions and spatiotemporally dynamic events.

This thesis, therefore, aims to make inroads into these unknowns. As Notch1, a receptor capable of interacting with Notch ligands, Jagged1 and Dll1, maintains HBC quiescence during OE homeostasis, its potential role in specifying HBC fate during OE regeneration was interrogated. Utilizing a mouse model that enables HBC-specific conditional knock out (cKO) of *Notch1*, it was discovered that Notch1 transduces signals critical to HBC proliferation and differentiation into neural progenitors during OE recovery from tissue injury. Moreover, decreased neural progenitor differentiation within *Notch1* cKO manifests as decreased density of HBC-derived olfactory sensory neurons within morphologically regenerated OE.

Work from this thesis also reveals that during acute OE regeneration, HBCs upregulate Rac1 to their apical domain. Multiple proteins that transduce stimuli via Rac1 also spatiotemporal synchronize with the small GTPase. These events correlate with JNK pathway activation, a process that can depend on Rac1-mediated signaling. Informed by *in vivo* observations, the cell autonomous influence that Rac1 has on HBCs during tissue repair was interrogated *in vitro*. Following phorbol ester treatment to model multiple molecular changes that occur in HBCs during acute tissue injury, primary HBCs subjected to concurrent Rac1 inhibition demonstrated impaired differentiation.

In total, the data generated by this thesis identify Notch1 and Rac1 as regulators of HBC biology as this resident stem cell population is called to action. By establishing these footholds, this thesis also implicates myriad potential interactions and non-cell autonomous events, thereby establishing bases from which future explorations can be launched to further understand how HBCs facilitate OE regeneration.

**Dedication**

For 公公, my first and best PI.

**Acknowledgements**

I would like to thank my advisor, Dr. Jim Schwob, for the opportunity to conduct my PhD thesis in his laboratory. The independence and support you afforded me over the years are privileges that I hope to parlay into my own independent research endeavors. I would also like to thank the members of the Schwob Lab for their camaraderie. It was an honor to share these trenches with you all.

Thank you to my Thesis Advisory Committee, Drs. Brent Cochran, Thomas Gridley, and Giuseppina Tesco, for their time and effort. My meetings with this trio helped steer me to this point. Furthermore, I am exceptionally appreciative of Dr. Bradley Goldstein for making the time to be my outside examiner.

My journey up to this point has followed a long and winding road. I would not have been able to make it even a quarter of the way without help from many people. To Drs. Jeanette Hyer, Nalin Gupta, and Tarik Tihan, thank you for your support from the very beginning, especially during my times of disappointment and uncertainty.

To Drs. Takashi Mikawa and Michael Bressan, thank you for providing me with a life-changing experience as your research technician. Your mentorship, attention to my scientific development, and overall dedication to maximizing my odds of success throughout those four years have propelled me to this point. I am forever in your debt. Additionally, these formative years would not have been what they were without the many Mikawa Lab members with whom I had the honor of working.

Most importantly, I would like to thank my family. Your faithful support has been and always will be a treasured and priceless constant in my life. Because of you all, I have always had everything I ever needed. To my mom, you have instilled in me resiliency and resolve. You and your unwavering love and support are elemental to my life. My successes are our successes. To my dad, you have imbued me with an appreciation for the power of self-reflection and self-improvement. I am extremely

fortunate to have had ingrained these traits from you two. To my sister, thank you for always listening and being my confidant. I am privileged to share the sibling bond that exists between us, and I look forward to making many more memories together. To my partner, you and your love, support, openness, and honesty have helped me grow immeasurably as a person and provided me a great sense of calm and security. Thank you for being my safe haven. Lastly, I have been extremely fortunate to share many years with all of my grandparents. To 奶奶 and 爷爷, your kindness and care provided me with great stability, and your story is an inspiration. For my 公公 and 婆婆, during my most difficult times when self-doubt was at its strongest, you and your imprint on my life provided me with the determination to fight on and overcome. I would not be who and where I am today without you. Words cannot even come close to adequately capturing the depth of love and affection I have for you. Always and forever, my achievements are our achievements.

**Table of Contents**

List of Tables

**List of Figures**

**List of Copyrighted Materials Used**

Bosco EE, Mulloy JC, Zheng Y (2009). Rac1 GTPase: A “Rac” of all trades. *Cell Mol Life Sci.* Feb; 66(3).

Brakebusch C, Bouvard D, Stanchi F, Sakai T, Fässler R (2002). Integrins in invasive growth. *J Clin Invest.* Apr 15; 109(8): 999-1006.

Chillakuri CR, Sheppard D, Lea SM, Handford PA (2012). Notch receptor-ligand binding and activation: Insights from molecular studies. *Semin Cell Dev Biol.*, Jun; 23(4).

Holbrook EH, Wu E, Curry WT, Lin DT, Schwob JE (2011). Immunohistochemical characterization of human olfactory tissue. *Laryngoscope,* Aug;121(8): 1687-1701.

Krolewski RC, Packard A, Jang W, Wildner H, Schwob JE (2012). Ascl1 (Mash1) knockout perturbs differentiation of nonneuronal cells in olfactory epithelium. *PLoS One*, 7(12).

Nakashima T, Kimmelman CP, Snow Jr. JB (1984). Structure of human fetal and adult olfactory neuroepithelium. *Arch Otolaryngol*, 110:641-646.

Olayioye MA, Noll B, Hausser A (2019). Spatiotemporal control of intracellular membrane trafficking by Rho GTPases. *Cells,* Dec; 8(12).

Schwob, JE, Jang W, Holbrook EH, Lin B, Herrick DB, Peterson JN, Coleman JH (2017). Stem and progenitor cells of the mammalian olfactory epithelium: Taking poietic license. *J Comp Neurol.* 1034-1054.

**List of Abbreviations**

ANK *Ankyrin*
CK *Cytokeratin*
FAK *Focal adhesion kinase*
GAP *GTPase-activating protein*
GBC *Globose basal cell*
GDI *Guanine nucleotide dissociation inhibitor*
GDP *Guanosine diphosphate*
GEF *Guanine nucleotide exchange factor*
GTP *Guanosine triphosphate*
HBC *Horizontal basal cell*
HD *Heterodimerization domain*
iOSN *Immature olfactory sensory neuron*
Itgb *Integrin β*
LNR *Lin-12-Notch*
mOSN *Mature olfactory sensory neuron*
MTZ *Methimazole*
NICD *Notch intracellular domain*
NRR *Negative regulatory region*
OE *Olfactory epithelium*
OMP *Olfactory marker protein*
PMA *Phorbol 12-myristate 13-acetate*
RAM *RBPJ-associated molecular*
Sus cell *Sustentacular cell*
TAD *Transcription activation domain*

## Chapter 1: Introduction

### 1.1 The olfactory epithelium

Located in the posterodorsal region of the nasal cavity[1] (Fig. 1.1A), the olfactory epithelium (OE) is multicellular tissue that, as the name implies, enables the sense of smell. This specialized neuroepithelium can be organized into apical and basal domains encompassing regions nearest the nasal cavity and closest to the basal lamina (Fig. 1.1B).

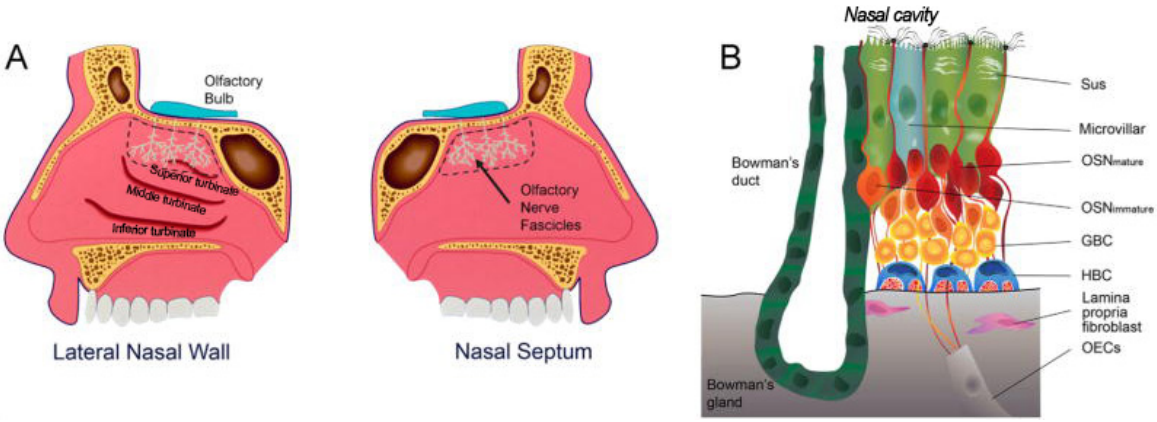


**Figure 1.1. Anatomical position and multicellularity of the OE.** The OE (area demarcated in dashes) is located in the posterodorsal region of the nasal cavity (A) and is composed of multiple cell types that are organized roughly in an apical (nearest naval cavity) to basal (nearest basal lamina, represented in cartoon as solid black line just below HBCs in blue) fashion (B). Adapted with permission from Schwob, JE, Jang W, Holbrook EH, Lin B, Herrick DB, Peterson JN, Coleman JH (2017). Stem and progenitor cells of the mammalian olfactory epithelium: Taking poietic license. *J Comp Neurol.* 1034-1054. Changes include text denoting superior, middle, and inferior turbinates (A), and the nasal cavity (B).

Most apically reside Sustentacular (Sus) cells (Fig. 1.1B), from whose cell bodies extend thin projections towards and through the basal lamina[2,3]. Molecularly defined by their expression of cytokeratins 8 and 18 (CK8 and CK18, respectively), Sus cells have been thought of as the glial-like OE cell type given similar characteristics of glial cell types in the central nervous system. Morphologically, Sus cells entwine olfactory sensory neurons (OSNs)[4], which resembles that of oligodendrocytes and Schwann cells

in the central and peripheral nervous systems, respectively[5,6]. Furthermore, functional resemblances also exist as Sus cells demonstrate metabolic, insulatory, phagocytic, and ion regulatory abilities[4,7-9].

In addition to Sus cell bodies, microvillar cells can be found within the OE's apical domain[10,11] (Fig. 1.1B). These cells are not well understood, but emerging evidence suggest that microvillar cells are morphologically, functionally, and molecularly diverse. Generally pear-shaped, microvillar cells under microscopic analyses demonstrate apical projections of varying complexity[11]. While some are thought to be epithelial-like because they lack features reminiscent of electrically active cells[10,12], other microvillar cells exhibit axonal processes that contact the olfactory bulb[13]. Those that are $CD73^{+}$ cycle intracellular Ca2+ when exposed to odorants[14]. Another distinct population of microvillar cells that are $TRPM5^{+}$, a cation channel first implicated in taste transduction[15], express choline acetyl transferase, which in turn may tune surrounding electrophysiological processes within the OE[16].

Mature OSNs (mOSNs) are the cell type that enables olfaction, and their cell bodies are found just below those of Sus and microvillar cells [2] (Fig. 1.1B). Their single dendritic process, however, extends through the apical domain and protrudes into the nasal cavity, where it terminates as a multi-ciliated, dendritic knob [17,18]. In the opposite direction, mOSNs extend an axon down towards and through the basal lamina that ultimately establish glutaminergic synapses onto the olfactory bulb in a highly stereotyped manner [19-21]. In addition to molecularly defining mOSNs, Olfactory Marker Protein (OMP) is functionally necessary for mOSN development as it facilitates electrophysiological maturation [22,23]. Another mOSN hallmark is the monoallelic expression of only one of the approximately 1,000 olfactory receptors encoded by the genome [24,25]. Not only is solitary olfactory receptor expression a unique molecular

characteristic, but mOSN failure to stabilize or maintain olfactory receptor expression via *Adcy3* or *Lhx2*, respectively, results in fewer mOSNs within the OE[26,27].

mOSN development failure, conversely, leads to increased Gap43$^+$ immature OSNs (iOSNs)[28] that reside below mature counterparts[2,26,27] (Fig. 1.1B). During the approximate seven days it takes to become a mOSN[29,30], iOSNs, unsurprisingly, upregulate transcriptional signatures associated with dendrite morphogenesis and axonogensis to achieve their mature form[18,31]. Accordingly, highly elaborate axons emanating from iOSNs contact the olfactory bulb[32]. As OSN maturation proceeds and all but one olfactory receptor becomes downregulated[33], these axons are pruned down to their olfactory receptor-specific glomerulus within the olfactory bulb[32].

Given the evolutionary importance of olfaction[34], it stands to reason that the OE possesses an ability to renew itself to buffer against homeostatic OSN turnover[35-37]. Indeed, this regenerative capacity is fulfilled by globose basal cells (GBCs)[38-40] that can become mOSNs and all differentiated OE cell types[39]. Found below iOSN cell bodies within the basal domain of the OE[2] (Fig. 1.1B), GBCs are morphologically distinguished by their round nucleus within an overall round cellular profile[2]. Based on the molecular expression of Sox2, Ascl1, and NeuroD1, this resident stem cell population can be divided into multiple subpopulations (Fig. 1.2). Of those 3 transcription factors, the most multipotent are exclusively Sox2$^+$, from which emerge GBCs that become more and more neurogenically biased[41-44]. From these arise GBCs expressing Ascl1, a transcription factor that positively regulates neuronal determination and also drives proliferation of these neuronal precursors[45-47]. Appearance of Ascl1$^+$ GBCs is followed by that of NeuroD1$^+$ GBCs[42,48]. As NeuroD1 supports terminal neuronal differentiation, this GBC subset functions as immediate neural precursors[49].


**Figure 1.2. Progression of GBC subpopulations.** Sox2+ GBCs are multipotent stem cells. They can differentiate into Ascl1+ GBCs, which are transit amplifying (i.e. proliferating) neuronal progenitors. These NeuroD1+ GBCs eventual become determined neuronal progenitors awaiting differentiation into OSNs. $GBC_{TA\text{-}OSN}$=transit amplifying GBCs that will become OSNs, $GBC_{INP}$=immediate neuronal precursor prior to OSN differentiation. Adapted with permission from Krolewski RC, Packard A, Jang W, Wildner H, Schwob JE (2012). Ascl1 (Mash1) knockout perturbs differentiation of nonneuronal cells in olfactory epithelium. *PLoS One*, 7(12). Changes include erasure of all images to the right of the intermediary line, the dividing line itself, and cartoon representing an HBC and line indicating derivation from the Sox2 GBC. Furthermore, "Normal Development" and "OPP" under the Sox2 GBC cartoon were erased, and remaining cartoons were moved to achieve vertical alignment.

Because nearly all are engaged in the cell cycle[39], GBCs preside as the OE's active stem cell population. Given this, they also predominant as the most proliferative cell type in the basal layer of the OE[50]. Within this compartment, however, they are accompanied by horizontal basal cells (HBCs)[2,3] (Fig. 1.1B). Morphologically flattened cells containing elongated nucleus and resting atop the basal lamina just below GBCs, $CK5^{+}/CK14^{+}$ HBCs are the OE's second resident stem cell. In contrast to GBCs, most HBCs remain quiescent[51,52], rarely contribute to normal tissue homeostasis[51], and thus,

constitute the tissue's reserve stem cell population. Their purpose is revealed when reconsidering the OE's function. To detect odors, the tissue is necessarily exposed to the environment that, in addition to carrying aromatics, harbors compounds that can be cytotoxic[53-55]. Therefore, HBCs, which can give rise to all OE cell types, mediate repair following severe OE injury[51,56]. Their ability to do so hinges on HBC expression of the transcription factor, p63[52]. Specifically, p63 expression must decrease following injury for HBCs to activate and mount an adequate regenerative response[56].

Within 24 hours after injury induction, a bifurcation that distinguishes self-renewing and differentiating HBCs appears, and by day 4, $p63^+$ quiescent HBCs are re-established[41]. In addition to the cell autonomous mechanisms that promote HBC activation within this temporal window, multiple extrinsic factors resulting from tissue injury play a critical role in promoting HBC-mediated OE regeneration. These include Sus cells, which mentioned previously, extend projections through the basal lamina. As they pass through the basal compartment, these projections come into close proximity with HBCs[3]. Perhaps unsurprisingly then, Sus cell-specific ablation leads to HBC activation and differentiation, presumably due to interrupting interactions between Jagged1 and Notch1 expressed by Sus cells and HBCs, respectively[57]. In addition to Jagged1, Sus cells express retinoic acid, which specifies HBC quiescence in homeostatic OE[58]. Therefore, compromised Sus cell integrity, can reshape the OE's environmental milieu, which in turn, alters the balance of HBC activity.

Following experimentally induced injury via intra-peritoneal methimazole (MTZ) injection[59], or of current relevance, SARS-CoV-2 infection that results in a grossly similar epithelial desquamation[60], numerous inflammatory markers are present within the OE[60-62]. Indeed, the inflammatory response promotes OE regeneration, and does so by directly acting on HBCs[61]. The idea that the post-injury environment influences HBC biology is further strengthened by a demonstration that HBC-associated cilia positively

regulate OE repair[63]. The signaling molecule(s) interacting with HBC cilia following OE injury, however, currently remain unidentified, and thus, exemplify the motivation of this thesis. To date, little is known about how HBC fate is specified during tissue repair, especially the role that cell-cell interactions may play. Moreover, since the discovery of p63 as a key regulator of HBC activity, only a handful of cell autonomous mechanisms that promote HBC-mediated OE regeneration have been validated *in situ*[61,64].

An appreciation for the need to develop a firm grasp on how HBCs facilitate proper OE regeneration can be had by recognizing the pathological findings within aged OE[65-68] and their association with a decline in olfaction that affects nearly three-quarters of Americans by age 80[69] and, of greatest concern, can negatively impact nutritional status, physical safety, and overall quality of life[70]. Olfactory impairment can be attributed to the loss of OSNs (Fig. 1.3A-F) and GBCs (Fig. 1.3G), the latter of which presumably disappear due to the lifelong demands of OE homeostasis. Interestingly, this pathological deterioration of the OE occurs despite the enduring presence of HBCs that remain quiescent atop the basal lamina (Fig. 1.3G).

Considering that the number of older individuals in our country is predicted to double in the next three decades[71] and younger individuals are experiencing olfactory-related sequelae resulting from SARS-CoV-2 infection[72,73], more and more may have to contend with decreasing olfaction. Therefore, reversing smell loss, may become increasingly important to an expanding population. Capitalizing on multipotent HBCs and their perdurance to regenerate the OE could restore a sense of well-being to those affected by olfactory impairments. Doing so, however, in a controlled manner will require intimate understanding of HBC biology. Consequently, work from this thesis hopes to aid the development of such clinical therapies that safely and appropriately restore the sense of smell.

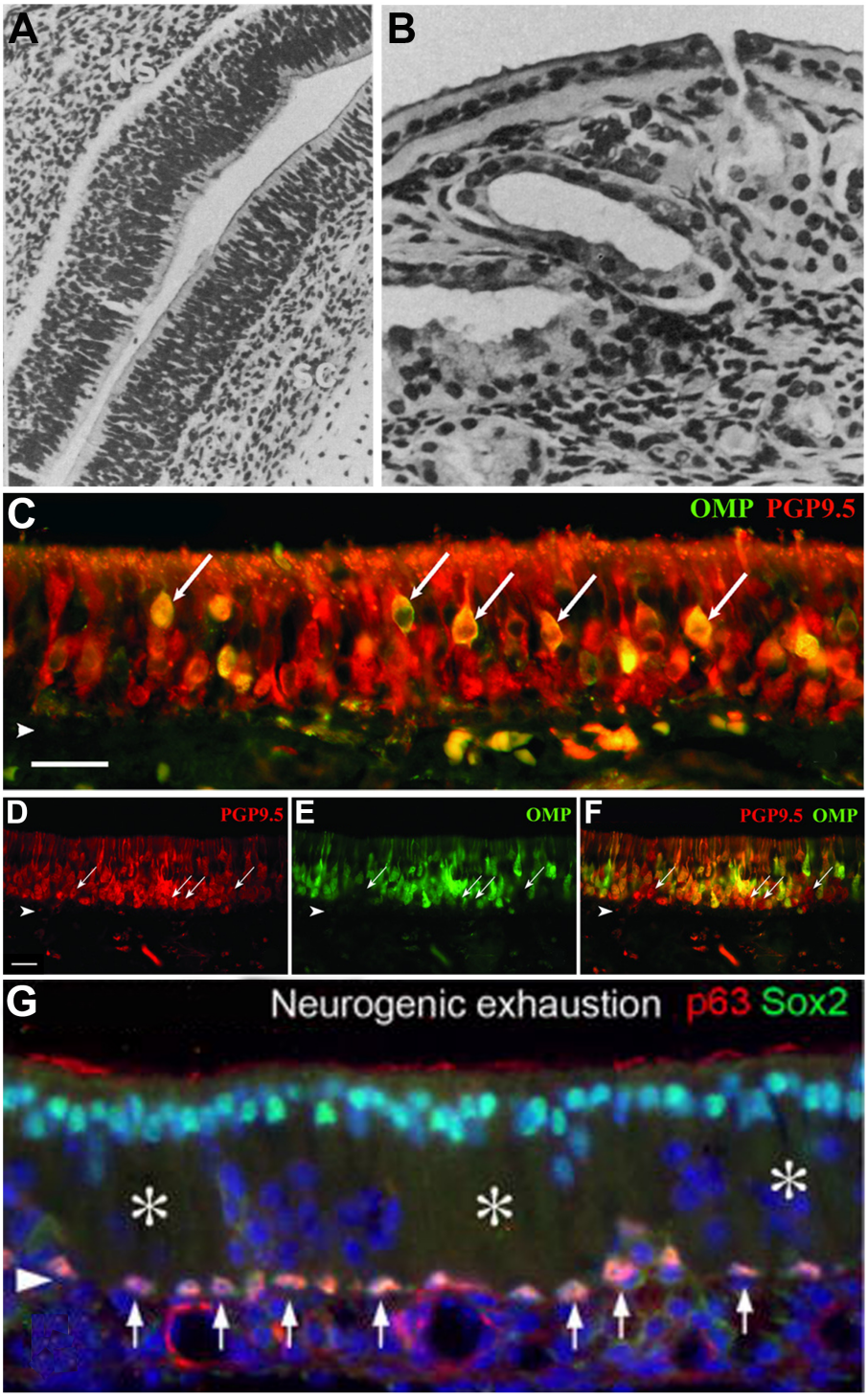


**Figure 1.3. Degradation of OE cellularity.** Hematoxylin and eosin staining of OE from a 7-month old fetus (A; NS = nasal septum; SC = superior concha) and adult (B) depicting OE thinning in the latter due to decreased cellularity. C) Immunofluorescence of human OE from a 75 year-old depicting decreased mOSNs (labeled by OMP); PGP9.5 = pan-OSN marker, arrow = OMP+/PGP9.5+ OSN, arrowhead = basement

membrane, scale bar = 25um). D-F) Compared to C, human OE illustrating increased mOSN population; arrow = OMP-/PGP9.5+ OSN, arrowhead = basement membrane, scale bar = 25um. G) A mouse model of aged OE demonstrating neurogenic exhaustion represented by decreased cellularity within the OE's intermediary region typically dominated by OSNs (asterisk = DAPI- swaths) and absence of p63-/Sox2+ GBCs within the basal compartment that typically regenerate OSNs during homeostasis. Neurogenically exhausted OE, however, still harbors quiescent HBCs (arrow = p63+/Sox2+ HBC) lying atop the basal lamina (arrowhead). Adapted with permission from (A, B) Nakashima T, Kimmelman CP, Snow Jr. JB (1984). Structure of human fetal and adult olfactory neuroepithelium. *Arch Otolaryngol*, 110:641-646; (C-F) Holbrook EH, Wu E, Curry WT, Lin DT, Schwob JE (2011). Immunohistochemical characterization of human olfactory tissue. *Laryngoscope,* Aug;121(8): 1687-1701; (G) Schwob, JE, Jang W, Holbrook EH, Lin B, Herrick DB, Peterson JN, Coleman JH (2017). Stem and progenitor cells of the mammalian olfactory epithelium: Taking poietic license. *J Comp Neurol.* 1034-1054. Changes include applying alphabetical panel indicators, transposing and color inverting the scale bar from the figure's original panel A (D), transposing color-coded protein indicators from the upper left to the upper right (C-F), transposing "Neurogenic exhaustion" from the upper left corner and eliminating "B" from the lower left corner (G). All erasures and transpositions were followed by clone healing the affected regions (C-G).

### 1.2 Notch signaling

Discovered in Drosophila, the Notch receptor is a single-pass transmembrane protein (Fig. 1.4A), and due to its post-translational cleavage in the trans-Golgi by a furin-like convertase at S1 that is necessary for receptor activity, inserts into the membrane as a heterodimer[74-76]. The mammalian genome possess four homologs, Notch1-4[77], and has multiple well-studied domains. Given that this thesis work examines Notch1, this receptor will be of particular focus. In its extracellular domain, Notch1 possesses 36 EGF-like domains, with EGF-like repeats 11-12 being both necessary and sufficient to mediate receptor-ligand interaction[78,79]. This EGF-like domain is followed by LNR (Lin-12-Notch) repeats and a heterodimerization domain. Together, they form a negative regulatory region (NRR) that shields the S2 cleavage site to prevent ligand-independent metalloprotease action[80,81]. Within the transmembrane domain lies the S3 cleavage site, which is acted on by γ-secretase (Fig. 1.4B). Cleavage at S3 by gamma-secretase leads to the release of the Notch intracellular domain (NICD)[77].

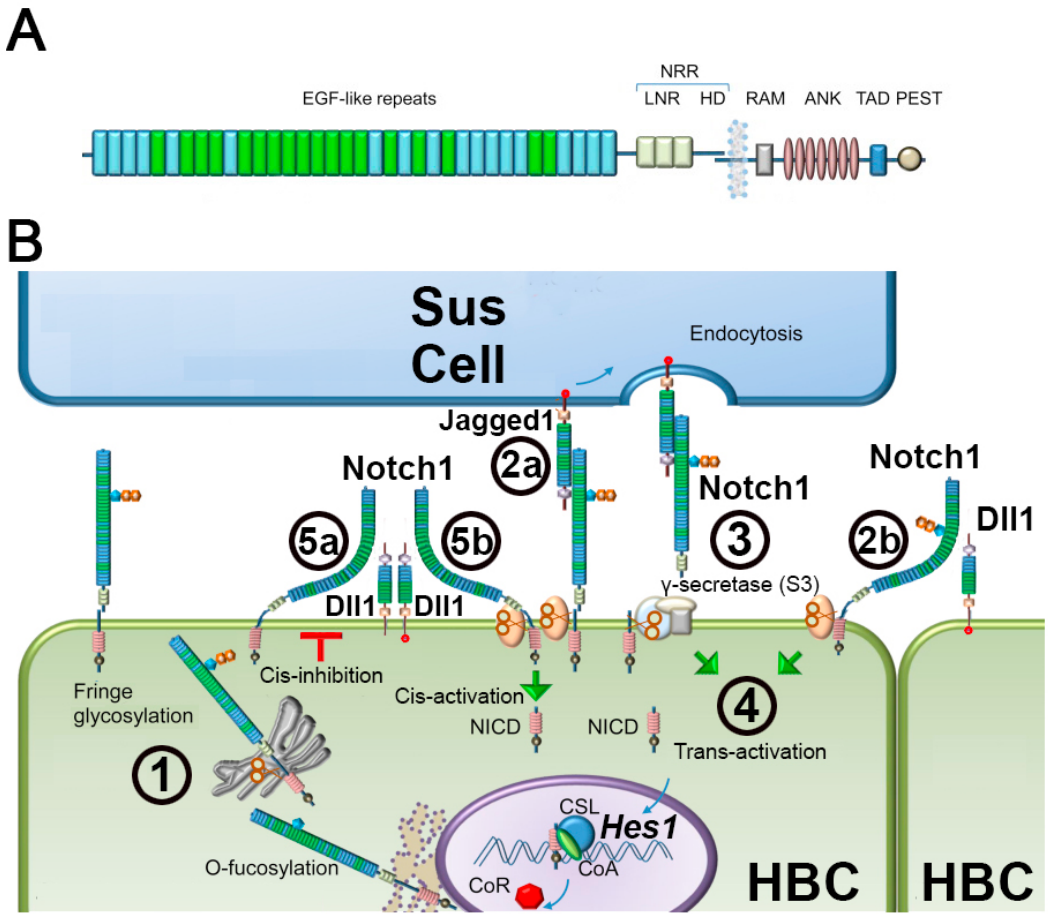


**Figure 1.4. Notch signaling basics.** A) Schematic of Notch receptor. Green and blue EGF-like repeats represent those that are and are not Ca2+ binding, respectively. LNR = Lin-12-Notch repeats; HD = heterodimerization domain; RAM = RBPJ-associated molecule (RAM); ANK = ankyrin repeats; TAD = transcription activation domain. B) Cartoon depicting the sequence of events in Notch signaling: 1) Receptors and ligands are post-translationally glycosylated by Fringe proteins, which tune the degree of effective ligand-receptor interaction and are dynamically expressed during tissue morphogenesis; 2a) Notch1 expressed by a HBC can potentially trans-interact with Jagged1 localized to an adjacent Sus cell and 2b) Dll1 expressed by a neighboring HBC; 3) Trans-interactions promote γ-secretase-mediated cleavage of Notch1, which enables 4) Notch1-Intracellular Domain (NICD) translocation to the nucleus to facilitate gene expression; 5a) Cis-interactions between Notch1 and Dll1 expressed by the same HBC can either attenuate or 5b) activate Notch signaling. Reprinted (A) and adapted (B) with permission from Chillakuri CR, Sheppard D, Lea SM, Handford PA (2012). Notch receptor-ligand binding and activation: Insights from molecular studies. *Semin Cell Dev Biol.*, Jun; 23(4). Changes include application of "Sus Cell," "HBC," "Hes1," and alphanumeric indicators, elimination of Notch cartoon elements in the blue cell, addition of Notch cartoon elements in the green cell, and addition of the partially shown green cell in the lower right corner.

Once free, NICD translocates to the nucleus and activates gene transcription. It accomplishes this by complexing with and inducing a conformation change of the DNA-binding protein, RBPJ. As a result, co-repressors dissociate from RBPJ and facilitate the association of additional co-activators, including Mastermind-like (MAML)[77]. NICD's capacity to engage in these interaction is due to its RBPJ-associated molecule (RAM) and ANK domains that engage with RBPJ and MAML, respectively[82,83]. Once formed, this complex canonically promotes transcription of Hes and Hey family transcription factors[77,84].

Among vertebrates, cleavage and activation of Notch receptors are initiated by two ligand families, Jagged and Delta-like (Dll), both of which are single-pass transmembrane proteins. Within the Jagged family exist two ligands, Jagged1 and Jagged2, while the Dll family encompasses Dll-1, Dll-3, and Dll-4. They share similar extracellular domains defined by N-terminal and DSL (Delta, Serrate, and Lag2) domains. Ligand interaction with Notch receptors has been shown to be dependent on the DSL domain[85]. The extracellular region continues with EGF-like repeats[86,87], which exhibit slight variability. Jagged ligands contain 15-16 EGF-like repeats and a von Willebrand (vWF) type C domain, whereas Dll ligands possess 6-8 EGF-like repeats and are void of the vWF domain[88].

Intracellularly, Notch ligands exhibit low sequence homology, however, most possess multiple lysine residues that act as ubiquitin ligase sites[87,89,90]. Reports have demonstrated that E3 ligases Mindbomb and Neuralized2 act on Dll1, which results in Notch signaling activity in target cells[91-94]. The subsequent ubiquitin-mediated endocytosis of Dll1 is thought to exert deforming biophysical forces on the bound

receptor, thereby exposing the receptor's S2 cleavage site and facilitating eventual NICD nuclear translocation[90].

Notch ligand-receptor interactions can be ascribed directionality. Those that occur between the same cell are termed cis-interactions, while those that occur between different cells are identified as trans-interactions. Cis-interactions are thought to typically inhibit pathway activation[95-97] and those occurring in trans serve to activate[98-100]. However, Notch signaling complexity is, in part, derived from the fact that directionality is an unreliable predictor of ligand-receptor response given that trans-interactions have been shown to inhibit[101] while cis-interactions can also activate[102].

Modulating Notch signaling pathway activity can also be accomplished with post-translational glycosylation of Notch receptors. In Drosophila, Fringe, a glycosyltransferase, can modify Notch receptor EGF-like repeats with the addition of a N-acetylgucosamine[77,103-106]. This results in enhanced binding with Delta, the Drosophila homolog of Dll, and concurrently decreases binding with Serrate, the Dorsophila homolog of Jagged. The mammalian genome possesses three homologs of Fringe. Manic fringe and Lunatic fringe can decrease the magnitude of productive interaction between Jagged1 and Notch1[107], while increasing it for Dll1[108]. Radical fringe, on the other hand, increases interaction for both Jagged1 and Dll1[109].

Notch signaling can also occur in a ligand-independent manner. In Drosophila, pathway activity follows receptor endocytosis mediated by the E3 ligase, Deltex[110,111]. Interestingly, receptor auto-activation can be attenuated by the Notch ligand, Delta[112].

Within resident stem cell niches, Notch signaling promotes proliferation and differentiation of intestinal and hair follicle bulge stem cells[98,113-115]. This contrasts with inhibition of spinal cord progenitor proliferation and differentiation mediated by Notch1[116]. Furthermore, Notch signaling within the subventricular zone (SVZ) specifies neural stem

cell quiescence[117]. Adding to these apparent functional contradictions, skeletal muscle satellite cells display differential responses depending on tissue status. Notch signaling typically sustains satellite cell quiescence, however, the pathway inverts to promote satellite cell proliferation and muscle repair after injury[118-120]. In total, these findings emphasize the need to study Notch signaling as it pertains to stem cells in a niche- and context-dependent manner. Although this well-conserved stem cell regulatory pathway maintains HBC quiescence via Notch1 during OE homeostasis[57], how this receptor regulates HBC-mediated OE regeneration remain unknown, thereby motivating the work that follows.

**1.3 Rac1**

First described in 1989 in human promyeoloblasts, Rac1 is a member of the Rho-GTPase family that resides within the larger Ras superfamily of small GTPases[121,122]. Although Rac1 shares ~60% and ~30% homology with rho and ras proteins[121], respectively, its N-terminal domain comprised of 5 alpha-helices surrounding a six-stranded beta-sheet that mediates binding of guanine nucleotides, GDP and GTP, are highly conserved throughout the superfamily[121,123-125].

In its inactive and active states, Rac1 binds GDP and GTP, respectively[126,127] (Fig. 1.5). Although Rac1 can spontaneously exchange GDP, the large difference between cytoplasmic GDP concentration (~$10^{-5}$M) and the GDP dissociation constant of GTPases (~$10^{-7}$-$10^{-11}$M)[126] suggests that exchanges occurring on an organismalcally-relevant timescale require a catalyst. Indeed, guanine nucleotide exchange factors (GEFs) serve this purpose by interacting with a domain just distal to the guanine nucleotide-interacting region[123]. Throughout the ras superfamily, the GEF-interacting domain demonstrates more variability and interfaces with family-specific GEFs[123]. Although GEFs specific to the Rho family of GTPases commonly contain a Dbl homology and pleckstrin homology domains, the basic principles of GDP-GTP exchange

can be generalized[123,128,129]. Briefly, GEF interaction with GTPase-GDP catalyzes GDP dissociation and stabilizes the now guanine nucleotide-free GTPase[130]. Given that the cytoplasmic concentration of GTP is ~10-fold greater than GDP[126,131], GTP more readily occupies the GTPase's free guanine nucleotide binding site and displaces the GEF[126]. Bound to GTP, the now activated GTPase can influence various cellular processes such as morphology, growth, proliferation, differentiation, and apoptosis[130,132-136].

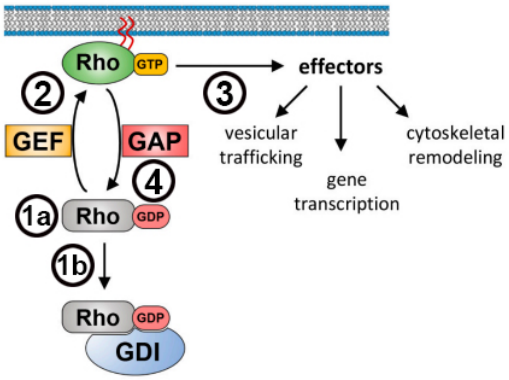


**Figure 1.5. Generalized cartoon of a small GTPase (Rho) activation and deactivation.** 1a) In its inactive form, GTPases are bound to GDP. 1b) GTPase inactivity can be enhanced by GDIs that stabilizing the GDP-bound state. 2) Active GTPase, which inserts into the plasma membrane, is formed by displacing bound GDP for GTP. GEFs facilitate GDP-to-GTP exchange on a biologically relevant timescale. 3) Active GTPases mediate myriad downstream functional effects. 4) GTPases are inactivated by hydrolyzing bound GTP to GDP. Given GTPases' inherently slow kinetics incompatible with proper biological function, GAPs catalyze GTP hydrolysis. Adapted with permission from Olayioye MA, Noll B, Hausser A (2019). Spatiotemporal control of intracellular membrane trafficking by Rho GTPases. *Cells,* Dec; 8(12). Changes include addition of alphanumeric indicators.

Persistent GTPase activation, however, can lead to tumorigensis[137]. While GTPases can perform the function that their name so implies, once again, the timescale at which they hydrolyze GTP into GDP is incompatible with proper cellular function[126]. Therefore, a GTPase interacting with its GTPase-activating proteins (GAPs) can catalyze GTP hydrolysis nearly five times faster than on its own. In the case of the well-studied Ras family of GTPases, $p120^{GAP}$ supplies an arginine side chain to H-Ras that catalyzes inherent GTPase function[138]. However, as with GEFs, there are five different

families of GAPs[123] with unidentical catalytic mechanisms[123,139]. GTPases can be further inhibited from activating by GDP dissociation inhibitors (GDIs)[140]. Once again disparate between GTPase families and named quite literally[141], GDIs prevent GDP-GTPase dissociation[142].

Rac1 inactivity, in particular, can be restored by GAPs within the ArhGAP family[143], or sustained by RhoGDI and D4GDI[144,145]. However, after binding with Rho-GEFs, such as Tiam1[129], activated Rac1 can participate in myriad biological functions. In phagocytes, Rac1 was first described to help generate the superoxide burst that functions to neutralize microorganisms[146]. Found in the leading edge of cells anchored to phosphatidylserine-rich plasma membrane via its C-terminal polybasic domain[147], Rac1 can promote actin filament polymerization, lamellipodia formation, and cellular migration[127,148]. Additionally, Rac1 at the plasma membrane can integrate signals received from multiple upstream modalities, including hormones, G protein-coupled receptors, receptor kinases, and adhesion proteins[149] (Fig. 1.6).

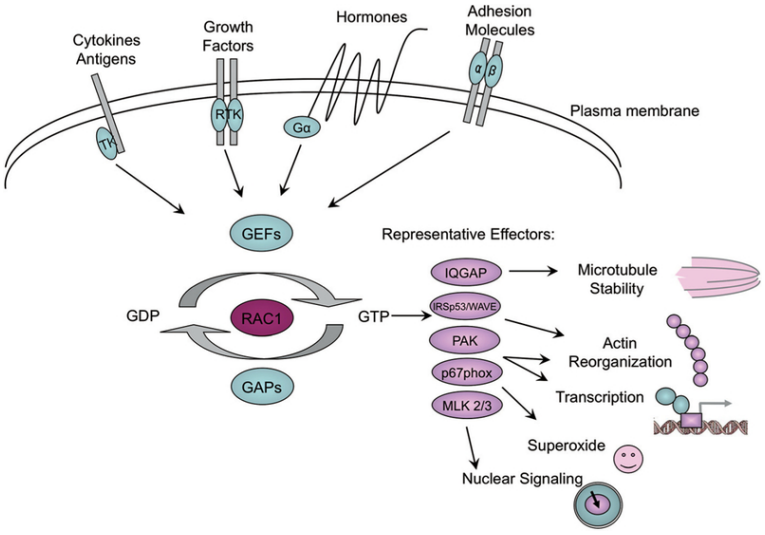


**Figure 1.6. Multiple upstream stimuli impinge on Rac1-mediated signaling.** Plasma membrane receptor interaction with cytokines, growth factors, hormones, or adhesion molecule interaction with extracellular matrix can activate Rac1. Subsequent Rac1-mediated signal transduction affects downstream intermediaries, and ultimately, influences various cellular processes. Reprinted with permission from Bosco EE, Mulloy JC, Zheng Y (2009). Rac1 GTPase: A "Rac" of all trades. *Cell Mol Life Sci.* Feb; 66(3).

Given the latter's relevancy to this thesis, specifically integrin beta 1 and 4 (Itgb1 and Itgb4, respectively), a brief overview of their relationship with Rac1 will be provided. The cytoplasmic tail of Itgb1, and integrin heterodimers comprised by Itgb4, positively regulate Rac1 activity[150-152]. Rac1 activation by Itgb1 and Itgb4, however, occurs via intermediary proteins, including focal adhesion kinase (FAK)[153]. Following integrin stimulation, FAK auto-phosphorylates its tyrosine 397 residue (pFAKY397)[153], which triggers additional phosphorylation at tyrosine residues 407, 576, 577, and 925[153-155]. Importantly, pFAKY925 facilitates eventual phosphorylation of Sos, a Rac1-GEF[156,157].

Following such protein interactions, active Rac1 initiates a signaling cascade canonically involving the cJun N-terminal kinase (JNK) pathway[158] (Fig. 1.7). Briefly, Rac1 via intermediary kinases activates JNK via phosphorylation at threonine 183 and tyrosine 185[159-161]. Subsequently, phospho-JNK (pJNK) phosphorylates cJun at serine residues 73 and 74 (pcJun)[158,162,163], thereby enabling pcJun to dimerize and form an AP-1 transcriptional complex[164,165] that can positively regulate proliferation[166-168].

Accordingly, Rac1 promotes proliferation of mammary epithelial and intestinal stem cells[133,134]. Interestingly, the inverse is true within the interfollicular epidermis as Rac1 supports stem cell quiescence in this context[169]. In addition to this seeming contradiction, Rac1 can also participate in hair follicle differentiation[135]. Morever, Rac1 promotes migration of hematopoietic stem cells during embryogenesis and keratinocyte stem cells during wound repair[170-172]. In light of its diverse array of functions within various stem cell populations, Rac1 deserves tissue-specific attention. Therefore, this thesis has aimed to begin revealing the regulatory function that Rac1 plays during HBC-mediated OE regeneration following injury.

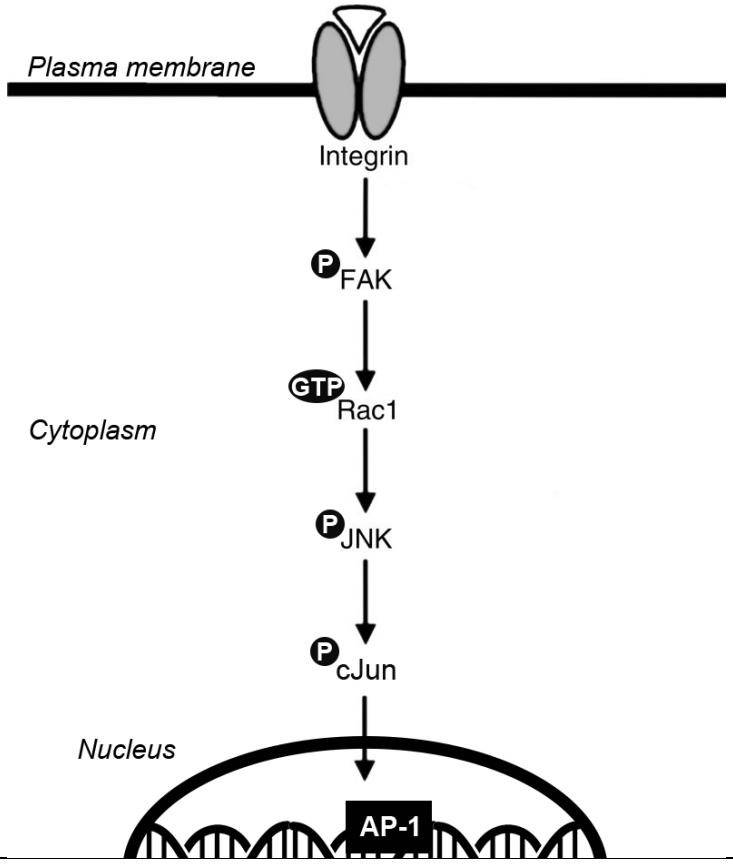


**Figure 1.7. Simplified cartoon of Rac1 activation by integrin receptors.** Integrin interaction with extracellular matrix can trigger subsequent phosphorylation of focal adhesion kinase at multiple tyrosine residues. Via additional downstream intermediaries, Rac1 is activated when bound to GTP. Active Rac1 can stimulate the JNK signaling pathway, which involves phosphorylation of JNK and cJun proteins. Phosphorylated cJun can contribute as a dimer in the homo- or heterodimeric transcription factor, AP-1. Adapted with permission from Brakebusch C, Bouvard D, Stanchi F, Sakai T, Fässler R (2002). Integrins in invasive growth. *J Clin Invest.* Apr 15; 109(8): 999-1006. Changes include addition of text to delineate cellular landmarks and modification of proteins within the signaling cascade, erasure of original text below "JNK" and replacement with "cJun," the proceeding arrow, the ellipse demarcating the nucleus, the DNA double helix within the nucleus, and the symbol representing AP-1.

### 1.4 Contributions

I wrote this entire chapter. Figure images belong to those authors cited in their respective figure legends.

## Chapter 2: Specification of horizontal basal cell fate during OE regeneration[*]

[*] Louie JD, Bromberg BH, Schwob JE. To be submitted to *Proc Natl Acad Sci U S A.*

## 2.1 Introduction

The olfactory epithelium (OE) harbors a population of resident stem cells called horizontal basal cells (HBCs) that contributes to OE regeneration following severe tissue injury[51]. In addition to discovering the various cell autonomous processes dictating HBC cell fate during OE regeneration facilitated by computational analysis of high-throughput transcriptomic sequencing data[41,52,57], there have been advances in our understanding that the local OE environment plays a critical role in supporting HBC contribution to OE regeneration. For example, inflammatory cytokines within the OE post-injury have been identified as a component that regulates HBC proliferation and contribution to tissue repair[61]. Moreover, HBC-specific ablation of cilia mitigates tissue repair[63], suggesting that HBCs must integrate extrinsic cues to mediate OE regeneration.

An aspect of the post-injury environment that has yet to be fully considered is the regenerating OE itself. Cell-cell interaction, especially via the Notch signaling pathway, is a well-conserved motif that regenerative tissues utilize to specify stem cell fate. During homeostasis, Notch signaling prompts intestinal stem cell progenitors to proliferate and specifies enterocyte differentiation[98,113,115]. Inversely, Notch signaling in neural stem cells of subventricular zone (SVZ) and satellite cells within skeletal muscle specifies their dormancy, thereby preventing proliferation and differentiation[117,118]. Similarly within the homeostatic OE, Notch signaling via the Notch1 receptor specifies HBC dormancy[57].

Following abrupt injury to various tissues, Notch signaling continues to positively regulate resident stem cells. Pathway activation is still critical to crypt base columnar cells following intestinal injury by promoting their proliferation and balancing their differentiation between secretory and absorptive cell fates[173]. In contrast to its inhibition of stem cell activity during homeostasis, Notch activity following injury to muscle becomes critical for satellite cells to contribute to regeneration[119,120]. Within the OE, however, little is known about how Notch signaling influences HBCs during regeneration.

Moreover, the Notch ligands that specify HBC fate, and their spatiotemporal dynamics during OE regeneration, remain unknown. Our data demonstrate that while they maintain Notch1 expression following OE injury, HBCs surprisingly enhance Notch pathway activation while concurrently downregulating their expression of the Notch ligand, Dll1. Soon thereafter when multiple cell layers emerge within the regenerating OE, HBCs concomitantly enrich for both Notch1 and Dll1. Conditional knockout (cKO) studies suggest that following injury, Notch1 transduces specification cues that promote HBCs to emerge from their niche by enhancing their entry into the cell cycle and mediating neuronal differentiation. In total, these data identify Notch1 as a bifunctional signal integrator that differentially specifies HBC identity depending on OE status.

## 2.2 Results

### 2.2.1 HBCs enhance Notch pathway activation during acute regeneration at 24hpi

Following intra-peritoneal injection of methimazole (MTZ), an agent known to induce OE injury and HBC-mediated regeneration[51,59], we analyzed Notch-related protein dynamics of cytokeratin 5$^{+}$ (CK5$^{+}$) HBCs during acute regeneration. Analyses were first performed at 24 hours post-MTZ injection (24hpi) when HBCs activate, defined by their significant downregulation of the transcription factor, p63 (Fig. 2.1A-E), a critical regulator of HBC quiescence and differentiation potential[52,56,174]. Because the Notch1 receptor specifies HBC quiescence in the unlesioned OE[57], we first assessed its expression. While HBCs at 24hpi maintain Notch1 expression at similar levels to HBCs in unlesioned OE (Fig. 2.1F-J), they interestingly enhance Notch pathway activation as evidenced by a 60.6% increase in expression of Hes1 (Fig. 2.1K-O), a transcription factor whose expression is predicated on Notch signaling[175,176]. We were then curious as to the expression of the two predominant Notch ligands found in the OE, Jagged1 and Dll1[57]. Given that MTZ-induced tissue destruction includes degeneration of Jagged1-expressing Sus cells, thus significantly diminishing the availability of this Notch ligand at

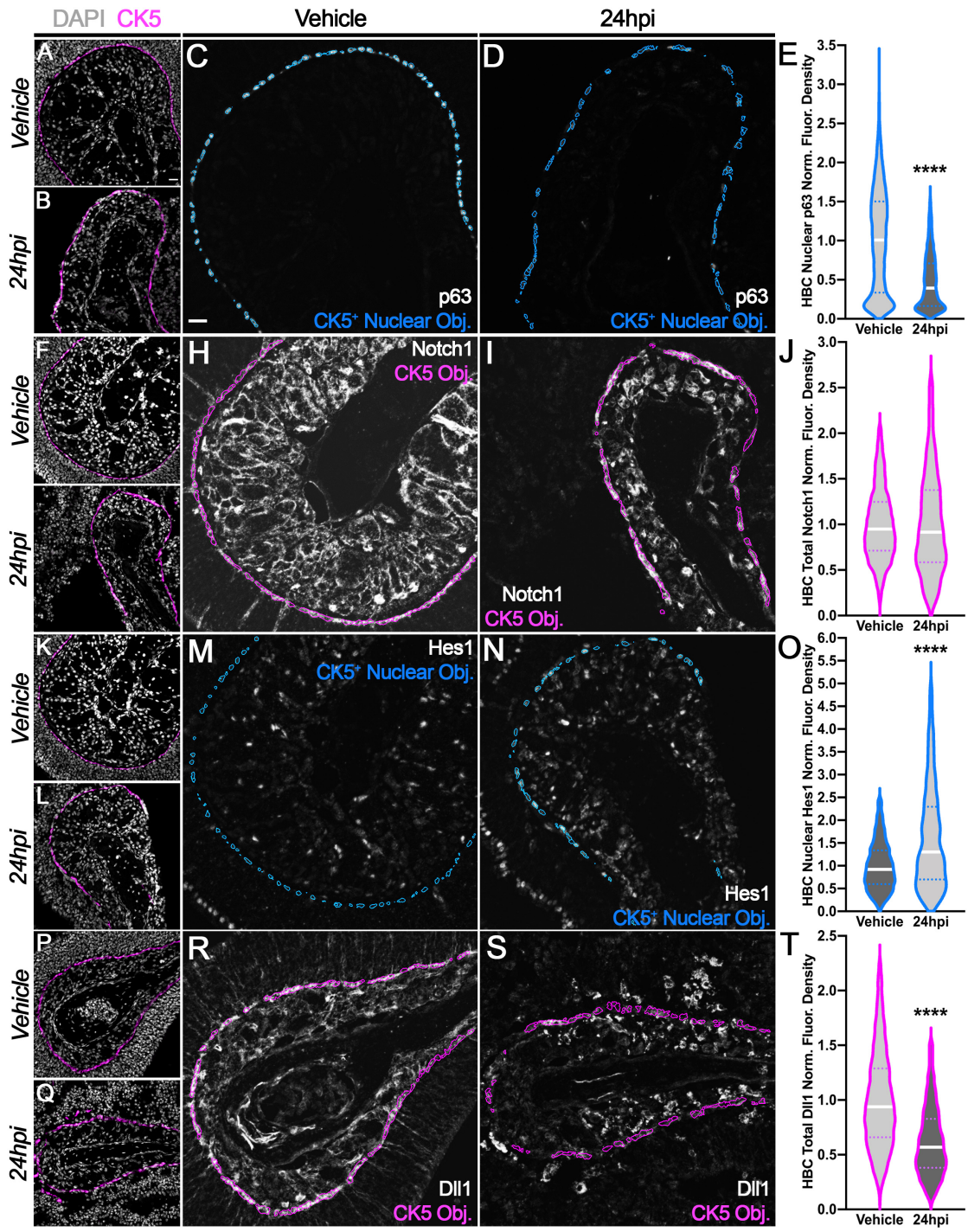


**Fig. 2.1: HBC expression dynamics of Notch signaling pathway components at 24hpi.** A-E: HBC nuclear p63 is significantly decreased (n=3 mice; 3,829 Vehicle HBCs and 1,419 24hpi HBCs). F-J: HBC total Notch1 remains statistically unchanged (n=3 mice; 2,833 Vehicle HBCs and 1,126 24hpi HBCs). K-O: HBC nuclear Hes1 significantly increases (n=3 mice; 2,201 Vehicle HBCs and 983 24hpi HBCs). P-T: HBC total Dll1 is significantly decreased (n=3 mice; 4,739 Vehicle HBCs and 2,688 24hpi HBCs). Solid line indicates median, dashed lines indicate upper and lower quartiles, Brown-Mood median test, ****p<0.0001 (E, J, O, T). Scale bar equals 10μm (A, C).

24hpi (Fig. 2.2A-D), we expected that Dll1 expressed by HBCs[57] (Fig. 2.1R) facilitates the observed Notch signaling enhancement. Surprisingly, HBCs at 24hpi downregulate Dll1 expression by nearly 40% (Fig. 2.1P-T). Therefore, these data suggest that Notch pathway activation is critical to HBC-mediated OE regeneration and HBCs potentially downregulate Dll1 to promote their activation.

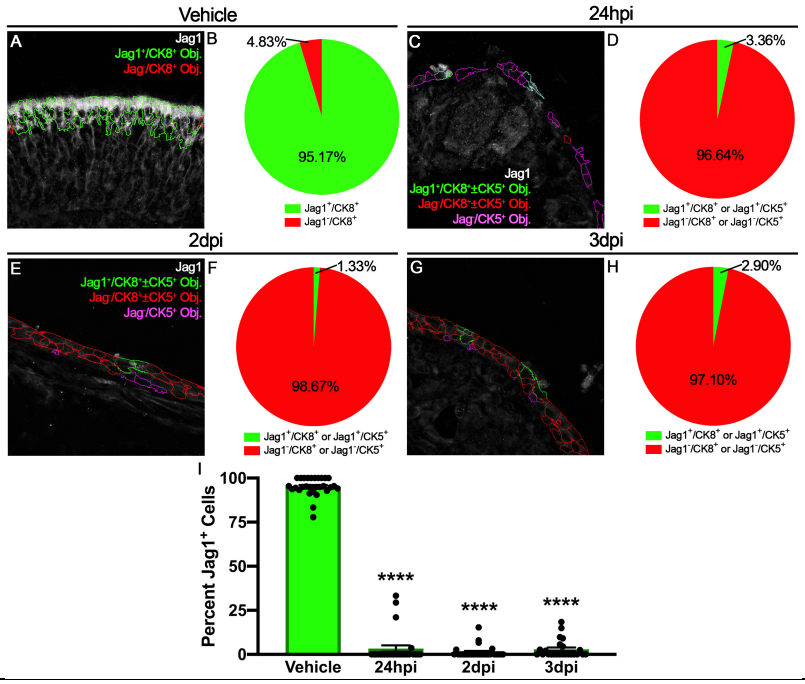


**Fig. 2.2: Jagged1 expression is negligible during early OE regeneration.** Jagged1 is highly expressed within the unlesioned OE and localizes to CK8$^+$ Sus cells (A, B). C-H: As regeneration proceeds from 24hpi (C, D), 2dpi (E, F), and 3dpi (G, H), scant CK5$^+$ and CK8$^+$ cells that compose the regenerating OE are Jagged1$^+$. I: Quantification of A-H (n=3 mice, 517 Vehicle CK8$^+$ cells across 29 regions, 583 24hpi CK8$^+$ or CK5$^+$ cells across 26 regions, 988 2dpi CK8$^+$ or CK5$^+$ cells across 27 regions, 1,102 3dpi CK8$^+$ or CK5$^+$ cells across 24 regions), error bars indicate mean ± SEM, Kruskal-Wallis test with post-hoc Dunn's multiple comparisons test, ****p<0.0001.

### 2.2.2 Re-establishment of Notch signaling pathway component polarity occurs as multiple cell layers become evident during OE regeneration

By 2 days post-MTZ injection (2dpi), the regenerating OE becomes multiple cell layers wherein two different CK5$^+$ populations can be found. Relative to the p63$^-$/CK5$^+$ cells that generally overlie them, p63$^+$/CK5$^+$ HBCs enrich for Notch1 (Fig. 2.3A,B,I) and

Dll1 (Fig. 2.3E,F,K), similar to unlesioned OE[57]. As OE regeneration proceeds at 3dpi, polarization of Notch1 (Fig. 2.3C,D,J) and Dll1 (Fig. 2.3G,H,L) increases with expression of these two Notch signaling pathway components continuing to segregate towards $p63^{+}/CK5^{+}$ HBCs.

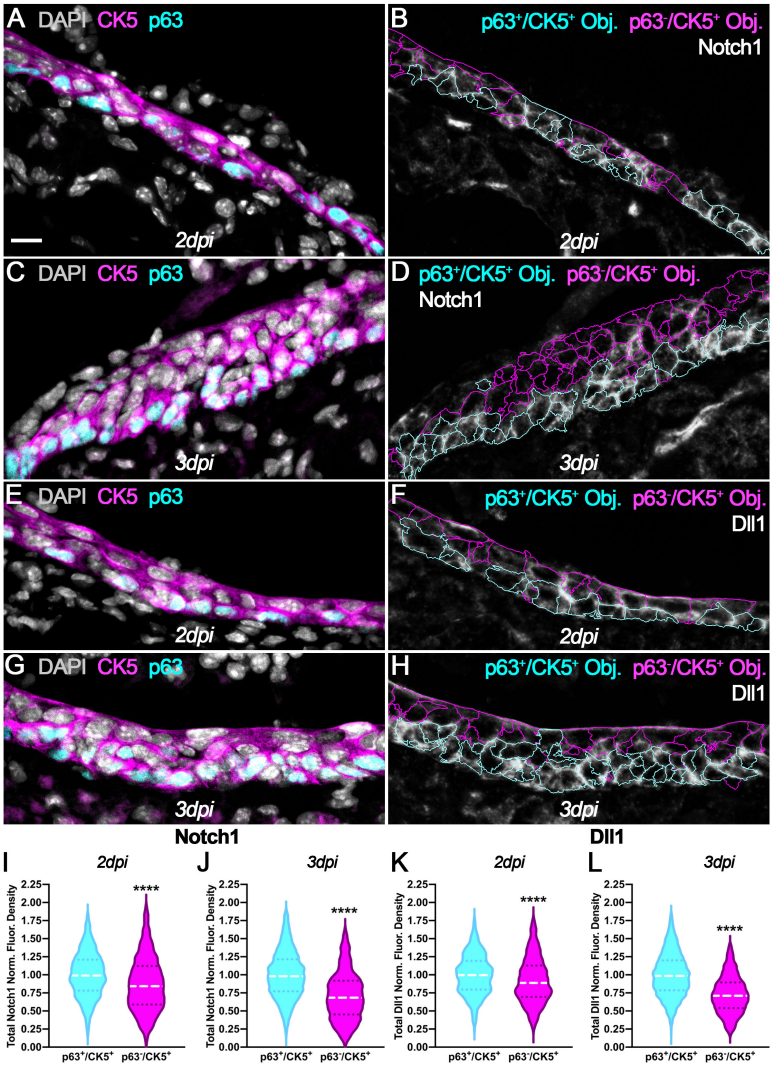


**Fig. 2.3: Polarization of Notch1 and Dll1 expression during OE regeneration.** A-D: dHBCs (p63+/CK5+) become increasingly enriched for Notch1 in the regenerating OE (2dpi: 13.1% increase, n=3 mice, 1,481 $p63^{+}/CK5^{+}$ dHBCs and 1,224 $p63^{-}/CK5^{+}$ cells; 3dpi: 39.3% increase, n=3 mice, 2,389 $p63^{+}/CK5^{+}$ dHBCs and 2,485 $p63^{-}/CK5^{+}$ cells). E-H: dHBCs become increasingly enriched for Dll1 in the regenerating OE (2dpi: 8.5% increase, n=3 mice, 1,470 $p63^{+}/CK5^{+}$ dHBCs and 1,226 $p63^{-}/CK5^{+}$ cells; 3dpi: 37.4% increase, n=3 mice, 2,143 $p63^{+}/CK5^{+}$ dHBCs and 2,333 $p63^{-}/CK5^{+}$ cells). I and J: quantification of B and D, respectively. K and L: quantification of F and H, respectively. Solid line indicates median, dashed lines indicate upper and lower quartiles, Brown-Mood median test, ****p<0.0001 (I-L). Scale bar equals 10μm (A).

### 2.2.3 *In vivo* HBC cKO of *Notch1* diminishes Notch signaling pathway activation within HBCs at 24hpi as the OE initiates regeneration

Given that HBCs maintain Notch1 receptor expression (Fig. 2.1J) and enhance Notch pathway activation at 24hpi (Fig. 2.1O), we interrogated whether HBC Hes1 expression is sensitive to Notch1-mediated signal transduction. Utilizing trigenic mice expressing tamoxifen-inducible Cre recombinase under the HBC-specific *CK5* promotor and tdTomato downstream of a floxed stop codon within the *Rosa26* locus that enables HBC lineage tracing, conditional knockout (cKO) of *Notch1* demonstrated that HBCs at 24hpi exhibited significantly diminished Notch signaling pathway activity as suggested by nuclear Hes1 expression (Fig. 2.4A-E). Interestingly, this reduction was not accompanied by a significant change in p63 expression (Fig. 2.4F-J). In sum, however, these data demonstrate that HBCs engage in Notch1-mediated signaling at 24hpi, which in turn, may encode specification cues that promote HBC contribution to OE regeneration.

Therefore, to determine the functional impact of *Notch1* cKO on OE regeneration, we assessed whether HBC fate specification is first affected at 3dpi when multiple cell layers become clearly evident. Suggested by enhanced p63 expression at 24hpi (Fig. 2.4F-J), there are significantly more quiescent, $Ki67^{-}/p63^{+}$ HBCs at 3dpi following *Notch1* cKO (26.7%) compared to *Notch1* WT control (15.1%) (Fig. 2.4K-S). Increased HBC quiescence within the regenerating OE at 3dpi is corroborated by localization of Sec8, a protein that exclusively marks all GBCs and excludes HBCs within the stem cell layer of unlesioned OE[63]. While regenerating *Notch1* WT OE at 3dpi is comprised of 11.2% $Sec8^{-}/p63^{+}$ HBCs, their frequency increases significantly to 23.7% within *Notch1* cKO OE (Fig. 2.5).

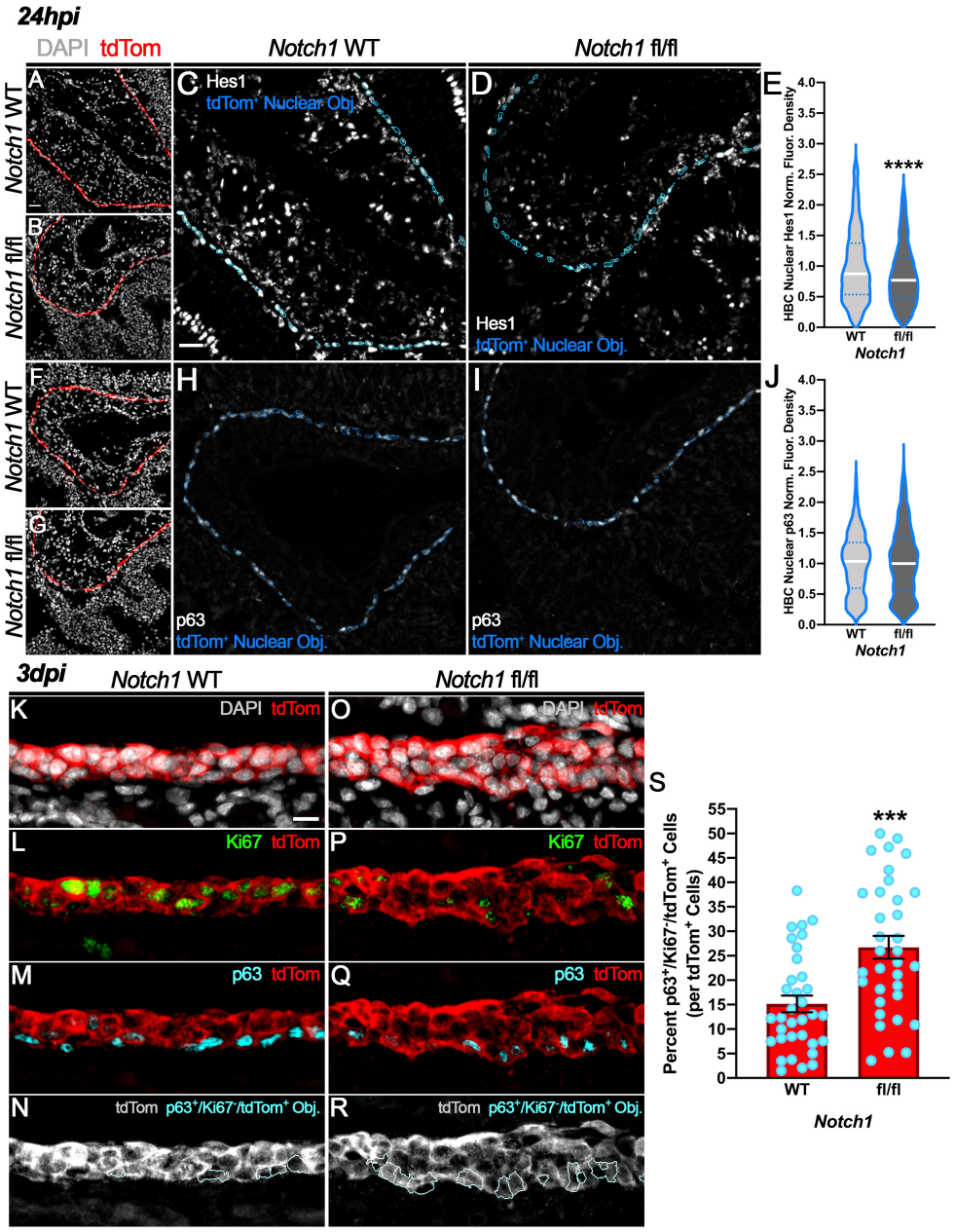


**Fig. 2.4: Abrogation of Notch1-mediated Notch signaling activity during OE regeneration at 24hpi correlates with increased quiescent HBCs at 3dpi.** A-D: At 24hpi, HBC cKO of *Notch1* leads to decreased Notch signaling activity as indicated by an ~16% decrease in HBC nuclear Hes1 expression. E: Quantification of A-D (n=3 mice, 1,229 *Notch1* WT HBCs and 1,109 *Notch1* fl/fl HBCs). F-I: No significant change in HBC nuclear p63 expression at 24hpi following *Notch1* cKO. J: Quantification of F-I (n=3 mice, 1,344 *Notch1* WT HBCs and 1,049 *Notch1* fl/fl HBCs). K-R: At 3dpi, HBC cKO of *Notch1* leads to increased quiescent HBCs ($p63^+/Ki67^-/tdTom^+$, cyan in N and R). S: Quantification of K-R (n=3 mice, 34 *Notch1* WT regions and 34 *Notch1* fl/fl regions). Solid line indicates median, dashed lines indicate upper and lower quartiles, Brown-Mood median test, ****p<0.0001 (E, J). Error bars indicate mean ± SEM, Mann-Whitney test, ***p<0.001 (S). Scale bar equals 10μm (A, C, K).

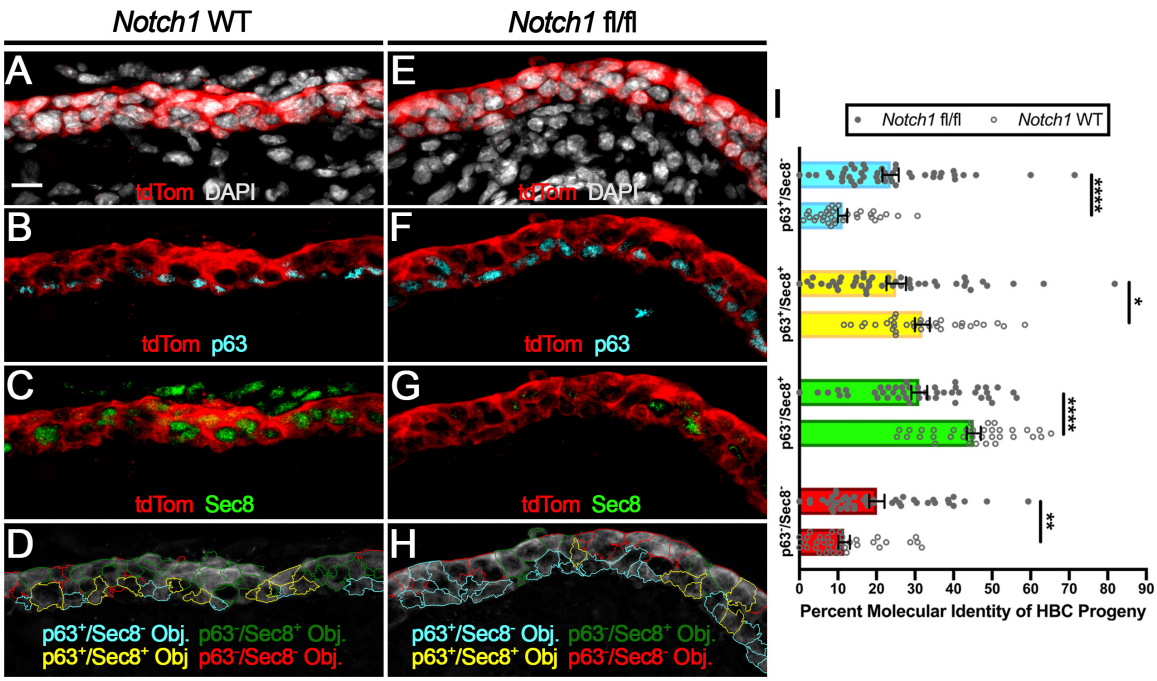


**Fig. 2.5: Molecularly distinct quiescent HBCs of the unlesioned OE are present at 3dpi.** A-H: At 3dpi, HBC cKO of *Notch1* leads to increased p63$^{+}$/Sec8$^{-}$/tdTom$^{+}$ quiescent HBCs (cyan, D and H) as seen in the unlesioned OE I: Quantification of A-H (n=3 mice, 35 *Notch1* WT regions and 46 *Notch1* fl/fl regions), error bars indicate mean ± SEM, Holm-Sidak t-test, *p<0.05, **p<0.01, ****p<0.0001. Scale bar equals 10μm (A).

As HBCs can give rise to GBCs[51] and transcriptome-based modeling suggests that this transition can happen directly[41], we interrogated whether HBC bias towards quiescence following HBC-specific *Notch1* cKO also interrupts GBC formation. To do so, we utilized a constellation of molecular markers to identify HBC-derived GBCs centered on the transcription factor, Sox2. Because HBCs and Sus cells are also Sox2$^{+}$[177] and present within the acutely regenerating OE[41,177], we excluded HBCs and Sus cells by their expression of p63 and CK18, respectively. Following negative selection of p63$^{+}$/Sox2$^{+}$/tdTom$^{+}$ HBCs and CK18$^{+}$/Sox2$^{+}$/tdTom$^{+}$ Sus cells, quantification of p63$^{-}$/CK18$^{-}$/Sox2$^{+}$/tdTom$^{+}$ GBCs at 3dpi demonstrated that *Notch1* cKO significantly diminishes the degree of GBCs arising from HBCs (13.0% v. 28.8% in *Notch1* WT OE)

(Fig. 2.6A-I). In total, these data indicate that Notch1 specifies quiescent HBCs towards GBC differentiation during acute injury-induced regeneration.

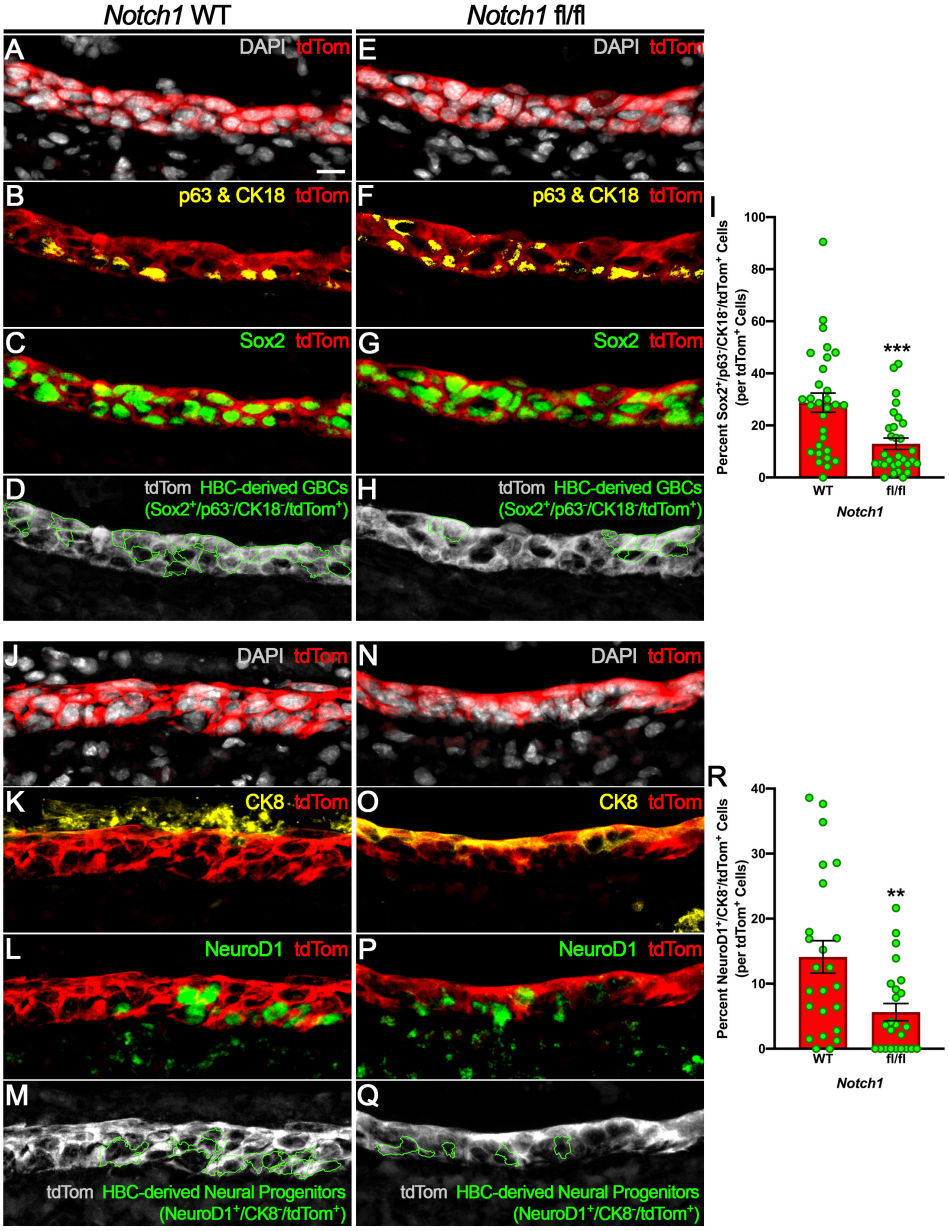


**Fig. 2.6: *Notch1* cKO decreases HBC differentiation towards GBCs and neuronal progenitors.** A-I: At 3dpi, Sox2$^+$/p63$^-$/CK18$^-$/tdTom$^+$ GBCs derived from HBCs (green, D and H) decreases following HBC-specific *Notch1* cKO. I: Quantification of A-H (n=3 mice, 30 *Notch1* WT regions and 30 *Notch1* fl/fl regions). J-Q: At 3dpi, NeuroD1$^+$/CK8$^-$/tdTom$^+$ neural progenitors derived from HBCs decreases (green, M and Q) following HBC-specific *Notch1* cKO. R: Quantification of J-Q (n=3 mice, 24 *Notch1* WT regions and 24 *Notch1* fl/fl regions). Error bars indicate mean ± SEM, Mann-Whitney test, **p<0.01, ***p<0.001 (I, R). Scale bar equals 10μm (A).

### 2.2.4 Notch1 transduces specification cues during acute OE regeneration that biases HBCs towards neuronal progenitor differentiation

As *Notch1* cKO within the acutely regenerating OE significantly compromises the effective pool of the two OE stem cell populations by increasing quiescent HBC (Fig. 2.4K-S) and decreasing GBC tissue compositions (Fig. 2.6A-I), we investigated what effect this may have on the differentiation of two major cell types within the OE, OSNs and Sus cells. While it has been demonstrated that HBCs can differentiate directly to Sus cells[41], OSNs are commonly derived from determined, NeuroD1$^+$ progenitors[42]. At 3dpi when multiple HBC-derived cell layers are present, HBC *Notch1* cKO resulted in no significant change in NeuroD1$^-$/CK8$^+$/ tdTom$^+$ HBC-derived Sus cells (54.7% v. 51.1% in *Notch1* WT OE) (Fig. 2.7). Interestingly, however, there was a significant decrease in NeuroD1$^+$/CK8$^-$/ tdTom$^+$ HBC-derived neural progenitors (5.6% v. 14.1% in *Notch1* WT OE) (Fig. 2.6J-R).

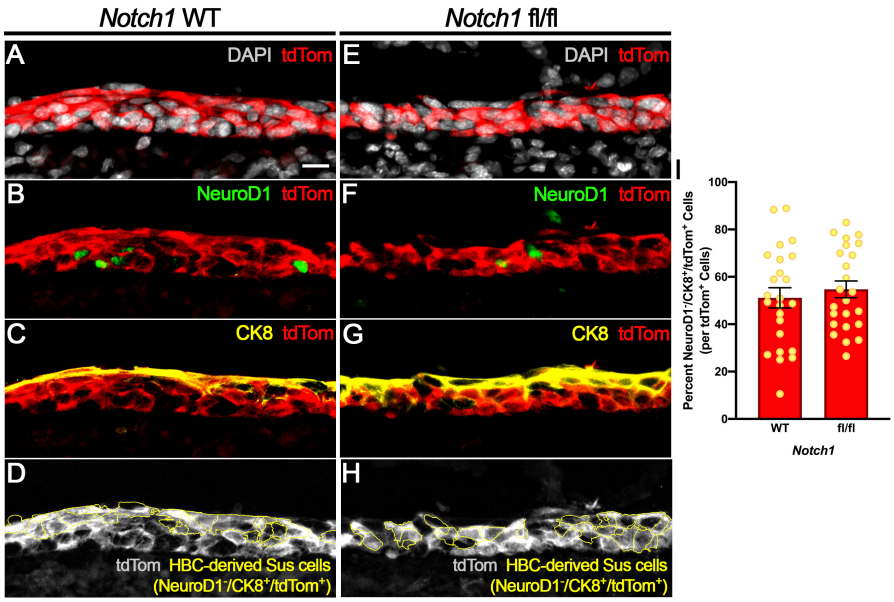


**Fig. 2.7: *Notch1* cKO has no appreciable effect on HBC differentiation towards Sus cells.** A-I: At 3dpi, there is no appreciable change in the percentage of NeuroD1$^-$/CK8$^+$/tdTom$^+$ Sus cells derived from HBCs (yellow, D and H) following HBC-specific *Notch1* cKO. I: Quantification of A-H (n=3 mice, 24 *Notch1* WT regions and 24 *Notch1* fl/fl regions). Error bars indicate mean ± SEM, Unpaired t-test. Scale bar equals 10μm (A).

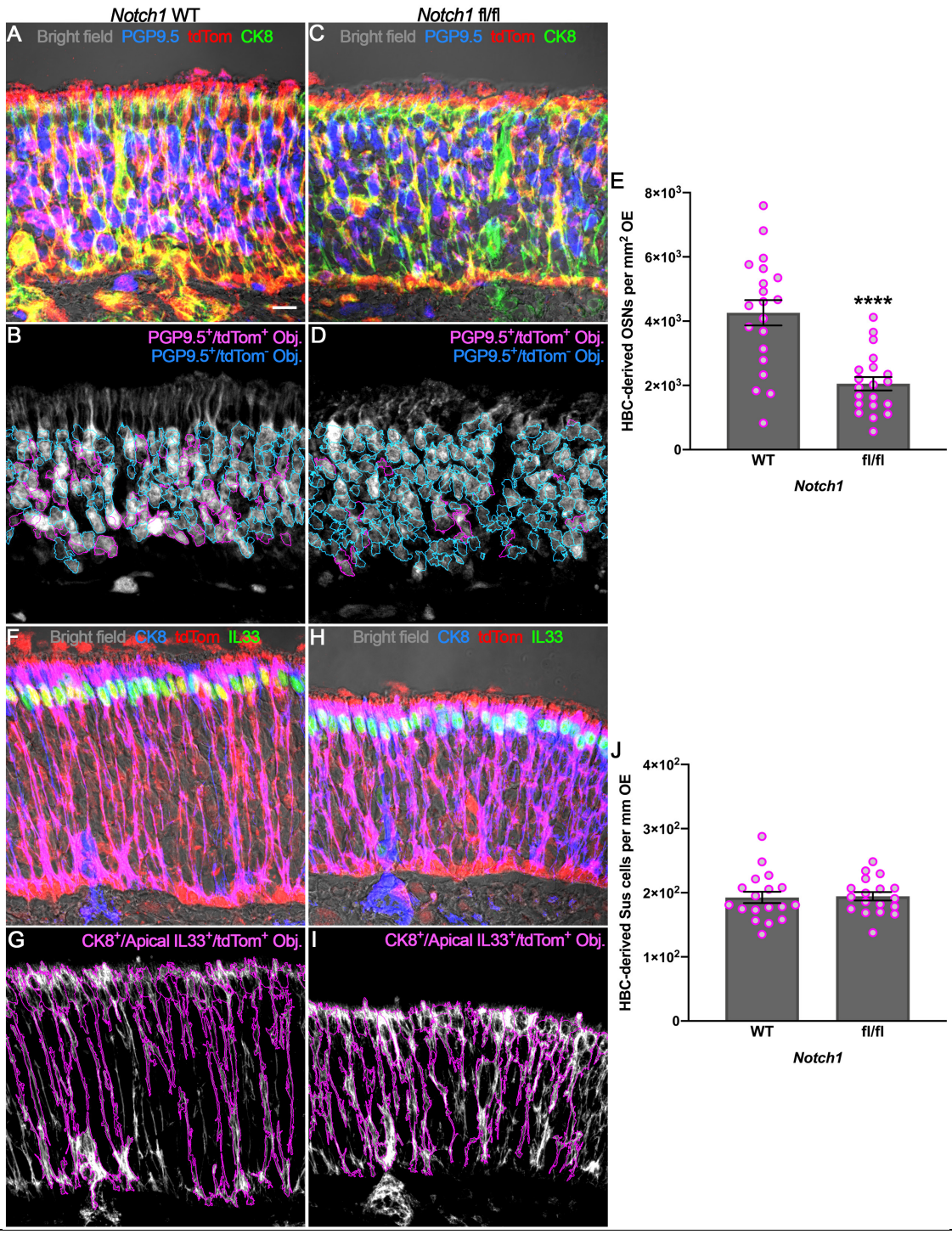


**Fig. 2.8: HBC-mediated neurogenesis following OE injury is diminished by *Notch1* cKO.** A-D: At 28dpi, PGP9.5$^+$/tdTom$^+$ OSNs derived from HBCs (magenta) decreases following HBC-specific *Notch1* cKO. E: Quantification of A-D (n=3 mice, 20 *Notch1* WT regions and 20 *Notch1* fl/fl regions). F-I: At 28dpi, CK8$^+$/apically localized IL33$^+$/tdTom$^+$ Sus cells derived from HBCs (magenta) demonstrates no significant change following HBC-specific *Notch1* cKO. J: Quantification of F-I (n=3 mice, 18 *Notch1* WT regions and 18 *Notch1* fl/fl regions). Error bars indicate mean ± SEM, Unpaired t-test, **p<0.01, ****p<0.0001 (E, J). Scale bar equals 10μm (A).

### 2.2.5 Notch1-mediated enhancement of HBC neuronal progenitor differentiation correlates with decreased HBC neurogenesis

To investigate whether these relative cell type compositions persist beyond acute OE regeneration, we assessed cellular density for Sus cells and OSNs at 28dpi when gross unlesioned OE morphology has regenerated. At this time point, Sus cell bodies are morphologically identifiable by their apical localization within the OE[2] and molecularly defined by CK8 and IL33[41,178], while both immature and mature OSNs express PGP9.5[66]. Within HBC *Notch1* cKO OE, HBC-derived PGP9.5$^+$/tdTom$^+$ OSN density within mutant OE decreased by nearly half (2,053 OSNs per mm2 v. 4,261 OSNs per mm2 in *Notch1* WT OE) (Fig. 2.8A-E). On the other hand, HBC-derived CK8$^+$/IL33$^+$/tdTom$^+$ Sus cell linear density remained relatively unchanged (193 Sus cells per mm v. 195 Sus cells per mm in *Notch1* WT OE) (Fig. 2.8F-J). Collectively, these data demonstrate that Notch1 contributes to normal OE regeneration by specifying adequate HBC neuronal differentiation. Furthermore, they suggest that HBC neuronal specification mediated by Notch1 occurs during acute OE regeneration and depends on HBC differentiation towards determined neural progenitors.

## 2.3 Discussion

While it is known that HBCs can give rise to all OE cell types, mechanisms governing HBC biology following tissue injury that ultimately enable HBC-mediated OE regeneration remain a relative black box. In recent years, HBC-specific genetic manipulations have revealed p63 as a critical cell autonomous regulator of HBC quiescence versus activation[52,56]. Similar experiments *in vivo* have also demonstrated that TNFR1 plays a central role in facilitating HBC-mediated OE regeneration[61], thereby implicating environmental cytokines as an HBC specification cue during injury repair. However, rigorous interrogation of the role that the injured tissue itself plays in promoting OE regeneration is lacking. Because Notch1 appears to positively regulate HBC

quiescence in uninjured OE, we therefore investigated this receptor's influence on HBC activity during OE regeneration elicited by tissue injury.

Exemplified by the disparate role that Notch signaling plays in skeletal muscle wherein the pathway specifies satellite cell quiescence during homeostasis[118] but functionally inverts following muscle injury to promote satellite cell proliferation and contribution to tissue regeneration[119,120], the Notch signaling pathway is an inherently complex pathway. As such, we could not assume that Notch1 influences HBC activity following OE injury in the same way as in uninjured OE. Indeed, rather than continue to promote HBC quiescence, Notch1 transduces cues that specify HBCs to proliferate and differentiate into neural progenitors during OE regeneration. Contrasted with spinal cord regeneration during which Notch1 inhibits spinal progenitor proliferation and motor neuron differentiation[116], our data further underscores the importance of studying this well-conserved stem cell regulatory pathway in a niche-specific manner.

The halving of HBC-derived OSNs within morphologically regenerated OE highlights the fundamental influence of Notch1 on HBC specification during regeneration. Considering that this is preceded by attenuated neural progenitor differentiation at 3dpi, this decreased neurogenesis suggests that a critical period for HBC fate determination occurs sometime during acute OE injury. Efforts to further narrow down this window when HBCs are receptive to Notch ligands would potentially enable more precise HBC manipulation towards one lineage or another.

While our study cannot definitively establish which Notch ligand specifies HBC fate during OE regeneration, we identify Dll1 as a promising candidate. Jagged1 and Dll1 are the predominant ligands detected within the uninjured OE[57], however following injury, the former becomes nearly absent while the latter is dynamically expressed during early regeneration. At 24hpi when HBCs are molecularly poised to contribute to tissue repair, HBC enhancement of nuclear Hes1 indicates that Notch signaling begins

to play an integral role soon after OE injury. Furthermore, it suggests that HBCs downregulate Dll1 to diminish a quiescence cue. Indeed, within the subventricular zone and interfollicular epidermis, Dll1 promotes quiescence of their respective resident stem cells[117,179]. Additionally, Dll1 has been shown to attenuate Notch-ligand independent signaling[112]. Therefore, it remains to be determined whether HBCs employ a similar process as OE regeneration initiates.

When multiple, molecularly heterogenous cell layers reappear during OE regeneration, Dll1 and Notch1 enrichment among HBCs suggest that the ligand continues to specify HBC quiescence, thus intimating that HBCs act as a niche element to regulate themselves. In drawing back and considering the regenerating tissue as a whole during this stage, it will be worthwhile to discern if HBCs variably express Dll1 to meter HBC differentiation and quiescence via lateral inhibition. Additionally, whether this balancing act occurs alongside of or instead due to precise temporal expression of Fringe proteins that tune Notch receptor-ligand interactions[107-109] deserves further attention.

In stark contrast to previous studies[57,180], we used high-throughput image analysis to determine the molecular identity of HBCs across multiple time points following OE injury. After quantifying thousands of HBCs and their progeny, we demonstrate that Notch1 enhances HBC proliferation and neuronal differentiation during OE regeneration. Our data also strongly implicates Dll1 as a specification cue that moderates these HBC functions. In total, these data provide previously unknown insight into HBC biology during tissue regeneration, thereby serving as a fundamental building block towards leveraging these resident stem cells in the treatment of olfactory diseases due to anatomic OE pathologies.

## 2.4 Materials and Methods

### 2.4.1 Mice

All mice were maintained on *ad libitum* chow and water in a heat and humidity controlled, AALAC-accredited vivarium. All protocols for the use of vertebrate animal were approved by the Committee for the Humane Use of Animals at Tufts University School of Medicine. Wild-type mice were F2 generation mice from an initial cross of C57BL/6J (Jax Stock #000664) and 129S1/SvlmJ (Jax Stock #002448) mice performed in-house. *K5CreER$^{T2}$* mice were generously provided by Dr. Pierre Chambon[181] (Jax Stock #018394). *Rosa26R(tdTomato)* (Jax Stock #007909) and B6.129X1-*Notch1$^{tm2Rko}$*/GridJ (Jax Stock #007181) mice were obtained from Jackson Labs. Bi-genic *K5CreER$^{T2}$*; *Rosa26R(tdTomato)* enabling HBC-specific inducible lineage tracing and tri-genic *K5CreER$^{T2}$*; *Notch1$^{tm2Rko}$*/GridJ; *Rosa26R(tdTomato)* enabling HBC-specific inducible *Notch1* KO and lineage tracing were generated in-house. All experiments used sex- and age-matched mice between 8-12 weeks old when initiated.

### 2.4.2 Tamoxifen induction of Cre-mediated recombination

Tamoxifen (Sigma-Aldrich, Cat. T5648) was dissolved in corn oil (Spectrum Chemical, Cat. CO136) at a stock concentration of 30mg/mL. For HBC lineage tracing only, the tamoxifen stock was intraperitoneally injected into *K5CreER$^{T2}$*; *Rosa26R(tdTomato)* mice at 150mg/kg for two consecutive days prior to subsequent experimentation. For combination HBC *Notch1* cKO and lineage tracing, *K5CreER$^{T2}$*; *Notch1$^{tm2Rko}$*/GridJ; *Rosa26R(tdTomato)* mice and their wild-type controls mice were intraperitoneally injected at 300mg/kg for two consecutive days prior to subsequent experimentation.

### 2.4.3 Methimazole-induced OE injury

Methimazole (Sigma-Aldrich Cat. M8506) was dissolved in PBS (Gibco, Cat. 10010-023) at a stock concentration of 5mg/mL. *K5CreER$^{T2}$*; *Rosa26R(tdTomato)* mice

were injected intra-peritoneally at 10uL of MTZ stock/g of mouse XX days after the initial tamoxifen injection. Because of OE over-lesioning seen at 24hpi as suggested by absence of tdTomato$^{+}$ HBC presumably due to increased metabolic load of the 300mg/kg tamoxifen required to induce *Notch1* recombination, *K5CreER$^{T2}$*; *Notch1$^{tm2Rko}$*/GridJ; *Rosa26R(tdTomato)* mice were injected intra-peritoneally at 5uL of MTZ stock/g of mouse 13 days after the initial tamoxifen injection.

### 2.4.4 Tissue processing

At indicated time points, mice were euthanized with an intra-muscular injection of ketamine (37.5mg/kg), xylazine (7.5mg/kg), and acepromazine (1.25mg/kg) triple cocktail. Following trans-cardial perfusion with 20mL PBS (Gibco Cat. 10010-023), mice were subsequently trans-cardially perfused with 40mL 1% PLP fixative (1% paraformaldehyde, 0.1M monobasic and dibasic phosphates, 90mM lysine, and 0.1M meta-sodium periodate). After dissecting away the surrounding cranial structures, the isolated OE was post-fixed in 1% PLP under vacuum for 1.5 hours. Following post-fixation, the OE was briefly rinsed three times in PBS to wash away residual fixative and allowed to incubate in decalcification buffer (0.35M EDTA [Sigma-Aldrich, Cat. ED2SS] and 0.35M NaOH) overnight at 4°C. To cryopreserve the tissue, OE was equilibrated overnight in 30% sucrose at 4°C, embedded and frozen in OCT (Sakura, Cat. 4583), and then stored at -80°C until cryosectioning. A Leica cryostat was used to collect 10µm coronal sections on positively-charged glass slides.

### 2.4.5 Immunofluorescence

Specific antibodies and conditions to detect the various antigens can be found in Table 2.1. All primary antibodies were diluted in Normal Donkey Block (NDB) (10% normal donkey serum v/v, 5% non-fat powdered milk w/v, 4% bovine serum albumin [BSA] w/v, and 0.1% Triton X-100 v/v in 1X PBS). Species-specific fluorophore- and

biotin-conjugated donkey secondary antibodies (Jackson ImmunoResearch) were diluted in NDB at 1:150 and 1:100, respectively. Streptavidin-conjugated horseradish peroxidase (SA-HRP) was diluted in TNB (0.5% blocking reagent w/v [Akoya Biosciences, Cat. FP1020], 0.15M NaCl, and 0.1M Tris-HCl pH 7.5) at 1:400. All washes performed on day 1 and day 2 were in 1X PBS and 3X PBS, respectively, with those following antibody incubation performed 3x5min. Slides were dried on a slide warmer at ~37C for 45-60min. after application of rubber cement (Elmer's) to isolate each section. Following a 10-15min. wash to remove OCT, sections used to detect antigens requiring antigen retrieval were incubated in antigen retrieval buffer (0.1M sodium citrate, pH 6) and placed in a pre-heated commercial steamer for 10min. After slides were washed for 10min., sections were incubated in 3% $H_2O_2$ diluted in MeOH or 90% MeOH depending on whether antigen detection required tyramide signal amplication (TSA), washed 3x5min., and blocked for 1hr. at room temperature with NDB. If a mouse primary antibody were to be used, those sections underwent additional blocking of promiscuous endogenous mouse antigens per manufacturer's protocol (Invitrogen, Cat. R37621). Following overnight primary antibody incubation at 4C, sections were incubated in secondary antibodies for 1hr. at room temperature in the dark. If antigen detection required TSA, appropriate sections were blocked for 30min. in TNB prior to incubation in SA-HRP for 1hr. at room temperature in the dark. TSA was achieved by incubating appropriate sections for 15min. in a solution consisting of 98% TSA Buffer (0.1M boric acid pH 8.5, 0.003% $H_2O_2$), 1% 10% BSA w/v in 1X PBS, and 1% FITC-tyramide. Nuclei were counterstained with DAPI. Sections were coverslipped in NPG (0.5% N-propyl gallate in 90% glycerol) mounting media and slides were stored at 4C in the dark until imaging.

| Antibody | Source | Identifier | Dilution | Antigen Retrieval Required | Signal Detection |
|---|---|---|---|---|---|
| Ms p63 | ATCC | Clone 4A4 | 1:100 | Yes | Secondary fluorophore |
| Rb Notch1 | Cell Signaling Technology | 3608 | 1:75 | Yes | TSA |
| Rb Hes1 | Cell Signaling Technology | 11988 | 1:50 | Yes | TSA |
| Shp Dll1 | R&D Systems | AF3970 | 1:20 | No | TSA |
| Ck CK5 | Biolegend | Clone Poly9059 | 1:200 | No | Secondary fluorophore |
| Ck mCherry | Novus | NBP2-25158 | 1:100 | No | Secondary fluorophore |
| Gt mCherry | Sicgen | AB0040-200 | 1:50 | No | Secondary fluorophore |
| Rb Ki67 | Abcam | ab15580 | 1:250 | Yes | Secondary fluorophore |
| Gt NeuroD1 | R&D Systems | AF2746 | 1:40 | Yes | TSA |
| Rat CK8 | Developmental Studies Hybridoma Bank | TROMA-I | 1:100 | No | Secondary fluorophore |
| Rb CK18 | Proteintech | 10830-1-AP | 1:400 | No | Secondary fluorophore |
| Rat Sox2 | Invitrogen | 14-9811-82 | 1:200 | Yes | Secondary fluorophore |
| Rb PGP9.5 | Proteintech | 14730-1-AP | 1:200 | Yes | Secondary fluorophore |
| Gt IL33 | R&D Systems | AF3626 | 1:10 | Yes | Secondary fluorophore |

**Table 2.1: Antibodies used and associated antigen labeling conditions**

### 2.4.6 Image analyses

ImageJ was used to process all uncompressed, 16bit tiff files obtained from confocal imaging. Z-planes were sum projected to maximize bit depth of captured fluorescence. The ImageJ Rolling ball background subtraction function was applied to every channel. CellProfiler (Version 3.1.9) was used to quantify total fluorescence intensity and generate images containing object overlays. Images of channels in which captured fluorescence was not intended for quantification were converted to 16bit so that CellProfiler could process those images, demarcate relevant cellular landmarks, and

quantify the area that those landmarks occupied to calculate total fluorescence densities. Templates for each CellProfiler pipeline used have been deposited on GitHub.

### 2.4.7 Statistical analyses and data presentation

All statistical analyses were performed within GraphPad Prism Version 8. Only brightness and contrast were adjusted for each representative image within ImageJ and Adobe Photoshop CS6, and these parameters were applied globally throughout the image. All graphs were generated using GraphPad Prism Version 8. All figures were constructed in Adobe Photoshop CS6.

## 2.5 Contributions

I wrote this entire chapter. Immunofluorescence labeling of Jagged1 was performed by Benjamin H. Bromberg. I performed all other experimentation. I performed all imaging, data analysis, and figure construction.

**Chapter 3: Spatiotemporal dynamics of horizontal basal cells during olfactory epithelium regeneration informs a mechanism of primary horizontal basal cell differentiation in vitro**[†]

[†] Louie JD, Bromberg BH, Schwob JE. To be submitted to *Stem Cell Reports*.

### 3.1 Introduction

Horizontal basal cells (HBCs) are a population of resident stem cells found within the olfactory epithelium (OE), an epithelium necessarily in contact with the external environment to fulfill its responsibility of enabling olfaction. Lying in reserve atop the basal lamina, HBCs are typically recruited for OE regeneration following severe tissue injury[51]. Such specific context can be explained by a number of mechanisms demonstrating that the tissue environment within the OE regulates HBC-mediated OE regeneration. Targeted ablation of Sustentacular cells, a glial-like cell whose cell body located at the top of the OE extends processes down towards HBCs[3], leads to HBC differentiation[57]. This consequence has been postulated to result from decreased cell-cell interactions between the Sus cell-expressed Notch ligand, Jagged1, and Notch1 receptor co-labeling with HBCs[57]. Additionally, Sus cell destruction is thought to cause a localized reduction of retinoic acid, a cytokine synthesized by Sus cells that specifies HBC dormancy[58]. Severe injury also elicits a tissue-wide inflammatory response[61]. Diminution of this response or impairing the ability of HBCs to respond to such environmental cues negatively impacts HBC proliferation and subsequent OE regeneration[61] Moreover, discovery that HBC-specific ablation of cilia compromises OE regeneration further underscores the importance of extrinsic, environmental cues[63].

Complementing these non-cell autonomous processes, high-throughput transcriptomic profiling identified the transcription factor, *p63*, as a positive regulator of HBC dormancy[52]. Subsequent investigation demonstrated that OE injury resulting in HBC-mediated regeneration begins with HBC activation as defined by decreased p63 expression. This critical event is corroborated by HBC-specific *p63* conditional knockout (cKO), which leads to HBC differentiation within uninjured OE[52,56]. Advancements in RNA sequencing technologies and their continued omnipresence have been a boon for computationally modeling HBCs and their highly dynamic nature following p63

downregulation[41,182]. To date, however, little is known about HBCs *in situ* and the spatiotemporally dynamic cell autonomous processes that occur soon after injury to promote their contribution to OE regeneration.

Despite prior evidence that p63 positively regulates expression of integrin β1 and β4 (Itgb1 and Itgb4)[183], HBCs interestingly do not downregulate these mediators of cellular adherence to the basal lamina following injury when p63 concurrently decreases. Instead, HBCs surprisingly increase their apical expression of Itgb1 and Itgb4. This spatiotemporal dynamicity occurs concomitant with increased apical Rac1, a member of the Rho family of small GTPases[121,122] that can be activated by Itgb1[150,151]or Itgb4[152,184]. Notably, Rac1 signaling activity can regulate stem cell functions[133-135,169-172], and indeed, spatiotemporal localization of additional molecular components further intimates that HBCs enact Rac1-mediated signaling during acute regeneration. These data gleaned during HBC activation *in vivo* implicating Rac1 as a mechanistic component of HBC-mediated OE regeneration were further interrogated *in vitro* to capitalize on the ease with which HBCs can be leveraged for future autologous stem cell therapies. In addition to diminishing phosphorylation of downstream molecular constituents, Rac1 inhibition functionally attenuates HBC differentiation, and importantly, does so without perturbing HBC activation. In total, keen observation that HBCs likely channel their regenerative response in part through Rac1 ultimately contributes to refining the ability to deftly manipulate a population of readily obtainable stem cells in order to broaden the therapeutic options intended to alleviate olfactory deficits.

## 3.2 Results

### 3.2.1 During acute regeneration, HBCs increase their apical expression of Itgb1 and Itgb4 at 24 hours post-OE injury (24hpi)

Within the OE, p63 is a critical regulator of HBC cell fate, with its decline a marker of HBC activation. Indeed, 24 hours after intra-peritoneal injection of

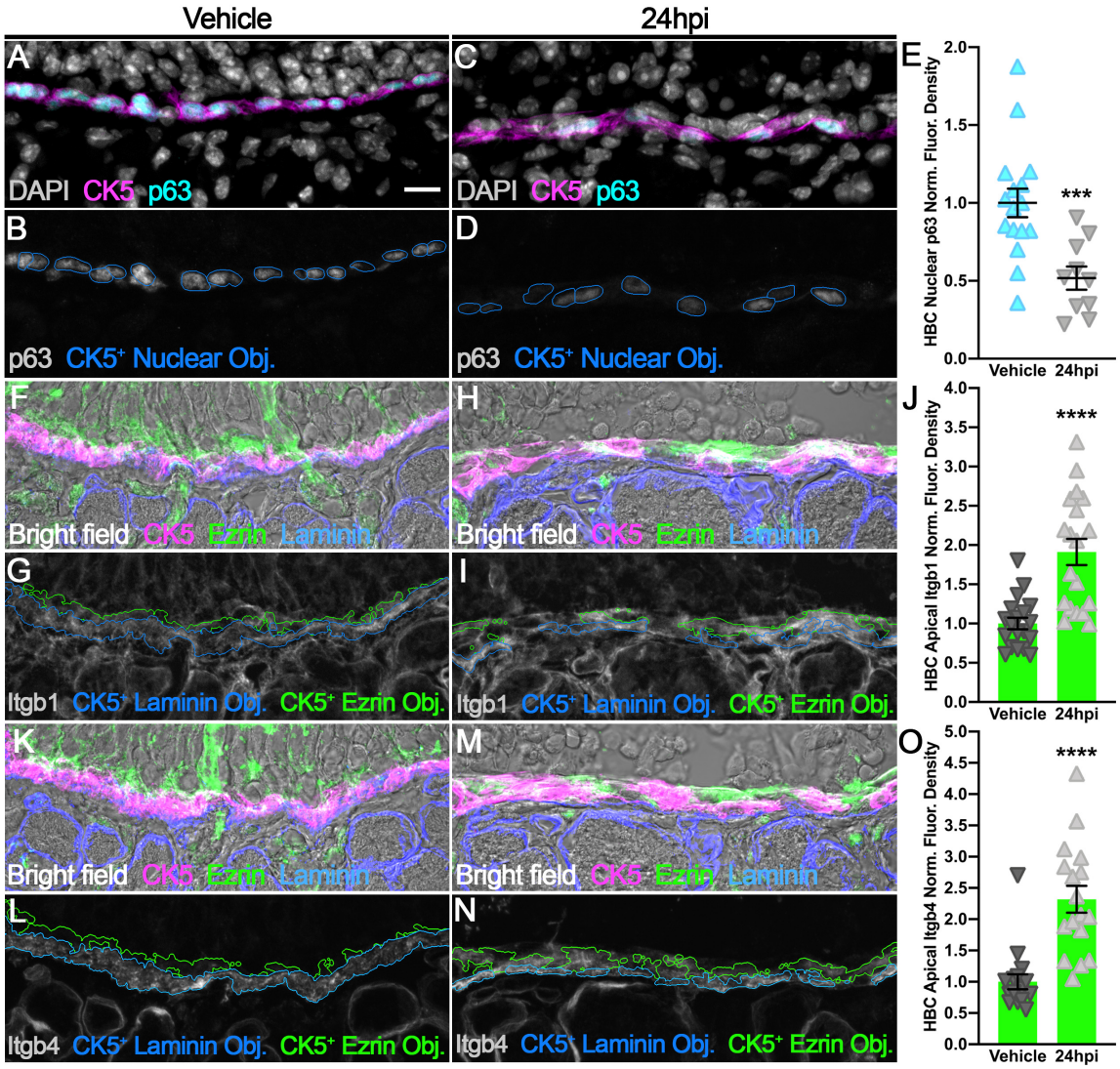


**Fig. 3.1: HBCs at 24hpi increase apical expression of Itgb1 and Itgb4.** A-D: Example of a region of 24hpi OE containing activated HBCs (aHBCs). E: Each point represents a $CK5^+$ nucleus from A-D. F-J: Adjacent section of region matched with A-D demonstrates aHBCs increase apical Itgb1 (n = 3 mice across 19 regions). K-O: Adjacent section of region matched with F-I demonstrates aHBCs increase apical Itgb4 (n = 3 mice across 17 regions). Error bars indicate mean ± SEM, Mann-Whitney test, ***p<0.001, ****p<0.0001 (E, J, O). Scale bar equals 10μm (A).

methimazole (MTZ), an agent known for its induction of OE injury and HBC-mediated regeneration[51,59], cytokeratin $5^+$ ($CK5^+$) HBCs significantly downregulate p63 expression (Fig. 3.1A-E). Given that p63 has been shown to positively regulate expression of Itgb1 and Itgb4[183], it was surprising that HBCs neither concomitantly decrease total nor basal

Itgb1 (Fig. 3.2A-D) and Itgb4 (Fig. 3.2E-H) coincident with CK5$^+$ or CK5$^+$/laminin$^+$ labeling, respectively. Instead at 24hpi, HBCs increase expression of Itgb1 and Itgb4 by 91.2% (Fig. 3.1F-J) and 131.9% (Fig. 3.1K-O), respectively, within CK5$^+$ domains exclusively co-labeled with ezrin (Fig. 3.1F-O), an apically-oriented protein that regulator of apical domain integrity by linking apically localized proteins and the cytoskeleton[185]. Therefore, these data demonstrate that at 24hpi, HBCs spatially modulate intracellular protein expression in part by enhancing apical expression of Itgb1 and Itgb4.

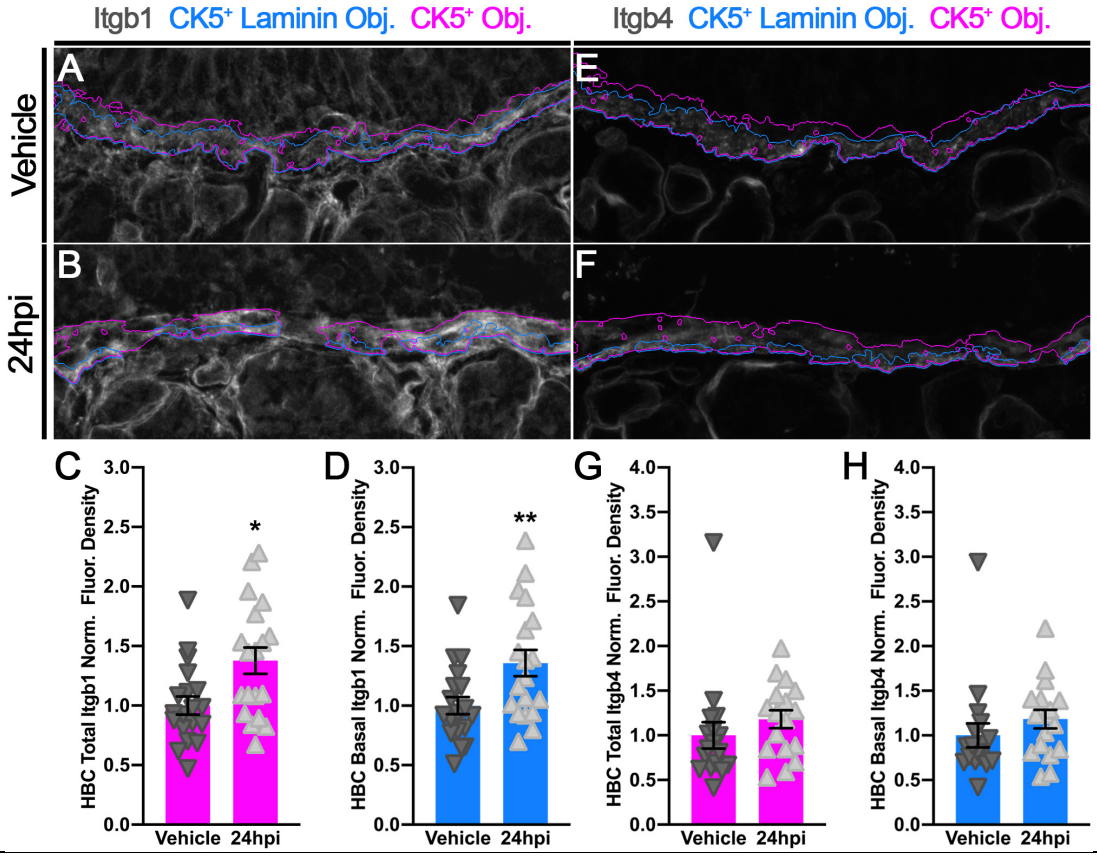


**Fig. 3.2: HBCs at 24hpi do not downregulate Itgb1 and Itgb4 despite p63 downregulation.** A-D: Identical image to Fig.1G (A) and Fig.1I (B) more clearly delineating total HBC area (CK5$^+$ Obj.) and HBC basal domain area (CK5$^+$ Laminin Obj.). HBCs at 24hpi upregulate both total and basal Itgb1 (C, D) (n=3 mice across 19 regions). E-H: Identical image to Fig.1L (E) and Fig.1N (F) more clearly delineating total HBC area (CK5$^+$ Obj.) and HBC basal domain area (CK5$^+$ Laminin Obj.). HBCs at 24hpi do not significantly alter their expression of both total and basal Itgb4 (G, H) (n=3 mice across 17 regions). Error bars indicate mean ± SEM, Mann-Whitney test, *p<0.05, **p<0.01 (C, D, G, H).

### 3.2.2 At 24hpi, HBCs spatiotemporally synchronize intracellular focal adhesion components concomitant with increased Rac1-mediated signaling pathway activation

As Itgb1 and Itgb4 can activate Rac1[150-152,184], a member of a family of small Rho GTPases[121,122] that has been implicated in mediating various stem cell functions[133-135,169-172], we interrogated whether HBCs concurrently upregulate Rac1 in a spatially similar manner. Indeed, HBCs at 24hpi increase apical Rac1 by 81.6% (Fig. 3.3A-E)

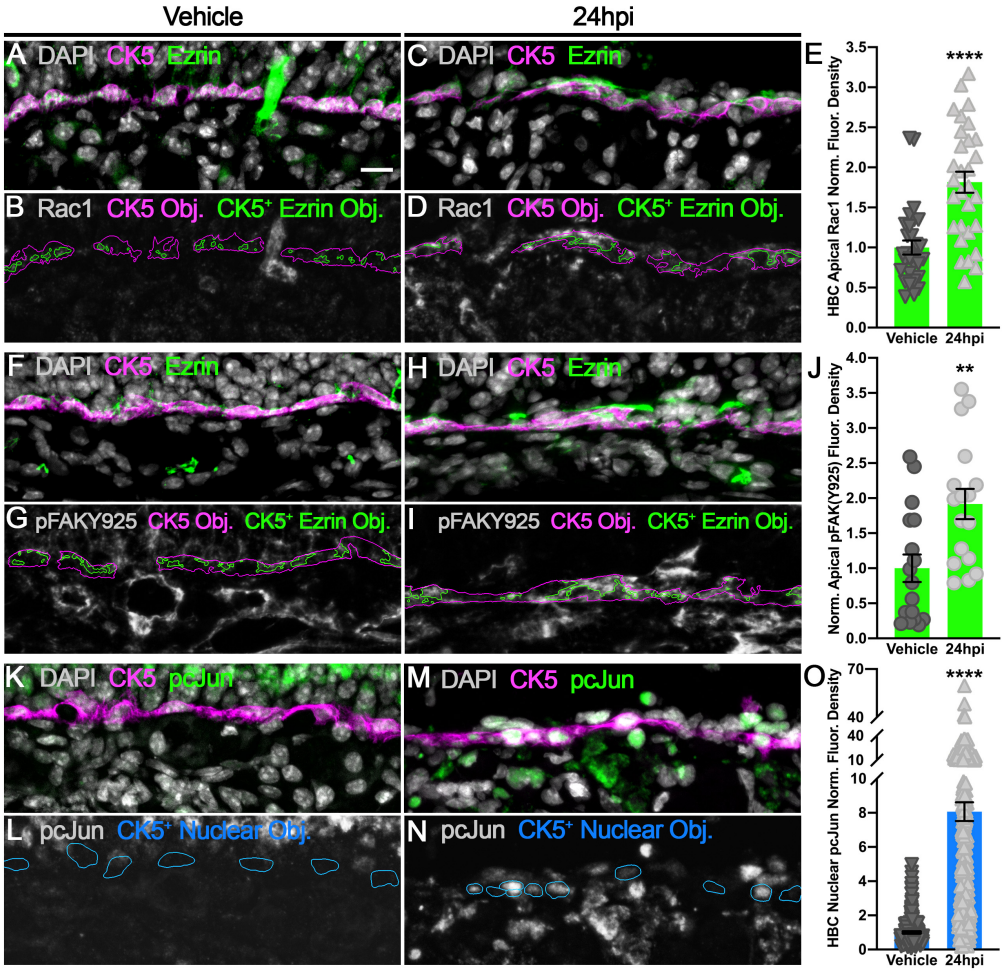


**Fig. 3.3: Downstream effector of Rac1-mediated signaling occurs concomitant with HBC spatiotemporal synchronization of intracellular focal adhesion components at 24hpi.** A-E: HBCs at 24hpi upregulate apical Rac1 (n=3 mice across 30 regions). F-J: HBCs at 24hpi upregulate apical pFAKY925 (n=3 mice across 17 regions.) K-O: HBCs at 24hpi upregulate nuclear pcJun (n=3 mice, 234 Vehicle HBCs and 258 24hpi HBCs). Error bars indicate mean ± SEM, Mann-Whitney test, **p<0.01, ****p<0.0001 (E, J, O). Scale bar equals 10μm (A).

concomitant with the increased spatial localization of Itgb1 and Itgb4 (Fig. 3.1 F-O). Furthermore, focal adhesion kinase phosphorylated at tyrosine 925 (pFAKY925), a critical intermediary that facilitates integrin-mediated Rac1 activation[186], is similarly increased by 91.7% in the apical domain at this time point during OE regeneration (Fig. 3.3F-J). Interestingly, the spatiotemporal synchronicity that HBCs demonstrate with enhanced Itgb1 and Itgb4, pFAKY925, and Rac1 apical localization juxtaposes an over 8-fold increase in HBC expression of phosphorylated cJun (pcJun) (Fig. 3.3K-O). As pcJun lies downstream of Rac1 activation, these data in sum suggest that HBCs at 24hpi activate Rac1-mediated signaling pathways.

### 3.2.3 Inhibiting Rac1 activity during activation of primary HBCs *in vitro* attenuates Rac1-mediated signaling

Rac1 activation most immediately leads to phosphorylation of cJun N-terminal kinase (JNK)[159-161]. Subsequently, phosphorylated JNK (pJNK) facilitates expression of

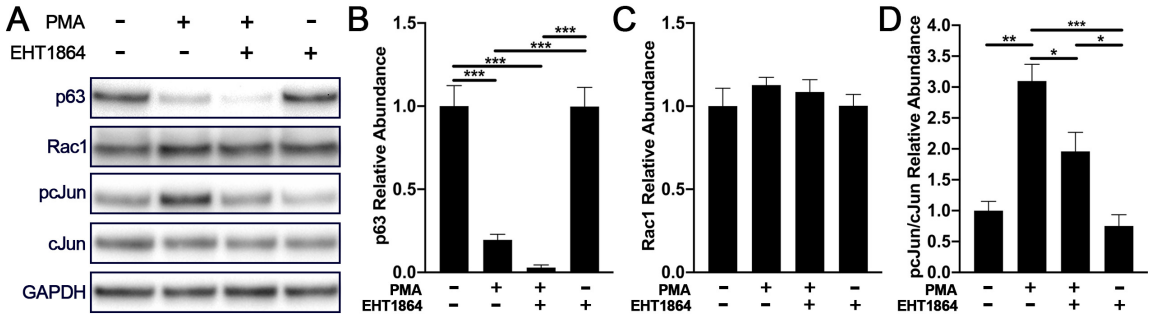


**Fig. 3.4: Enhancement of Rac1-mediated signaling during primary HBC activation *in vitro*.** A: Representative western blots depicting abundance of p63, Rac1, pcJun, total cJun, and GAPDH (n=3 independent trials). B-D: Quantification of densitometric measurements for p63 (B), Rac1 (C), and normalized pcJun per normalized total cJun (D) abundances, error bar indicates mean + SEM, one-way ANOVA with post-hoc Tukey's multiple comparisons test, *<0.05, **p<0.01, ***p<0.001.

pcJun[158,162,163], a transcription factor subunit that can regulate proliferation and tissue morphognesis[164-168,187,188]. Therefore, we utilized our primary HBC culture system that can model HBC activation[189] (Camila Barrios-Camacho, unpublished data) to begin

interrogating the potential relationship between HBC and Rac1 activation. Treating HBCs with 50nM phorbol 12-myristate 13-acetate (PMA) induces their activation as evidenced by decreased p63 abundance (Fig. 3.4A,B), and HBC activation occurs concurrently with increased pcJun abundance (Fig. 3.4A,D). To determine whether this increase was a result of Rac1 activation, PMA-induced HBC activation was coupled with 50μM EHT1864, an inhibitor of Rac1 activation[190]. PMA and EHT1864 treatment together attenuated pcJun abundance by nearly 40% (Fig. 3.4A,D). The same treatment paradigm similarly decreased pJNK abundance (Fig. 3.5), thereby underscoring involvement of Rac1-mediated signaling. Importantly, these effects were not due to any significant change in total Rac1 abundance following EHT1864 treatment (Fig. 3.4A,C). Notably, HBC activation was not curtailed by inhibition of Rac1 activation, as treatment with both small molecules together did not significantly affect the magnitude of decreased p63 abundance (Fig. 3.4B). Collectively, these data demonstrate that primary HBCs initiate Rac1-mediated signaling following their activation, and furthermore, suggest that HBCs do so to regulate a currently undefined process independent of their activation.

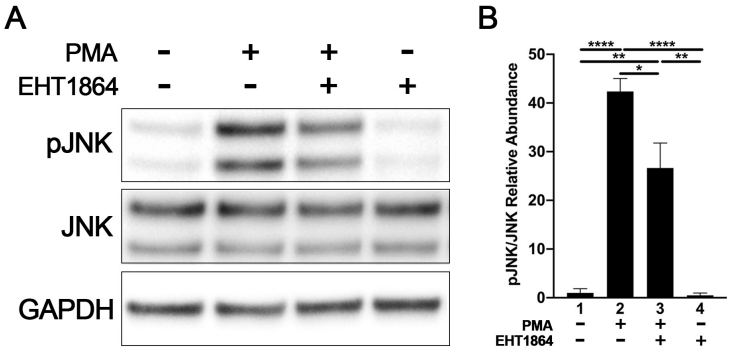


**Fig. 3.5: Inhibition of Rac1 *in vitro* concomitant with primary HBC activation perturbs multiple components of Rac1-mediated signaling.** A: Representative western blots depicting abundance of pJNK, JNK, and GAPDH (n=3 independent trials). C: Quantification of densitometric measurements for normalized pJNK per normalized total JNK abundance, error bar indicates mean + SEM, one-way ANOVA with post-hoc Tukey's multiple comparisons test, *<0.05, **p<0.01, ****p<0.0001.

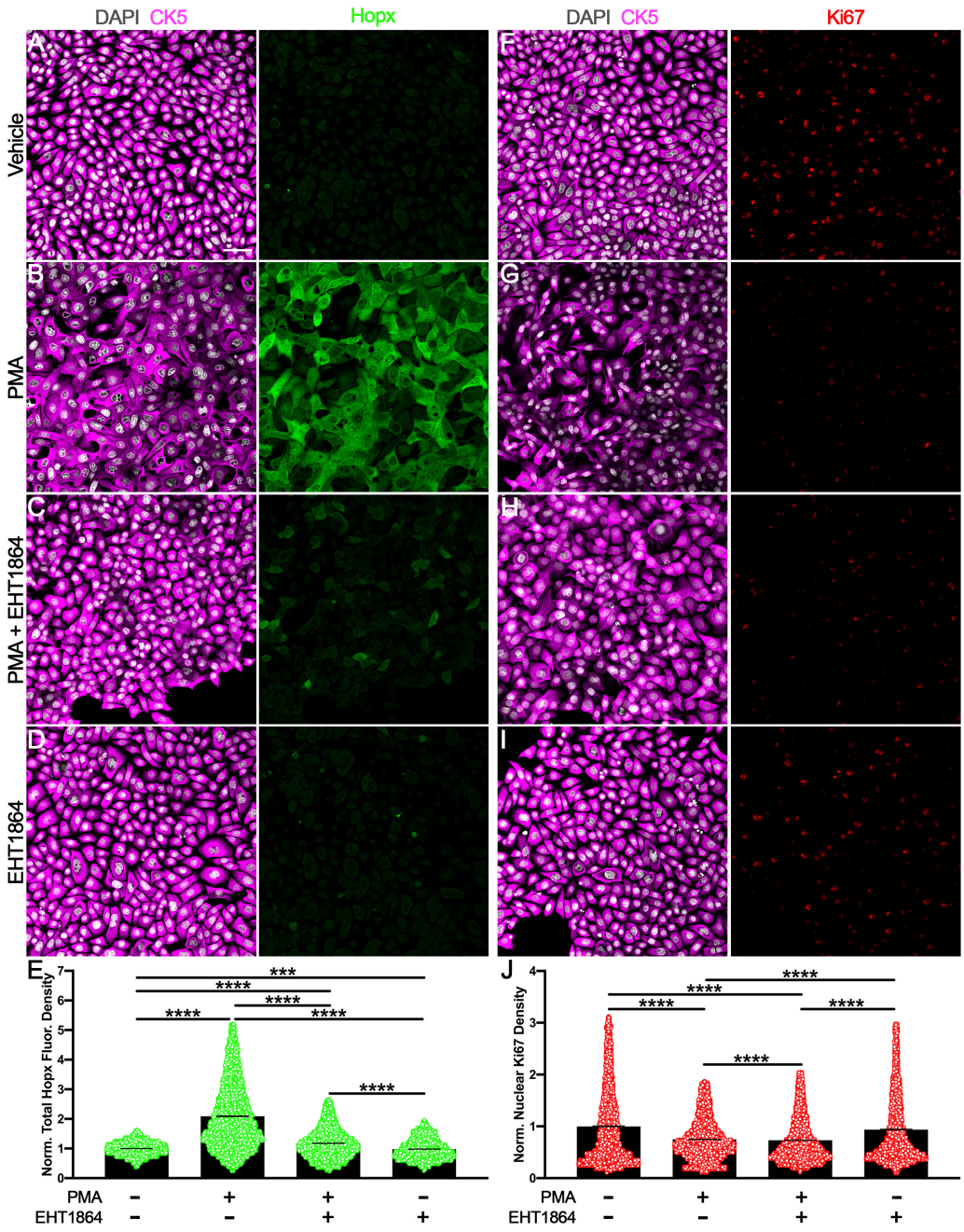


**Fig. 3.6: Rac1 facilitates primary HBC differentiation.** A-D: Representative images of Hopx expression after treating primary HBCs with vehicle (A; 4,927 cells analyzed), PMA (B; 8,065 cells analyzed), PMA+EHT1864 (C, 7,235 cells analyzed), or EHT1864 (D, 5,358 cells analyzed). E: Quantification of Hopx fluorescence density for conditions represented by A-D. F-I: Representative images of Ki67 expression after treating primary HBCs with vehicle (F; 4,716 cells analyzed), PMA (G; 7,325 cells analyzed), PMA+EHT1864 (H; 7,297 cells analyzed), or EHT1864 (I; 5,228 cells analyzed). J: Quantification of Ki67 fluorescence density for conditions represented by F-I. n=4 independent trials. Error bars indicate mean ± SEM, Kruskal-Wallis test with post-hoc Dunn's multiple comparisons test, ***p<0.001, ****p<0.0001 (E, J). Scale bar equals 50μm (A).

### 3.2.4 Rac1-mediated signaling functionally impacts primary HBC differentiation

Shortly following their activation *in vivo*, HBCs become increasingly proliferative[52] and upregulate *Hopx*, an HBC differentiation marker[41]. Therefore, to begin elucidating whether Rac1-mediated signaling governs either HBC proliferation or differentiation, we again utilized our primary HBC culture activation model (Fig. 3.6A-J). PMA treatment alone more than doubled overall Hopx expression (Fig. 3.6A,B,E). Surprisingly, *in vitro* HBCs following pharmacological activation attenuated Ki67 expression by nearly 25% (Fig. 3.6F,G,J). When concurrently treated with PMA and EHT1864, primary HBC expression of Hopx was significantly abrogated Fig. 3.6B,C,E). Interestingly, treatment with both small molecules also resulted in a small, but statistically significant, decrease in overall Ki67 expression relative to PMA treatment alone (Fig. 3.6G,H,J). Together, these data demonstrate that inhibition of Rac1-mediated signaling *in vitro* functionally disrupts HBCs following their activation.

## 3.3 Discussion

While it has been known for more than a decade that HBCs can help repair the OE following tissue injury[51], only relatively recently have mechanisms that enable HBCs to contribute to OE regeneration, such as transcription downregulation and integration of environmental cues, been uncovered[56,61,63]. However, it remains unknown whether HBCs undergo any spatiotemporally dynamic processes during OE regeneration. For the first time, we demonstrate that HBCs reorganize Rac1 apically following OE injury and establish that Rac1 regulates the molecular and functional identity of primary HBCs in culture.

The ability to harvest, expand, activate, and differentiate HBCs, especially those from human patients[189], represents a powerful tool in developing a potential therapy to treat hyposmia or anosmia. These pathologies of olfaction can be attributed to aneuronal regions within the OE that are exhausted of the active stem cell population comprised by

globose basal cells[68] and contain persistently dormant HBCs that do not facilitate OE regeneration despite the apparent need[68,191]. One strategy to ameliorate these diseases includes activating the endogenous HBC population. A complementary or parallel approach involves culturing HBCs harvested from a patient and infusing these activated autologous stem cells back into the nasal cavity. Notably, however, a rodent model of stem cell infusion into the auditory cochlea demonstrated an inverse relationship between cell survival and degree of cellular differentiation[192]. As primary HBCs upregulate the differentiation marker, Hopx, following PMA treatment (Fig. 3.4A-I), this may explain why PMA-activated HBCs infused into the nasal cavity of multiple rodent models also demonstrate low engraftment efficiency within injured OE (Camila Barrios-Camacho, personal communication). Therefore, our work identifying Rac1 as a positive regulator of *in vitro* HBC differentiation offers insight into strategies that could increase HBC engraftment efficiency *in vivo*. Additionally, reversible Rac1 inhibition that temporarily attenuates HBC differentiation (Fig. 3.4E) but does not significantly affect HBC activation (Fig. 3.3B) intimates that enhanced HBC engraftment would be accompanied by those HBCs remaining receptive to critical endogenous specification and differentiation cues within the injured OE.

Multiple considerations suggest that PMA activation of HBCs occurs in a physiologically relevant manner. HBCs activated by OE injury downregulate p63 (Fig. 3.3.1A-E)[56] and upregulate *Hopx*[41], which is recapitulated by PMA-treated primary HBCs *in vitro* (Fig. 3.4B,E). Additionally, HBC-mediated regeneration *in vivo* is positively regulated by NF-κB pathway activation[61], and this is mirrored *in vitro* as HBCs increase nuclear RelA following PMA treatment (Camila Barrios-Camacho, personal communication). Furthermore, Itgb1- and Rac1-mediated signaling pathways promote appropriate proliferation of mammary epithelial stem cells during mammary morphogenesis[193] and keratinocyte stem cells following skin wounding[171,172],

respectively. PMA is known to also activate these pathways[194,195], and the *in vivo* data presented here following injury demonstrating that HBCs mobilize the molecular machinery integral to both Itgb1- and Rac1-mediated signaling (Fig. 3.3.1 and Fig. 3.3.2) suggest that further mechanistic interrogation of these pathways within the OE will bear fruit.

PMA treatment of HBCs, however, did not recapitulate the increase in Ki67 seen during *in vivo* HBC activation[52]. Therefore, the decrease in Ki67 following PMA-induced HBC activation (Fig. 3.4F,G,J) simultaneously exemplifies the inherent limitations with studying HBCs as an isolated population and heightens the potential for environmental cues influencing HBCs following OE injury. Considering that skin wounding can prompt increased fibronectin deposition[196] and skeletal muscle damage is followed by changes in laminin expression[197], the extracellular matrix (ECM) represents a promising candidate. Hematopoietic stem cell proliferation within bone marrow is dependent on interaction with tenascin-C[198], while collagen VI in skeletal muscle acts as an instructive cue for satellite cells to proliferate[199]. In addition to positively regulating proliferation, chondroitin sulfate proteoglycans specify embryonic neural stem cell differentiation towards neuronal rather than glial fates[200]. Moreover, stem cell function dependent on ECM interactions can be mediated by Itgb1[201-203]. Therefore, our demonstration that *in vivo* HBCs spatiotemporally synchronize components of a signaling axis known to occur following Itgb1-ECM interactions[204,205], further intensifies the need for additional inquiry into the role that ECM proteins play in regulating HBC biology following OE injury.

Our novel observation that HBCs redistribute various proteins following OE injury provides a launching point from which myriad additional inquires can be made into mechanisms that govern HBCs during OE regeneration. Importantly, this discovery *in vivo* led to our identification that Rac1 regulates primary HBC differentiation *in vitro* without impinging on their activation. Although harvesting HBCs from and reintroducing

them back into the same patient remains a promising personalized strategy to treat diseases of pathologic OE deterioration, data from current animal models suggest the differentiation process that accompanies the necessary activation of primary HBCs to achieve any engraftment[56,189] is what also accounts for their sparse engraftment. Therefore, the ability to reversibly uncouple HBC differentiation from activation with commercially available small molecules that target Rac1 represents a potential strategy to overcome the pitfalls of therapeutic primary stem cell infusion.

### 3.4 Materials and Methods

#### 3.4.1 Animals

All animals were maintained on *ad libitum* chow and water in a heat and humidity controlled, AALAC-accredited vivarium. All protocols for the use of vertebrate animal were approved by the Committee for the Humane Use of Animals at Tufts University School of Medicine. Wild-type (WT) mice were F2 generation mice from an initial cross of C57BL/6J (Jax Stock #000664) and 129S1/SvlmJ (Jax Stock #002448) mice performed in-house. *In vivo* experiments used sex- and age-matched mice that were 8-12 weeks old when initiated. *In vitro* primary HBCs were harvested from Sprague-Dawley rats (Taconic Biosciences).

#### 3.4.2 Methimazole-induced OE injury

Methimazole (MTZ) (Sigma-Aldrich, Cat. M8506) was dissolved in 1X PBS (Gibco, Cat. 10010-023) at a stock concentration of 5mg/mL. WT mice were injected intra-peritoneally at 10uL of MTZ stock/g of mouse.

#### 3.4.3 Tissue processing

At 24 hours post-MTZ injection, mice were euthanized with an intra-muscular injection of ketamine (37.5mg/kg), xylazine (7.5mg/kg), and acepromazine (1.25mg/kg) triple cocktail. Following trans-cardial perfusion with 20mL PBS (Gibco Cat. 10010-023), mice were trans-cardially fixed with 40mL 1% PLP (1% paraformaldehyde, 0.1M

monobasic and dibasic phosphates, 90mM lysine, and 0.1M meta-sodium periodate). After dissecting away the surrounding cranial structures, the isolated OE was post-fixed in 1% PLP under vacuum for 1.5hrs. Following post-fixation, the OE was briefly rinsed three times in 1X PBS to wash away residual fixative and then incubated in decalcification buffer (0.35M EDTA [Sigma-Aldrich, Cat. ED2SS] and 0.35M NaOH) overnight at 4°C. To cryopreserve the tissue, OE was equilibrated overnight in 30% sucrose (w/v in 1X PBS) at 4°C, embedded and frozen in OCT (Sakura, Cat. 4583), and then stored at -80°C until cryosectioning. To capture the approximate diameter of one cell per section, a Leica cryostat was used to collect three 10um coronal sections per positively-charged glass slides.

### 3.4.4 Immunofluorescence

Specific antibodies and conditions to detect the various antigens can be found in Table 3.1. All primary antibodies were diluted in Normal Donkey Block (NDB) (10% normal donkey serum v/v, 5% non-fat powdered milk w/v, 4% bovine serum albumin [BSA] w/v, and 0.1% Triton X-100 v/v in 1X PBS). Species-specific fluorophore- and biotin-conjugated donkey secondary antibodies (Jackson ImmunoResearch) were diluted in NDB at 1:150 and 1:100, respectively. Streptavidin-conjugated horseradish peroxidase (SA-HRP) was diluted in TNB (0.5% blocking reagent w/v [Akoya Biosciences, Cat. FP1020], 0.15M NaCl, and 0.1M Tris-HCl pH 7.5) at 1:400. All washes performed on day 1 and day 2 were in 1X PBS and 3X PBS, respectively, with those following antibody incubation performed 3x5min. Slides were dried on a slide warmer at ~37C for 45-60min. after application of rubber cement (Elmer's) to isolate each section. Following a 10-15min. wash to remove OCT, sections used to detect antigens requiring antigen retrieval were incubated in antigen retrieval buffer (0.1M sodium citrate, pH 6) and placed in a pre-heated commercial steamer for 10min. After slides were washed for

10min., sections were incubated in 3% $H_2O_2$ diluted in MeOH or 90% MeOH depending on whether antigen detection required tyramide signal amplication (TSA), washed 3x5min., and blocked for 1hr. at room temperature with NDB. Following overnight primary antibody incubation at 4C, sections were incubated in secondary antibodies for 1hr. at room temperature in the dark. If antigen detection required TSA, appropriate sections were blocked for 30min. in TNB prior to incubation in SA-HRP for 1hr. at room temperature in the dark. TSA was achieved by incubating appropriate sections for 15min. in a solution consisting of 98% TSA Buffer (0.1M boric acid pH 8.5, 0.003% $H_2O_2$), 1% 10% BSA w/v in 1X PBS, and 1% FITC-tyramide. Nuclei were counterstained with DAPI. Sections were coverslipped in NPG (0.5% N-propyl gallate in 90% glycerol) mounting media and slides were stored at 4C in the dark until imaging.

| Antibody | Source | Identifier | Dilution | Antigen Retrieval Required | Signal Detection |
|---|---|---|---|---|---|
| Ms p63 | ATCC | Clone 4A4 | 1:100 | Yes | Secondary fluorophore |
| Ms Ezrin | Developmental Studies Hybridoma Bank | CPTC-Ezrin-1 | 1:25 | No | Secondary fluorophore |
| Rb Laminin | Novus Biologicals | NB300-144 | 1:100 | No | Secondary fluorophore |
| Gt Itgb1 | R&D Systems | AF2405 | 1:13 | No | Secondary fluorophore |
| Rat Itgb4 | R&D Systems | MAB4054 | 1:20 | No | Secondary fluorophore |
| Ck CK5 | BioLegend | Clone Poly9059 | 1:200 | No | Secondary fluorophore |
| Rb Rac1 | Proteintech | 24072-1-AP | 1:200 | Yes | TSA |
| Rb pFAKY925 | Cell Signaling Technology | 3284 | 1:100 | Yes | TSA |
| Rb pcJun | Cell Signaling Technology | 3270 | 1:40 | Yes | TSA |

**Table 3.1: Antibodies used and associated antigen labeling conditions**

### 3.4.5 Primary HBC culture

Isolation, maintenance, and passaging of primary HBCs have been previously described in detail[189]. Passage 10 HBCs were used for experimentation. HBCs cultured for immediate western blot analyses were grown on 6-well plates coated with poly-D-lysine/laminin (Corning, Cat. 354595). HBCs cultured for immediate immunocytochemical analyses were grown on 8-well culture slides coated with poly-D-lysine/laminin (Corning, Cat. 354688). PMA (Sellekchem, Cat. S7791) and EHT1864 (SellekChem, Cat. S7482) were dissolved in DMSO. HBCs determined to undergo Rac1 inhibition during the 12hr. treatment paradigm were pre-incubated in EHT1864 for 1hr, and DMSO concentration for all conditions was identical at all times.

### 3.4.6 Western blot of primary HBCs

Primary HBCs were lysed by applying 200uL Lysis Buffer (RIPA buffer [Thermo Scientific, Cat. 89901] supplemented with a protease and phosphatase inhibitor cocktail [Thermo Scientific, Cat. 78442]) per well and freezing the 6-well plate at -80C overnight. All subsequent steps were performed on ice. Immediately after thawing, an additional 100uL Lysis Buffer was applied to each well and mechanical cell lysis was performed with a cell scraper. The entire volume of lysate from each well was transferred to a pre-chilled 2mL microcentrifuge tube, and debris pelleted via centrifugation at maximum rpm for 10min. at 4C. Supernatant from each experimental condition was transferred to a new pre-chilled 2mL microcentrifuge tube and total protein abundance was determined by BCA protein assay per manufacturer's protocol (Thermo Scientific, Cat. 23227). Working protein stocks were prepared by diluting supernatant with 4X LDS Sample Buffer (Invitrogen, Cat. B0007), 10X Sample Reducing Agent (Invitrogen, Cat. B0009), and Lysis Buffer. These stocks were placed in a heating block set at 70C for 10min and then stored at -80C.

Protein from working stocks were loaded at ~5µg in 4-12% Bis-Tris gels (Invitrogen, Cat. NW04120BOX) and bracketed by a protein ladder standard (Proteintech, Cat. PL00002). Gels were run per manufacturer's protocol (Invitrogen, Cat. A25977) in MES SDS running buffer (Invitrogen, Cat. B0002). Protein was transferred to a 0.2um PVDF membrane (Invitrogen, Cat. LC2002) at 20V per manufacturer's protocol (Invitrogen, Cat. BT00061).

Following protein transfer, membranes were rinsed in 1X TBST (Tris-buffered saline with 1% Tween 20) and blocked for 1hr at room temperature in Blocking Buffer (5% BSA w/v in 1X TBST). Primary antibodies against ΔNp63 (BioLegend, Cat. 619002; 1:500), cJun (Cell Signaling Technology, Cat. 9165; 1:1000), pcJun (Cell Signaling Technology, Cat. 3270; 1:1000), JNK (Cell Signaling Technology, Cat. 9252; 1:1000), pJNK (Cell Signaling Technology, Cat. 4668; 1:1000), Rac1 (Proteintech, Cat. 66122-I-Ig; 1:2000), and GAPDH (Cell Signaling Technology, Cat. 97166; 1:1000) were diluted in Block Buffer and incubated with membranes overnight at 4C. The following day, membranes were washed 6x7min in 1X TBST, incubated in the appropriate HRP-conjugated donkey secondary antibodies (Jackson ImmunoResearch) diluted 1:5000 in Blocking Buffer, and washed 6x5min in 1X TBST. Proteins were visualized in a gel dock system (Bio-Rad, Universal Hood II) after membranes were incubated in SuperSignal West Pico Plus Chemiluminescent substrate (Thermo Scientific, Cat. 34577). Bio-Rad Image Lab software was used to export TIFF files that were subsequently imported into ImageJ to perform densitometric analyses.

**3.4.7 Immunocytochemistry**

Primary HBCs were fixed with 10% buffered formalin (Fisher, Cat. SF100) for 15min. at room temperature, washed 3x5min in 1X PBS, then stored at 4C in fresh 1X PBS until further processing. To note, all washes prior to primary antibody incubation and during day 2 were in 1X PBS and 3X PBS, respectively, with those following

antibody incubation performed 3x5min. HBCs were subsequently permeabilized on ice with ice-cold 100% MeOH for 10min. and washed 3x5min. After 1hr. of blocking in NDB at room temperature, HBCs were incubated overnight at 4C in antibodies against Hopx (1:150; Proteintech, Cat. 11419-1-AP), Ki67 (1:75; BD Biosciences, Cat. 556003), and CK5 (1:400; BioLegend, Clone Poly9059) in NDB diluent. The next day, HBCs were incubated in the dark with species-specific fluorophore-conjugated donkey secondary antibodies (Jackson ImmunoResearch) at 1:250 in NDB diluent. Nuclei were counterstained with DAPI and chamber slide walls removed per manufacturer's protocol. Slides were coverslipped with NPG mounting media and stored at 4C in the dark until imaging.

### 3.4.8 Imaging

All sections and cells were imaged on a Zeiss LSM800 confocal microscope. Zeiss Zen 2.6 software was used to set imaging parameters to eliminate spectral overlap between channels, which included capturing fluorescence in multi-track mode, adjusting the variable secondary dichroics, and enabling appropriate emission filters. For proteins quantified by relative fluorescence intensity, all excitation and emission capture settings were identical between control and experimental conditions. Imaging OE included capturing multiple z-planes stepped at 2um intervals to sample from a minimum of approximately 5 cellular cross-sections. First and last z-planes were established when the maximum fluorescence intensity of the channel to be quantified fell within lowest quartile of a 16bit display range. Because primary HBCs can pile on top of each another in culture, imaging HBC islands *in vitro* involved capturing the z-plane in which $CK5^{+}$ HBCs appeared most confluent.

### 3.4.9 Image analyses

ImageJ was used to process all uncompressed, 16bit tiff files obtained from confocal imaging. Z-planes were sum projected to maximize bit depth of captured

fluorescence. The ImageJ Rolling ball background subtraction function was applied to every channel. CellProfiler (Version 3.1.9) was used to quantify total fluorescence intensity. Images of channels in which captured fluorescence was not intended for quantification were converted to 16bit so that CellProfiler could process those images, demarcate relevant cellular landmarks, and quantify the area that those landmarks occupied to calculate total fluorescence densities. Templates for each CellProfiler pipeline used have been deposited on GitHub.

### 3.4.10 Statistical analyses and data presentation

All statistical analyses were performed within GraphPad Prism Version 8. Only brightness and contrast were adjusted for each representative image within ImageJ and Adobe Photoshop CS6, and these parameters were applied globally throughout the image. All graphs were generated using GraphPad Prism Version 8. All figures were constructed in Adobe Photoshop CS6.

## 3.5 Contributions

I wrote this entire chapter. Immunofluorescence labeling of pFAKY925 was performed by Benjamin H. Bromberg. I performed all other experimentation. I performed all imaging, data analysis, and figure construction.

## Chapter 4: Discussion

### 4.1 Notch1

During OE regeneration following severe tissue injury, Notch1 enables HBCs to contribute to OE regeneration by appropriately promoting this resident stem cell population's ability to proliferate and differentiate (Fig. 4.1). This contradicts the receptor's function during OE homeostasis when Notch1 specifies HBC quiescence[57]. The functional inversion could be explained by chromatin remodeling, a biological process observed during pluripotency induction[206] and embryonic stem cell differentiation[207,208]. Chromatin remodeling has also been demonstrated during differentiation of adult stem cells, namely satellite cells[209,210] resident within skeletal muscle in which Notch1 demonstrates a similar functional inversion[118-120]. Moreover, satellite cell chromatin remodeling is critical to proper skeletal muscle regeneration[211]. This functional finding mirrors that previously described in the regenerating OE, wherein inhibition of the epigenetic regulator, Ezh2, perturbs chromatin methylation, cellular multipotency, and progenitor differentiation[44]. HBCs during early OE regeneration, therefore, may warrant interrogation via methods such as methylation sequencing and ATAC-seq that, in combination, can provide deeper insight into their chromatin dynamics.

Although spontaneous HBC differentiation following HBC-specific *Notch1* cKO within uninjured OE can be explained molecularly by decreased *p63* transcription, p63 protein expression was, interestingly, never assessed[57]. Therefore, no significant change in p63 expression by HBCs at 24hpi despite *Notch1* cKO may not be as counterintuitive as it seems. Indeed, precedence is found via HBC-expressed Dll1, which demonstrates an inverse relationship between mRNA[57] and protein abundance soon after OE injury. Alternatively, p63 expression during acute regeneration may become independent of

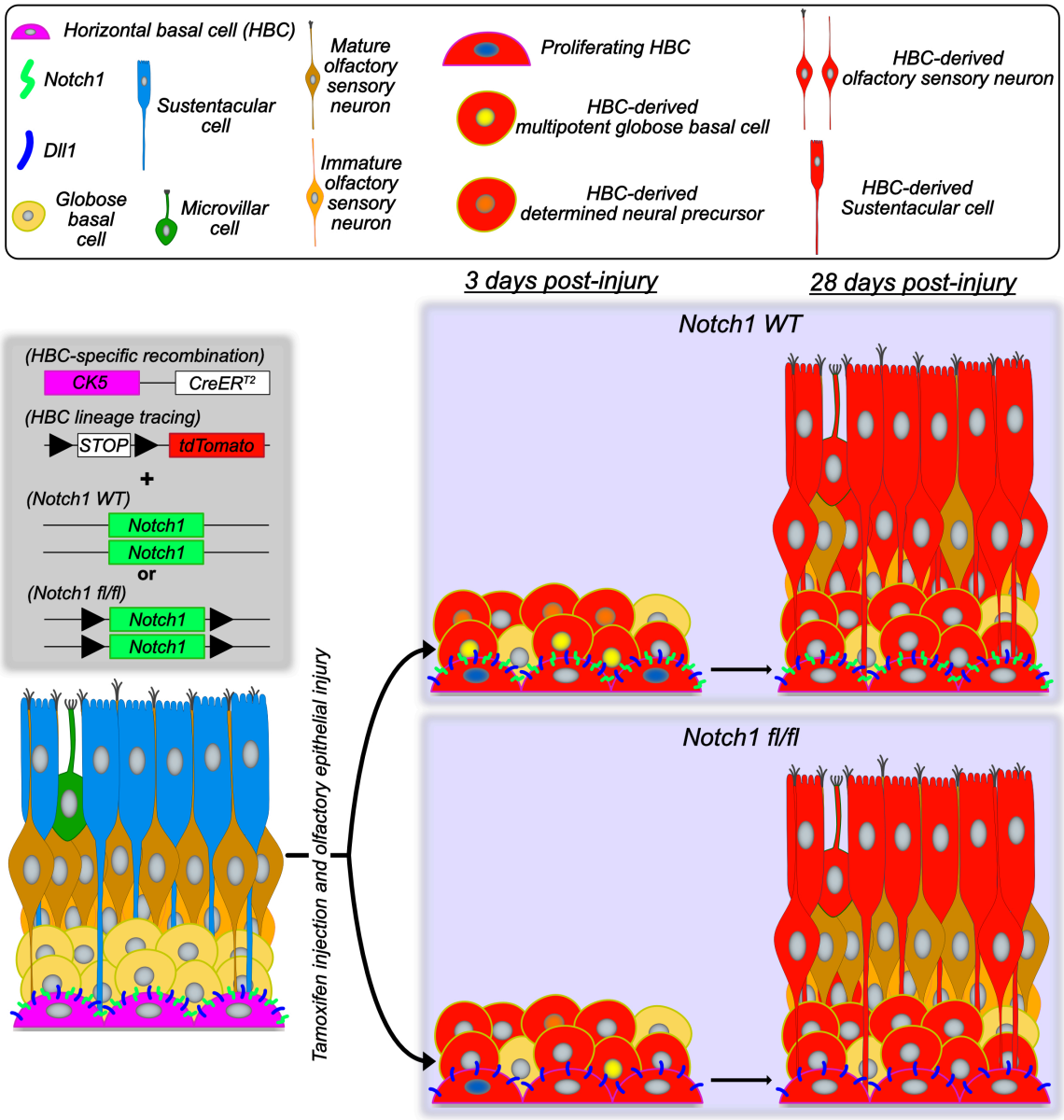


**Fig. 4.1: Notch1 specifies HBC proliferation and neuronal differentiation during OE regeneration.** Cartoon depicting the working model that following HBC-specific *Notch1* cKO, more HBCs are quiescent during OE regeneration. As a consequence, fewer HBCs differentiate into multipotent and neuronally-determined GBCs. In turn, this leads to fewer HBC-derived OSNs in morphologically regenerated OE.

Notch1-transduced signaling, especially considering the functional inversion mediated by the receptor during OE regeneration and possibility of HBC epigenomic alterations. Profiling the p63 promoter region for protein interaction partners at 24hpi may reveal

alternative upstream signaling cascades critical for differential p63 regulation depending on OE integrity.

Alternatively, HBC-expressed Notch1 and its functional inversion following OE injury could potentially be an artifact in that the receptor consistently functions to promote HBC activation regardless of tissue status. This possibility would reconcile with the receptor's role in basal stem cells of the interfollicular epidermis where Notch1 promotes p63 downregulation and stem cell differentiation[212]. Moreover, this scenario also intimates that the Notch ligands closely approximated to HBCs function to inhibit Notch pathway activity. Indeed, Jagged1 can negatively regulate Notch signaling, and its potential inhibitory role correlates well with the interpretation that HBC activation following Sus cell ablation is secondary to destruction of these Jagged1-expressing cells[57]. Additionally, Dll1 expression dynamics exhibited by HBCs, namely downregulation at 24hpi when HBCs are activating and enrichment at 3dpi when surrounded by non-HBCs, suggest that Dll1 also inhibits Notch pathway activation to specify HBC quiescence. Determining whether these ligands do indeed inhibit Notch signaling could include assessing HBC expression of Hes1 in the face of simultaneous HBC-specific Dll1 and Sus cell-specific Jagged1 recombination, and whether this functionally results in enhanced spontaneous HBC differentiation. If validated, the role of non-canonical or ligand-independent Notch signaling pathway activity could initially be investigated via conditional expression of Notch1 resistant to proteolytic cleavage or HBC-specific gamma-secretase defect.

In addition to Notch1 playing a consistent but functionally marginalized role due to inhibitory ligand expression, apparent Notch1 functional inversion may also result if the receptor has no direct impact on HBC function within homeostatic OE. This could be possible when considering that prior to injury, HBC-specific cKO of *Rbpj*, a critical intermediary during Notch pathway transduction[77,213], yields no observable HBC

differentiation[57]. Moreover, HBC-specific *Notch1* cKO results in only sparse spontaneous HBC differentiation even at 3 months following initial genetic recombination[57]. In contrast, Sus cell ablation more rapidly results in HBC differentiation[57], thereby raising the potential that rather than specifying HBC status directly, Notch1 may indirectly influence HBCs by regulating Sus cell biology. This hypothesis comes into clearer focus in light of the fact that retinoic acid expressed by Sus cells helps maintain HBC quiescence[58]. Additionally, retinoic acid production has been shown to be sensitive to Notch signaling pathway activity[214]. In concert with the potential for increased availability of HBC-expressed Dll1 to interact with Sus cell-expressed Notch2 due to *Notch1* recombination, these data prompt investigation into a HBC-Sus cell feedback circuit. Initial interrogation could include quantifying relative magnitude of RALDH2 in Sus cells following *Notch1* cKO in HBCs.

Given how Dll1 is dynamically expressed by HBCs – downregulated at 24hpi concurrent with HBC activation and enriched at 3dpi as HBCs reside in a regenerating OE also composed of non-HBCs – this ligand may instruct HBC quiescence. Because HBCs express both Notch1 and Dll1, however, whether these stem cells engage in both cis- and trans-interactions remains unknown. As such, the functional impact of cis and trans Notch1-Dll1 interactions on HBC biology is murkier still. Therefore, it would be worthwhile to discover the directionality and effect of Dll1-Notch1 interactions. To begin interrogating these questions, sparsely culturing WT HBCs could establish the effect of cis-interactions on Notch signaling activity and HBC molecular status. Additionally, growing *Notch1* and *Dll1* cKO HBCs together and focusing on adjacent cells expressing unique fluorescent tags associated with each genotype could help establish the influence of trans-interactions on pathway activity and HBC response. In turn, these findings *in vitro* would provide insight into how *in vivo* HBCs might respond following HBC-specific *Dll1* cKO. By achieving sparse and mosaic recombination within uninjured

and injured OE, this would ideally place a single WT HBC in between two recombined HBCs. In such a case, the WT and recombined HBCs may reveal whether Dll1-Notch1 interactions in cis and trans, respectively, promote activity that recapitulates those observed *in vitro*.

If Dll1 does indeed interact with Notch1 in both cis and trans, with each producing functionally divergent responses, another question arises of how does Dll1 achieve its net effect within an HBC population enriched for both ligand and receptor. Depending on the assays investigating which interaction, cis or trans, promotes which HBC activity, quiescence or activation, HBCs may upregulate Dll1 such that interactions with Notch1 that specify quiescence outnumber those promoting activation. As this thesis demonstrates that overlying non-HBCs still express Dll1, it may be the case that Dll1-Notch1 trans-interactions specify HBC quiescence. The sparse recombination strategy mentioned previously along with cKO of *Dll1* in non-HBCs during acute OE regeneration could more definitively identify the functional import of each interaction.

The differential impact of Dll1-Notch1 interactions if the functional outcome depends on the ligand's origin can also be modified by Fringe proteins. Given that Radical fringe increases receptor interaction with both Jagged1 and Dll1, HBCs may enrich for this glycosyltransferase within homeostatic OE to ensure their quiescence. At 24hpi, HBCs may downregulate Radical fringe to minimize quiescence cues from downregulated, but still present, Dll1. As regeneration proceeds, HBCs could again upregulate Radical fringe to re-establish cues that instruct HBCs to re-quiesce. However, as this thesis demonstrated, HBC-expressed Notch1 promotes HBC proliferation and differentiation, thereby implying that Dll1-Notch1 interactions specifying HBC quiescence are not uniformly distributed, but rather spatially regulated. Consequently, any analysis to determine the role of the various mammalian Fringe proteins during OE regeneration should pay close attention to their spatiotemporal distribution.

### 4.2 Rac1

This thesis demonstrates that *in vitro* primary HBCs depend, in part, on Rac1-mediated signaling to differentiate (Fig. 4.2). Whether Rac1 plays a similar role *in vivo* remains open to interrogation. Regardless, however, increased and decreased Ki67 expression of HBCs following activation *in vivo* and *in vitro*, respectively, indicate that neither Rac1 activation nor p63 downregulation cell autonomously promote HBC proliferation. Instead, these data derived from differing environments suggest that this process is driven, in part, by non-cell autonomous factors. Indeed, acute exposure to inflammatory cytokines is a critical factor that supports HBC proliferation and HBC-mediated OE regeneration. A high-throughput proteomics screen of the OE at 24hpi may facilitate identification of additional cytokines central to HBC function following OE injury. Prospective hits may include bFGF, EGF, and TGFa as they have been previously implicated in enhancing OSN regeneration[215].

The discrepancy in pcJun expression between control HBCs *in vivo* and *in vitro*, highlighted by the latter's decrease in fold-change relative to activated HBCs (Fig. 3.2O and Fig. 3.3D), opens another potential avenue of inquiry. Just recently, it was discovered that Yap positively regulates HBC proliferation and proper OE regeneration following injury[64]. Additionally, Yap is sensitive to cellular density[216,217] and can activate the JNK signaling pathway[218]. In sum, these findings suggest that increased pcJun abundance in cultured HBCs at baseline may result from HBC sensitivity to cellular density. Moreover, this introduces the possibility that physical displacement of OE alone after tissue injury initiates HBC proliferation and prepares these stem cells to facilitate regeneration. Alternatively, given that Itgb1-dependent Rac1 activity has been shown to regulate Yap[219], HBC expression of Yap triggered by a sudden decrease in cellular density may also reside downstream of HBC Rac1 activation.

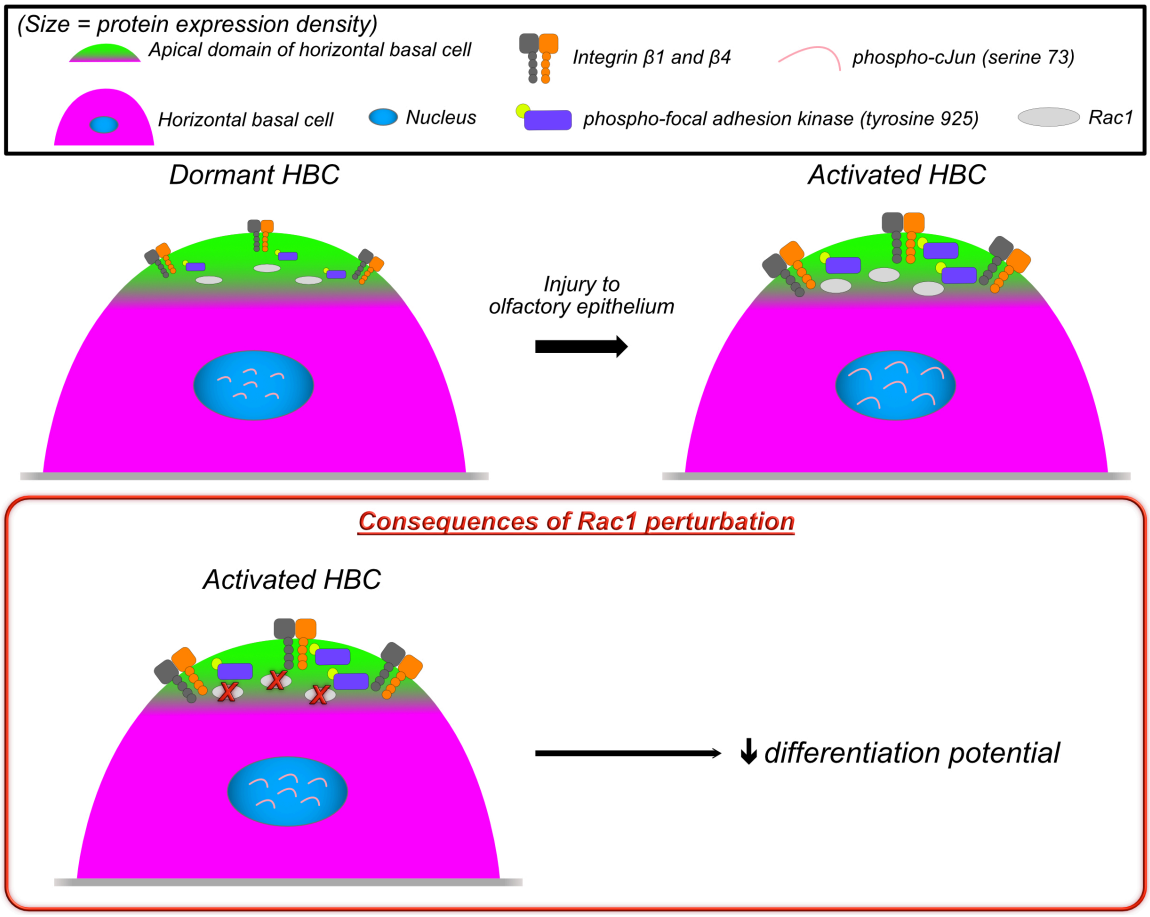


**Fig. 4.2: Following activation, Rac1 promotes primary HBC differentiation *in vitro*.** Following OE injury, HBCs upregulate multiple proteins that can activate Rac1-mediated signaling. These data informed *in vitro* investigations demonstrating that activated HBCs are molecularly and functionally dependent on Rac1.

Spatial reorganization of integrin expression density following OE injury may imply that dynamic ECM deposition occurs during tissue regeneration. Following damage to other tissues, including skin and skeletal muscle, the wounded environment alters composition of fibronectin[196] and laminin[197], respectively. Additionally, ECM proteins such tenascin-C and collagen VI instruct hematopoietic stem cells and skeletal muscle satellite cells, respectively, to proliferate[198,199], while chondroitin sulfate proteoglycans specify embryonic neural stem cells to preferentially differentiate into neurons rather than glia[200]. Given these precedents, it would be worthwhile to survey the

OE's ECM landscape following injury. Expression and distribution of collagen could be assessed via second harmonic imaging[220], with subsequent antibody probing to identify the subtypes if imaging yields positive results. Additional antibody probing for various other ECM proteins would provide a richer perspective, however, the fullest view could be achieved by an unbiased proteomics screen.

In addition to potentially identifying most ECM proteins relevant to the OE's post-injury environment, a proteomics screen may also highlight wound-associated cytokines, including EGF and TGFα. These two cytokines in particular are found in wounds of burn patients and animal models[221-224]. EGF receptor (EGFR), which binds with both EGF and TGFα, is also localized to undifferentiated keratinocytes in burn wounds[225], and indeed, wound repair is attenuated with EGFR KO[226]. Within the OE, HBCs express EGFR[3,227] and are responsive to EGF and TGFα[228]. Interestingly, EGFR within the OE's basal compartment decreases with age[229], which correlates with the tissue's decreasing regenerative capacity. Moreover, reduced EGFR signaling has been implicated in impaired olfactory neurogenesis[230]. As EGFR is also able to activate Rac1 during signal transduction[231-233], HBC-specific *EGFR* cKO may significantly impair OE regeneration following injury in part by dysregulating Rac1 apical localization.

Given that Rac1 can promote actin reorganization and filopodia formation[127,148,234,235], this small GTPase may also support HBC-mediated regeneration by facilitating detection of environmental cytokines like EGF and TGFα. As Rac1 has been implicated in lamellipodia formation as well[236,237], HBCs may very well adopt a migratory phenotype following OE injury. This possibility is supported by observations that HBCs may decrease contacts with the basal lamina based on their morphological changes following OE injury. Following development of techniques that enable OE live imaging, it would be intriguing to see if HBCs extend protrusions into their environment and whether *Rac1* cKO abrogates these membrane dynamics.

### 4.3 Crosstalk between Notch signaling and Rac1

Interestingly, HBC-mediated OE regeneration may also rely on crosstalk between Rac1 and Notch signaling. Notch1-mediated signaling positively regulates Rac1 activity in cells derived from human hepatic cholangiocarcinoma[238]. This molecular mechanism supports these cells' ability to migrate and adopt of morphology reminiscent of cells undergoing epithelial-to-mesenchymal transition (EMT). While comparing a cancer cell line to HBCs can be tenuous, both cell types demonstrate sensitivity Notch1 and Rac1 perturbations. Moreover, following p63 downregulation, HBCs *in vivo* and *in vitro* respectively exhibit morphological and molecular hallmarks of EMT[56] (Louie, unpublished data). To determine whether Notch1 does in fact function upstream of Rac1 to specify HBC fate, active Rac1 abundance within *Notch1* cKO HBCs isolated at 24hpi would be revealing. A decrease, however, would not clarify whether Notch1 transduces signals that run in parallel with or converge solely on Rac1. To elucidate this, one possibility includes quantifying HBC fates following HBC-specific *Rac1* cKO and comparing these values to those after HBC-specific *Notch1* cKO. Similar results would suggest that Rac1 resides at a centralized signaling junction while no change or an intermediary phenotype could indicate that Notch1 mediates additional parallel or compensatory signals.

Inversely, Rac1 has been implicated to lie upstream of Notch signaling positively regulates transcription of pathway-dependent genes[133]. To determine whether this scenario is relevant to HBCs, the converse cKO experiment proposed above could be performed to assess Hes1 downregulation follows HBC-specific *Rac1* recombination. If Rac1 indeed mediates Notch pathway activity in the OE, one potential mechanism may relate to Rac1's ability to remodel actin filament organization and the changing biophysical forces that HBCs experience as a result. As applying a mechanical load onto murine tibial osteocytes and subjecting bone marrow-derived mesenchymal stromal cells

to cyclic stretching *in vitro* results in increased Notch signaling pathway activity[239], it would be interesting to observe whether HBCs engage in a similar mechanotransduction.

Interestingly, Rac1 can also negatively regulate Notch signaling as seen during thymus development[240] and T cell leukemia pathogenesis[241]. This antagonistic relationship may result from Rac1 activity attenuating presenilin-1, a catalytic component of gamma-secretase[242], and the enzymatic subunit's affinity for Notch1. While increased Rac1 activation correlating with decreased Notch pathway activity runs counter to this thesis' results within acutely regenerating OE, this axis furthers the idea that Notch1 may be engaged in non-canonical signal transduction in uninjured OE when Rac1 is relatively inactive based on its decreased apical localization in HBCs. Moreover, this hypothesis continues to intimate that the Notch ligands, Jagged1 and Dll1, serve to abate pathway activity and specify HBC quiescence. These possibilities could be interrogated by constitutively expressing active Rac1 during OE homeostasis to see if HBC differentiation increases. In addition, concurrent HBC-specific *Dll1* cKO and Sus cell-specific *Jagged1* cKO could examine the proposed inhibitory role played by Notch ligands to abrogate Rac1-mediated, non-canonical Notch pathway activity.

**4.4 Contributions**

I wrote this entire chapter.

## Chapter 5: Bibliography


1. Naessen, R. The identification and topographical localisation of the olfactory epithelium in man and other mammals. *Acta Otolaryngol.* **70,** 51–57 (1970).
2. Graziadei, P. P. & Graziadei, G. A. Neurogenesis and neuron regeneration in the olfactory system of mammals. I. Morphological aspects of differentiation and structural organization of the olfactory sensory neurons. *J. Neurocytol.* **8,** 1–18 (1979).
3. Holbrook, E. H., Szumowski, K. E. & Schwob, J. E. An immunochemical, ultrastructural, and developmental characterization of the horizontal basal cells of rat olfactory epithelium. *J. Comp. Neurol.* **363,** 129–146 (1995).
4. Breipohl, W., Laugwitz, H. J. & Bornfeld, N. Topological relations between the dendrites of olfactory sensory cells and sustentacular cells in different vertebrates. An ultrastructural study. *J. Anat.* **117,** 89–94 (1974).
5. Taveggia, C. *et al.* Neuregulin-1 type III determines the ensheathment fate of axons. *Neuron* **47,** 681–694 (2005).
6. Simons, M. & Trajkovic, K. Neuron-glia communication in the control of oligodendrocyte function and myelin biogenesis. *J. Cell. Sci.* **119,** 4381–4389 (2006).
7. Dahl, A. R., Hadley, W. M., Hahn, F. F., Benson, J. M. & McClellan, R. O. Cytochrome P-450-dependent monooxygenases in olfactory epithelium of dogs: possible role in tumorigenicity. *Science* **216,** 57–59 (1982).
8. Suzuki, Y., Takeda, M. & Farbman, A. I. Supporting cells as phagocytes in the olfactory epithelium after bulbectomy. *J. Comp. Neurol.* **376,** 509–517 (1996).
9. Rafols, J. A. & Getchell, T. V. Morphological relations between the receptor neurons, sustentacular cells and Schwann cells in the olfactory mucosa of the salamander. *Anat Rec* **206,** 87–101 (1983).
10. Carr, V. M., Farbman, A. I., Colletti, L. M. & Morgan, J. I. Identification of a new non-neuronal cell type in rat olfactory epithelium. *Neuroscience* **45,** 433–449 (1991).
11. Lin, W., Ezekwe, E. A. D., Zhao, Z., Liman, E. R. & Restrepo, D. TRPM5-expressing microvillous cells in the main olfactory epithelium. *BMC Neurosci* **9,** 114–13 (2008).
12. Asan, E. & Drenckhahn, D. Immunocytochemical characterization of two types of microvillar cells in rodent olfactory epithelium. *Histochem. Cell Biol.* **123,** 157–168 (2005).
13. Rowley, J. C., Moran, D. T. & Jafek, B. W. Peroxidase backfills suggest the mammalian olfactory epithelium contains a second morphologically distinct class of bipolar sensory neuron: the microvillar cell. *Brain Res* **502,** 387–400 (1989).
14. Pfister, S. *et al.* Characterization and turnover of CD73/IP(3)R3-positive microvillar cells in the adult mouse olfactory epithelium. *Chem. Senses* **37,** 859–868 (2012).
15. Pérez, C. A. *et al.* A transient receptor potential channel expressed in taste receptor cells. *Nat. Neurosci.* **5,** 1169–1176 (2002).
16. Genovese, F. & Tizzano, M. Microvillous cells in the olfactory epithelium express elements of the solitary chemosensory cell transduction signaling cascade. *PLoS ONE* **13,** e0202754 (2018).
17. Schwob, J. E. Neural regeneration and the peripheral olfactory system. *Anat Rec* **269,** 33–49 (2002).
18. McClintock, T. S., Khan, N., Xie, C. & Martens, J. R. Maturation of the Olfactory Sensory Neuron and Its Cilia. *Chem. Senses* **45,** 805–822 (2020).

19. Mombaerts, P. *et al.* Visualizing an olfactory sensory map. *Cell* **87,** 675–686 (1996).
20. Berkowicz, D. A., Trombley, P. Q. & Shepherd, G. M. Evidence for glutamate as the olfactory receptor cell neurotransmitter. *J Neurophysiol* **71,** 2557–2561 (1994).
21. Tatti, R. *et al.* A population of glomerular glutamatergic neurons controls sensory information transfer in the mouse olfactory bulb. *Nat Commun* **5,** 3791–16 (2014).
22. Margolis, F. L. A brain protein unique to the olfactory bulb. *PNAS* **69,** 1221–1224 (1972).
23. Lee, A. C., He, J. & Ma, M. Olfactory marker protein is critical for functional maturation of olfactory sensory neurons and development of mother preference. *J. Neurosci.* **31,** 2974–2982 (2011).
24. Buck, L. & Axel, R. A novel multigene family may encode odorant receptors: a molecular basis for odor recognition. *Cell* **65,** 175–187 (1991).
25. Mombaerts, P. Axonal wiring in the mouse olfactory system. *Annu Rev Cell Dev Biol* **22,** 713–737 (2006).
26. Lyons, D. B. *et al.* An epigenetic trap stabilizes singular olfactory receptor expression. *Cell* **154,** 325–336 (2013).
27. Zhang, G., Titlow, W. B., Biecker, S. M., Stromberg, A. J. & McClintock, T. S. Lhx2 Determines Odorant Receptor Expression Frequency in Mature Olfactory Sensory Neurons. *eNeuro* **3,** (2016).
28. McIntyre, J. C., Titlow, W. B. & McClintock, T. S. Axon growth and guidance genes identify nascent, immature, and mature olfactory sensory neurons. *J Neurosci Res* **88,** 3243–3256 (2010).
29. Rodriguez-Gil, D. J. *et al.* Odorant receptors regulate the final glomerular coalescence of olfactory sensory neuron axons. *Proc. Natl. Acad. Sci. U.S.A.* **112,** 5821–5826 (2015).
30. Liberia, T., Martin-Lopez, E., Meller, S. J. & Greer, C. A. Sequential Maturation of Olfactory Sensory Neurons in the Mature Olfactory Epithelium. *eNeuro* **6,** (2019).
31. Nickell, M. D., Breheny, P., Stromberg, A. J. & McClintock, T. S. Genomics of mature and immature olfactory sensory neurons. *Journal of …* **520,** 2608–2629 (2012).
32. Marcucci, F., Maier-Balough, E., Zou, D.-J. & Firestein, S. Exuberant growth and synapse formation of olfactory sensory neuron axonal arborizations. *Journal of …* **519,** 3713–3726 (2011).
33. Mombaerts, P. Odorant receptor gene choice in olfactory sensory neurons: the one receptor-one neuron hypothesis revisited. *Curr. Opin. Neurobiol.* **14,** 31–36 (2004).
34. Sarafoleanu, C., Mella, C., Georgescu, M. & Perederco, C. The importance of the olfactory sense in the human behavior and evolution. *J Med Life* **2,** 196–198 (2009).
35. Moulton, D. G. Dynamics of cell populations in the olfactory epithelium. *Annals of the New York Academy of Sciences* **237,** 52–61 (1974).
36. Farbman, A. I. Olfactory neurogenesis: genetic or environmental controls? *Trends Neurosci* **13,** 362–365 (1990).
37. Cowan, C. M. & Roskams, A. J. Apoptosis in the mature and developing olfactory neuroepithelium. *Microsc. Res. Tech.* **58,** 204–215 (2002).
38. Caggiano, M., Kauer, J. S. & Hunter, D. D. Globose basal cells are neuronal progenitors in the olfactory epithelium: a lineage analysis using a replication-

incompetent retrovirus. *Neuron* **13,** 339–352 (1994).
39. Chen, M. *et al.* Wnt-responsive Lgr5$^{+}$ globose basal cells function as multipotent olfactory epithelium progenitor cells. *J. Neurosci.* **34,** 8268–8276 (2014).
40. Li, Z. *et al.* Sox2 regulates globose basal cell regeneration in the olfactory epithelium. *Int Forum Allergy Rhinol* **12,** 286–292 (2022).
41. Gadye, L. *et al.* Injury Activates Transient Olfactory Stem Cell States with Diverse Lineage Capacities. *Cell Stem Cell* **21,** 775–790.e9 (2017).
42. Packard, A., Giel-Moloney, M., Leiter, A. & Schwob, J. E. Progenitor cell capacity of NeuroD1-expressing globose basal cells in the mouse olfactory epithelium. *Journal of …* **519,** 3580–3596 (2011).
43. Packard, A. I., Lin, B. & Schwob, J. E. Sox2 and Pax6 Play Counteracting Roles in Regulating Neurogenesis within the Murine Olfactory Epithelium. *PLoS ONE* **11,** e0155167 (2016).
44. Lin, B. *et al.* Injury Induces Endogenous Reprogramming and Dedifferentiation of Neuronal Progenitors to Multipotency. *Cell Stem Cell* **21,** 761–774.e5 (2017).
45. Cau, E., Gradwohl, G., Fode, C. & Guillemot, F. Mash1 activates a cascade of bHLH regulators in olfactory neuron progenitors. *Development* **124,** 1611–1621 (1997).
46. Farah, M. H. *et al.* Generation of neurons by transient expression of neural bHLH proteins in mammalian cells. *Development* **127,** 693–702 (2000).
47. Castro, D. S. *et al.* A novel function of the proneural factor Ascl1 in progenitor proliferation identified by genome-wide characterization of its targets. *Genes Dev.* **25,** 930–945 (2011).
48. Krolewski, R. C., Packard, A., Jang, W., Wildner, H. & Schwob, J. E. Ascl1 (Mash1) knockout perturbs differentiation of nonneuronal cells in olfactory epithelium. *PLoS ONE* **7,** e51737 (2012).
49. Boutin, C. *et al.* NeuroD1 induces terminal neuronal differentiation in olfactory neurogenesis. *Proc. Natl. Acad. Sci. U.S.A.* **107,** 1201–1206 (2010).
50. Huard, J. M. & Schwob, J. E. Cell cycle of globose basal cells in rat olfactory epithelium. *Dev. Dyn.* **203,** 17–26 (1995).
51. Leung, C. T., Coulombe, P. A. & Reed, R. R. Contribution of olfactory neural stem cells to tissue maintenance and regeneration. *Nat. Neurosci.* **10,** 720–726 (2007).
52. Fletcher, R. B. *et al.* p63 regulates olfactory stem cell self-renewal and differentiation. *Neuron* **72,** 748–759 (2011).
53. Upadhyay, U. D. & Holbrook, E. H. Olfactory loss as a result of toxic exposure. *Otolaryngol Clin North Am* **37,** 1185–1207 (2004).
54. Ajmani, G. S., Suh, H. H. & Pinto, J. M. Effects of Ambient Air Pollution Exposure on Olfaction: A Review. *Environ Health Perspect* **124,** 1683–1693 (2016).
55. Zhang, Z. *et al.* Exposure to Particulate Matter Air Pollution and Anosmia. *JAMA Netw Open* **4,** e2111606–e2111606 (2021).
56. Schnittke, N. *et al.* Transcription factor p63 controls the reserve status but not the stemness of horizontal basal cells in the olfactory epithelium. *Proc. Natl. Acad. Sci. U.S.A.* **112,** E5068–77 (2015).
57. Herrick, D. B., Lin, B., Peterson, J., Schnittke, N. & Schwob, J. E. Notch1 maintains dormancy of olfactory horizontal basal cells, a reserve neural stem cell. *Proc. Natl. Acad. Sci. U.S.A.* **114,** E5589–E5598 (2017).
58. Håglin, S., Berghard, A. & Bohm, S. Increased Retinoic Acid Catabolism in Olfactory Sensory Neurons Activates Dormant Tissue-Specific Stem Cells and Accelerates Age-Related Metaplasia. *J. Neurosci.* **40,** 4116–4129 (2020).

59. Genter, M. B., Deamer, N. J., Blake, B. L., Wesley, D. S. & Levi, P. E. Olfactory toxicity of methimazole: dose-response and structure-activity studies and characterization of flavin-containing monooxygenase activity in the Long-Evans rat olfactory mucosa. *Toxicol Pathol* **23,** 477–486 (1995).
60. Bryche, B. *et al.* Massive transient damage of the olfactory epithelium associated with infection of sustentacular cells by SARS-CoV-2 in golden Syrian hamsters. *Brain Behav Immun* **89,** 579–586 (2020).
61. Chen, M., Reed, R. R. & Lane, A. P. Acute inflammation regulates neuroregeneration through the NF-κB pathway in olfactory epithelium. *Proc. Natl. Acad. Sci. U.S.A.* **114,** 8089–8094 (2017).
62. Zhang, A. J. *et al.* Severe Acute Respiratory Syndrome Coronavirus 2 Infects and Damages the Mature and Immature Olfactory Sensory Neurons of Hamsters. *Clin Infect Dis* **73,** e503–e512 (2021).
63. Joiner, A. M. *et al.* Primary Cilia on Horizontal Basal Cells Regulate Regeneration of the Olfactory Epithelium. *J. Neurosci.* **35,** 13761–13772 (2015).
64. Wu, Q. *et al.* YAP signaling in horizontal basal cells promotes the regeneration of olfactory epithelium after injury. *Stem Cell Reports* **17,** 664–677 (2022).
65. Nakashima, T., Kimmelman, C. P. & Snow, J. B. Structure of human fetal and adult olfactory neuroepithelium. *Arch Otolaryngol* **110,** 641–646 (1984).
66. Holbrook, E. H., Wu, E., Curry, W. T., Lin, D. T. & Schwob, J. E. Immunohistochemical characterization of human olfactory tissue. *The Laryngoscope* **121,** 1687–1701 (2011).
67. Choi, R. & Goldstein, B. J. Olfactory epithelium: Cells, clinical disorders, and insights from an adult stem cell niche. *Laryngoscope Investig Otolaryngol* **3,** 35–42 (2018).
68. Child, K. M., Herrick, D. B., Schwob, J. E., Holbrook, E. H. & Jang, W. The neuroregenerative capacity of olfactory stem cells is not limitless: implications for aging. *J. Neurosci.* **38,** 6806–6824 (2018).
69. Doty, R. L. *et al.* Smell identification ability: changes with age. *Science* **226,** 1441–1443 (1984).
70. DOTY, R. L. Clinical studies of olfaction. *Chem. Senses* **30 Suppl 1,** i207–9 (2005).
71. Ortman, J. M., Velkoff, V. A. & Hogan, H. *An aging nation: the older population in the United States*. (United States Census Bureau, 2014).
72. Kumar, L. *et al.* Loss of smell and taste in COVID-19 infection in adolescents. *Int J Pediatr Otorhinolaryngol* **142,** 110626 (2021).
73. Yan, Q., Qiu, D., Liu, X., Guo, X. & Hu, Y. Prevalence of Smell or Taste Dysfunction Among Children With COVID-19 Infection: A Systematic Review and Meta-Analysis. *Front Pediatr* **9,** 686600 (2021).
74. Salazar, J. L. & Yamamoto, S. Integration of Drosophila and Human Genetics to Understand Notch Signaling Related Diseases. *Adv Exp Med Biol* **1066,** 141–185 (2018).
75. Blaumueller, C. M., Qi, H., Zagouras, P. & Artavanis-Tsakonas, S. Intracellular cleavage of Notch leads to a heterodimeric receptor on the plasma membrane. *Cell* **90,** 281–291 (1997).
76. Logeat, F., Bessia, C., Brou, C. & LeBail, O. The Notch1 receptor is cleaved constitutively by a furin-like convertase. *Proceedings of the …* (1998).
77. Kopan, R. & Ilagan, M. X. G. The canonical Notch signaling pathway: unfolding the activation mechanism. *Cell* **137,** 216–233 (2009).
78. Chillakuri, C. R., Sheppard, D., Lea, S. M. & Handford, P. A. Notch receptor-ligand binding and activation: insights from molecular studies. *Seminars in cell*

\& *developmental biology* **23,** 421–428 (2012).
79. Rebay, I. *et al.* Specific EGF repeats of Notch mediate interactions with Delta and Serrate: implications for Notch as a multifunctional receptor. *Cell* **67,** 687–699 (1991).
80. Sanchez-Irizarry, C. *et al.* Notch Subunit Heterodimerization and Prevention of Ligand-Independent Proteolytic Activation Depend, Respectively, on a Novel Domain and the LNR Repeats. *… and cellular biology* **24,** 9265–9273 (2004).
81. van Tetering, G. *et al.* Metalloprotease ADAM10 is required for Notch1 site 2 cleavage. *J. Biol. Chem.* **284,** 31018–31027 (2009).
82. Lubman, O. Y., Ilagan, M. X., Kopan, R. & Barrick, D. Quantitative dissection of the Notch:CSL interaction: insights into the Notch-mediated transcriptional switch. *J. Mol. Biol.* **365,** 577–589 (2007).
83. Nam, Y., Sliz, P., Song, L., Aster, J. C. & Cell, B. S. Structural basis for cooperativity in recruitment of MAML coactivators to Notch transcription complexes. *Cell* (2006).
84. Fischer, A. & Gessler, M. Delta-Notch--and then? Protein interactions and proposed modes of repression by Hes and Hey bHLH factors. *Nucleic Acids Res.* **35,** 4583–4596 (2007).
85. Shimizu, K., Chiba, S., Kumano, K. & of Biological, H. N. Mouse jagged1 physically interacts with notch2 and other notch receptors assessment by quantitative methods. *Journal of Biological~…* (1999).
86. Tax, F. E., Yeargers, J. J. & Thomas, J. H. Sequence of C. elegans lag-2 reveals a cell-signalling domain shared with Delta and Serrate of Drosophila. *Nature* **368,** 150–154 (1994).
87. D'Souza, B., Meloty-Kapella, L. & Weinmaster, G. Canonical and non-canonical Notch ligands. *Current Topics in Developmental Biology* **92,** 73–129 (2010).
88. Andersson, E. R. & Lendahl, U. Therapeutic modulation of Notch signalling--are we there yet? *Nature reviews Drug discovery* **13,** 357–378 (2014).
89. Glittenberg, M., Pitsouli, C., Garvey, C., Delidakis, C. & Bray, S. Role of conserved intracellular motifs in Serrate signalling, cis-inhibition and endocytosis. *EMBO J.* **25,** 4697–4706 (2006).
90. Parks, A. L., Klueg, K. M., Stout, J. R. & Muskavitch, M. A. Ligand endocytosis drives receptor dissociation and activation in the Notch pathway. *Development* **127,** 1373–1385 (2000).
91. Itoh, M. *et al.* Mind bomb is a ubiquitin ligase that is essential for efficient activation of Notch signaling by Delta. *Developmental cell* **4,** 67–82 (2003).
92. Lai, E. C., Roegiers, F., Qin, X., Jan, Y. N. & Rubin, G. M. The ubiquitin ligase Drosophila Mind bomb promotes Notch signaling by regulating the localization and activity of Serrate and Delta. *Development* **132,** 2319–2332 (2005).
93. Song, R. *et al.* Neuralized-2 regulates a Notch ligand in cooperation with Mind bomb-1. *J. Biol. Chem.* **281,** 36391–36400 (2006).
94. Weinmaster, G. & Fischer, J. A. Notch ligand ubiquitylation: what is it good for? *Developmental cell* **21,** 134–144 (2011).
95. Bray, S. Notch signalling in Drosophila: three ways to use a pathway. *Seminars Cell Dev Biology* **9,** 591–597 (1998).
96. Jacobsen, T. L., Brennan, K. & Development, A. A. Cis-interactions between Delta and Notch modulate neurogenic signalling in Drosophila. *Development* (1998).
97. del Álamo, D., Rouault, H. & Schweisguth, F. Mechanism and significance of cis-inhibition in Notch signalling. *Curr. Biol.* **21,** R40–7 (2011).
98. Pellegrinet, L. *et al.* Dll1- and dll4-mediated notch signaling are required for

homeostasis of intestinal stem cells. *Gastroenterology* **140,** 1230–1240.e1–7 (2011).
99. Shimizu, H. *et al.* Distinct expression patterns of Notch ligands, Dll1 and Dll4, in normal and inflamed mice intestine. *PeerJ* **2,** e370 (2014).
100. Nandagopal, N. *et al.* Dynamic Ligand Discrimination in the Notch Signaling Pathway. *Cell* **172,** 869–880.e19 (2018).
101. Yatsenko, A. S. & Shcherbata, H. R. Distant activation of Notch signaling induces stem cell niche assembly. *PLoS Genet.* **17,** e1009489 (2021).
102. Nandagopal, N., Santat, L. A. & Elowitz, M. B. Cis-activation in the Notch signaling pathway. *Elife* **8,** 323 (2019).
103. Brückner, K., Perez, L., Clausen, H. & Cohen, S. Glycosyltransferase activity of Fringe modulates Notch-Delta interactions. *Nature* **406,** 411–415 (2000).
104. Panin, V. M., Papayannopoulos, V., Wilson, R. & Irvine, K. D. Fringe modulates Notch-ligand interactions. *Nature* **387,** 908–912 (1997).
105. Rana, N. A. & Haltiwanger, R. S. Fringe benefits: functional and structural impacts of O-glycosylation on the extracellular domain of Notch receptors. *Curr Opin Struct Biol* **21,** 583–589 (2011).
106. Fleming, R. J. Structural conservation of Notch receptors and ligands. **9,** 599–607 (1998).
107. Moloney, D. J. *et al.* Fringe is a glycosyltransferase that modifies Notch. *Nature* **406,** 369–375 (2000).
108. LeBon, L., Lee, T. V., Sprinzak, D., Jafar-Nejad, H. & Elowitz, M. B. Fringe proteins modulate Notch-ligand cis and trans interactions to specify signaling states. *Elife* **3,** e02950 (2014).
109. Yang, L.-T. *et al.* Fringe glycosyltransferases differentially modulate Notch1 proteolysis induced by Delta1 and Jagged1. *Mol. Biol. Cell* **16,** 927–942 (2005).
110. Yamada, K. *et al.* Roles of Drosophila deltex in Notch receptor endocytic trafficking and activation. *Genes Cells* **16,** 261–272 (2011).
111. Steinbuck, M. P. & Winandy, S. A Review of Notch Processing With New Insights Into Ligand-Independent Notch Signaling in T-Cells. *Front Immunol* **9,** 1230 (2018).
112. Palmer, W. H., Jia, D. & Deng, W.-M. Cis-interactions between Notch and its ligands block ligand-independent Notch activity. *Elife* **3,** e04415 (2014).
113. Fre, S. *et al.* Notch signals control the fate of immature progenitor cells in the intestine. *Nature …* **435,** 964–968 (2005).
114. Vauclair, S., Nicolas, M., Barrandon, Y. & Radtke, F. Notch1 is essential for postnatal hair follicle development and homeostasis. *Dev. Biol.* **284,** 184–193 (2005).
115. Beumer, J. & Clevers, H. Cell fate specification and differentiation in the adult mammalian intestine. *Nature Reviews Molecular Cell Biology 2009 10:1* **22,** 39–53 (2021).
116. Dias, T. B., Yang, Y.-J., Ogai, K., Becker, T. & Becker, C. G. Notch signaling controls generation of motor neurons in the lesioned spinal cord of adult zebrafish. *J. Neurosci.* **32,** 3245–3252 (2012).
117. Kawaguchi, D., Furutachi, S., Kawai, H., Hozumi, K. & Gotoh, Y. Dll1 maintains quiescence of adult neural stem cells and segregates asymmetrically during mitosis. *Nat Commun* **4,** 1880 (2013).
118. Bjornson, C. R. R. *et al.* Notch signaling is necessary to maintain quiescence in adult muscle stem cells. *Stem Cells* **30,** 232–242 (2012).
119. Conboy, I. M. & Rando, T. A. The regulation of Notch signaling controls satellite cell activation and cell fate determination in postnatal myogenesis.

*Developmental cell* **3,** 397–409 (2002).
120. Luo, D., Renault, V. M. & Rando, T. A. The regulation of Notch signaling in muscle stem cell activation and postnatal myogenesis. *Seminars Cell Dev Biology* **16,** 612–622 (2005).
121. Didsbury, J., Weber, R. F., Bokoch, G. M., Evans, T. & Snyderman, R. rac, a novel ras-related family of proteins that are botulinum toxin substrates. *J. Biol. Chem.* **264,** 16378–16382 (1989).
122. Klooster, ten, J. P. & Hordijk, P. L. Targeting and localized signalling by small GTPases. *Biol Cell* **99,** 1–12 (2007).
123. Cherfils, J. & Zeghouf, M. Regulation of small GTPases by GEFs, GAPs, and GDIs. *Physiol Rev* **93,** 269–309 (2013).
124. Barbacid, M. ras genes. *Annu Rev Biochem* **56,** 779–827 (1987).
125. Ménard, L. *et al.* Rac1, a low-molecular-mass GTP-binding-protein with high intrinsic GTPase activity and distinct biochemical properties. *Eur J Biochem* **206,** 537–546 (1992).
126. Bourne, H. R., Sanders, D. A. & McCormick, F. The GTPase superfamily: conserved structure and molecular mechanism. *Nature* **349,** 117–127 (1991).
127. Etienne-Manneville, S. & Hall, A. Rho GTPases in cell biology. *Nature* **420,** 629–635 (2002).
128. Soisson, S. M., Nimnual, A. S., Uy, M., Bar-Sagi, D. & Kuriyan, J. Crystal structure of the Dbl and pleckstrin homology domains from the human Son of sevenless protein. *Cell* **95,** 259–268 (1998).
129. Worthylake, D. K., Rossman, K. L. & Sondek, J. Crystal structure of Rac1 in complex with the guanine nucleotide exchange region of Tiam1. *Nature* **408,** 682–688 (2000).
130. Cherfils, J. & Chardin, P. GEFs: structural basis for their activation of small GTP-binding proteins. *Trends in biochemical sciences* **24,** 306–311 (1999).
131. Mondal, S., Hsiao, K. & Goueli, S. A. A Homogenous Bioluminescent System for Measuring GTPase, GTPase Activating Protein, and Guanine Nucleotide Exchange Factor Activities. *Assay Drug Dev Technol* **13,** 444–455 (2015).
132. Ridley, A. J., Paterson, H. F., Johnston, C. L., Diekmann, D. & Hall, A. The small GTP-binding protein rac regulates growth factor-induced membrane ruffling. *Cell* **70,** 401–410 (1992).
133. Olabi, S., Ucar, A., Brennan, K. & Streuli, C. H. Integrin-Rac signalling for mammary epithelial stem cell self-renewal. *Breast Cancer Res.* **20,** 128 (2018).
134. Myant, K. B. *et al.* Rac1 drives intestinal stem cell proliferation and regeneration. *Cell Cycle* **12,** 2973–2977 (2013).
135. Behrendt, K. *et al.* A function for Rac1 in the terminal differentiation and pigmentation of hair. *J. Cell. Sci.* **125,** 896–905 (2012).
136. Jin, S., Ray, R. M. & Johnson, L. R. Rac1 mediates intestinal epithelial cell apoptosis via JNK. *Am J Physiol Gastrointest Liver Physiol* **291,** G1137–47 (2006).
137. Hobbs, G. A., Der, C. J. & Rossman, K. L. RAS isoforms and mutations in cancer at a glance. *J. Cell. Sci.* **129,** 1287–1292 (2016).
138. Scheffzek, K., Lautwein, A., Scherer, A., Franken, S. & Wittinghofer, A. Crystallization and preliminary X-ray crystallographic study of the Ras-GTPase-activating domain of human p120GAP. *Proteins* **27,** 315–318 (1997).
139. Zhang, B., Chernoff, J. & Zheng, Y. Interaction of Rac1 with GTPase-activating proteins and putative effectors. A comparison with Cdc42 and RhoA. *J. Biol. Chem.* **273,** 8776–8782 (1998).
140. Dovas, A. & Couchman, J. R. RhoGDI: multiple functions in the regulation of

Rho family GTPase activities. *Biochem J* **390,** 1–9 (2005).
141. DerMardirossian, C. & Bokoch, G. M. GDIs: central regulatory molecules in Rho GTPase activation. *Trends Cell Biol* **15,** 356–363 (2005).
142. Ueda, T., Kikuchi, A., Ohga, N., Yamamoto, J. & Takai, Y. Purification and characterization from bovine brain cytosol of a novel regulatory protein inhibiting the dissociation of GDP from and the subsequent binding of GTP to rhoB p20, a ras p21-like GTP-binding protein. *J. Biol. Chem.* **265,** 9373–9380 (1990).
143. Seoh, M. L., Ng, C. H., Yong, J., Lim, L. & Leung, T. ArhGAP15, a novel human RacGAP protein with GTPase binding property. *FEBS Lett* **539,** 131–137 (2003).
144. Ando, S. *et al.* Post-translational processing of rac p21s is important both for their interaction with the GDP/GTP exchange proteins and for their activation of NADPH oxidase. *J. Biol. Chem.* **267,** 25709–25713 (1992).
145. Hiraoka, K. *et al.* Both stimulatory and inhibitory GDP/GTP exchange proteins, smg GDS and rho GDI, are active on multiple small GTP-binding proteins. *Biochem. Biophys. Res. Commun.* **182,** 921–930 (1992).
146. Abo, A. *et al.* Activation of the NADPH oxidase involves the small GTP-binding protein p21rac1. *Nature* **353,** 668–670 (1991).
147. Payapilly, A. & Malliri, A. Compartmentalisation of RAC1 signalling. *Curr. Opin. Cell Biol.* **54,** 50–56 (2018).
148. Nobes, C. D. & Hall, A. Rho, rac, and cdc42 GTPases regulate the assembly of multimolecular focal complexes associated with actin stress fibers, lamellipodia, and filopodia. *Cell* **81,** 53–62 (1995).
149. Bosco, E. E., Mulloy, J. C. & Zheng, Y. Rac1 GTPase: a 'Rac' of all trades. *Cell Mol Life Sci* **66,** 370–374 (2009).
150. Berrier, A. L., Mastrangelo, A. M., Downward, J., Ginsberg, M. & LaFlamme, S. E. Activated R-ras, Rac1, PI 3-kinase and PKCepsilon can each restore cell spreading inhibited by isolated integrin beta1 cytoplasmic domains. *J. Cell Biol.* **151,** 1549–1560 (2000).
151. Berrier, A. L., Martinez, R., Bokoch, G. M. & LaFlamme, S. E. The integrin β tail is required and sufficient to regulate adhesion signaling to Rac1. *J. Cell. Sci.* **115,** 4285–4291 (2002).
152. Russell, A. J. *et al.* Alpha 6 beta 4 integrin regulates keratinocyte chemotaxis through differential GTPase activation and antagonism of alpha 3 beta 1 integrin. *J. Cell. Sci.* **116,** 3543–3556 (2003).
153. Schlaepfer, D. D., Hanks, S. K., Hunter, T. & van der Geer, P. Integrin-mediated signal transduction linked to Ras pathway by GRB2 binding to focal adhesion kinase. *Nature* **372,** 786–791 (1994).
154. Calalb, M. B., Polte, T. R. & Hanks, S. K. Tyrosine phosphorylation of focal adhesion kinase at sites in the catalytic domain regulates kinase activity: a role for Src family kinases. *… and cellular biology* **15,** 954–963 (1995).
155. Schlaepfer, D. D. & Hunter, T. Evidence for in vivo phosphorylation of the Grb2 SH2-domain binding site on focal adhesion kinase by Src-family protein-tyrosine kinases. *… and cellular biology* **16,** 5623–5633 (1996).
156. Khanday, F. A. *et al.* Sos-mediated activation of rac1 by p66shc. *J. Cell Biol.* **172,** 817–822 (2006).
157. Gerboth, S. *et al.* Phosphorylation of SOS1 on tyrosine 1196 promotes its RAC GEF activity and contributes to BCR-ABL leukemogenesis. *Leukemia* **32,** 820–827 (2018).
158. Dérijard, B. *et al.* Independent human MAP-kinase signal transduction pathways defined by MEK and MKK isoforms. *Science* **267,** 682–685 (1995).
159. Teramoto, H. *et al.* Signaling from the small GTP-binding proteins Rac1 and

Cdc42 to the c-Jun N-terminal kinase/stress-activated protein kinase pathway. A role for mixed lineage kinase 3/protein-tyrosine kinase 1, a novel member of the mixed lineage kinase family. *J. Biol. Chem.* **271,** 27225–27228 (1996).
160. Ichijo, H. From receptors to stress-activated MAP kinases. *Oncogene* **18,** 6087–6093 (1999).
161. Lu, X., Nemoto, S. & Lin, A. Identification of c-Jun NH2-terminal protein kinase (JNK)-activating kinase 2 as an activator of JNK but not p38. *J. Biol. Chem.* **272,** 24751–24754 (1997).
162. Smeal, T., Binetruy, B., Mercola, D. A., Birrer, M. & Karin, M. Oncogenic and transcriptional cooperation with Ha-Ras requires phosphorylation of c-Jun on serines 63 and 73. *Nature* **354,** 494–496 (1991).
163. Smeal, T. *et al.* Oncoprotein-mediated signalling cascade stimulates c-Jun activity by phosphorylation of serines 63 and 73. *… and cellular biology* **12,** 3507–3513 (1992).
164. Bohmann, D. *et al.* Human proto-oncogene c-jun encodes a DNA binding protein with structural and functional properties of transcription factor AP-1. *Science* **238,** 1386–1392 (1987).
165. Rauscher, F. J., Voulalas, P. J., Franza, B. R. & Curran, T. Fos and Jun bind cooperatively to the AP-1 site: reconstitution in vitro. *Genes Dev.* **2,** 1687–1699 (1988).
166. Herber, B., Truss, M., Beato, M. & Müller, R. Inducible regulatory elements in the human cyclin D1 promoter. *Oncogene* **9,** 1295–1304 (1994).
167. Albanese, C. *et al.* Transforming p21ras mutants and c-Ets-2 activate the cyclin D1 promoter through distinguishable regions. *J. Biol. Chem.* **270,** 23589–23597 (1995).
168. Shaulian, E. & Karin, M. AP-1 in cell proliferation and survival. *Oncogene* **20,** 2390–2400 (2001).
169. Benitah, S. A., Frye, M., Glogauer, M. & Watt, F. M. Stem cell depletion through epidermal deletion of Rac1. *Science* **309,** 933–935 (2005).
170. Ghiaur, G. *et al.* Rac1 is essential for intraembryonic hematopoiesis and for the initial seeding of fetal liver with definitive hematopoietic progenitor cells. *Blood* **111,** 3313–3321 (2008).
171. Castilho, R. M. *et al.* Requirement of Rac1 distinguishes follicular from interfollicular epithelial stem cells. *Oncogene* **26,** 5078–5085 (2007).
172. Castilho, R. M. *et al.* Rac1 is required for epithelial stem cell function during dermal and oral mucosal wound healing but not for tissue homeostasis in mice. *PLoS ONE* **5,** e10503 (2010).
173. Carulli, A. J. *et al.* Notch receptor regulation of intestinal stem cell homeostasis and crypt regeneration. *Dev. Biol.* **402,** 98–108 (2015).
174. Packard, A., Schnittke, N., Romano, R.-A., Sinha, S. & Schwob, J. E. DeltaNp63 regulates stem cell dynamics in the mammalian olfactory epithelium. *J. Neurosci.* **31,** 8748–8759 (2011).
175. Ohtsuka, T. *et al.* Hes1 and Hes5 as notch effectors in mammalian neuronal differentiation. *EMBO J.* **18,** 2196–2207 (1999).
176. Fryer, C. J., White, J. B. & Jones, K. A. Mastermind recruits CycC:CDK8 to phosphorylate the Notch ICD and coordinate activation with turnover. *Mol. Cell* **16,** 509–520 (2004).
177. Guo, Z. *et al.* Expression of pax6 and sox2 in adult olfactory epithelium. *Journal of …* **518,** 4395–4418 (2010).
178. Maurya, D. K. *et al.* Development of the Olfactory Epithelium and Nasal Glands in TMEM16A-/- and TMEM16A+/+ Mice. *PLoS ONE* **10,** e0129171 (2015).

179. Estrach, S., Cordes, R., Hozumi, K., Gossler, A. & Watt, F. M. Role of the Notch ligand Delta1 in embryonic and adult mouse epidermis. *J. Invest. Dermatol.* **128,** 825–832 (2008).
180. Herrick, D. B., Guo, Z., Jang, W., Schnittke, N. & Schwob, J. E. Canonical Notch Signaling Directs the Fate of Differentiating Neurocompetent Progenitors in the Mammalian Olfactory Epithelium. *J. Neurosci.* **38,** 5022–5037 (2018).
181. Indra, A. K. *et al.* Temporally-controlled site-specific mutagenesis in the basal layer of the epidermis: comparison of the recombinase activity of the tamoxifen-inducible Cre-ER(T) and Cre-ER(T2) recombinases. *Nucleic Acids Res.* **27,** 4324–4327 (1999).
182. Fletcher, R. B. *et al.* Deconstructing Olfactory Stem Cell Trajectories at Single-Cell Resolution. *Cell Stem Cell* **20,** 817–830.e8 (2017).
183. Carroll, D. K. *et al.* p63 regulates an adhesion programme and cell survival in epithelial cells. *Nat. Cell Biol.* **8,** 551–561 (2006).
184. Cruz-Monserrate, Z. & O'Connor, K. L. Integrin alpha 6 beta 4 promotes migration, invasion through Tiam1 upregulation, and subsequent Rac activation. *Neoplasia* **10,** 408–417 (2008).
185. Casaletto, J. B., Saotome, I., Curto, M. & McClatchey, A. I. Ezrin-mediated apical integrity is required for intestinal homeostasis. *Proc. Natl. Acad. Sci. U.S.A.* **108,** 11924–11929 (2011).
186. Deramaudt, T. B. *et al.* FAK phosphorylation at Tyr-925 regulates cross-talk between focal adhesion turnover and cell protrusion. *Mol. Biol. Cell* **22,** 964–975 (2011).
187. Rorke, E. A., Adhikary, G., Jans, R., Crish, J. F. & Eckert, R. L. AP1 factor inactivation in the suprabasal epidermis causes increased epidermal hyperproliferation and hyperkeratosis but reduced carcinogen-dependent tumor formation. *Oncogene* **29,** 5873–5882 (2010).
188. Young, C. A., Rorke, E. A., Adhikary, G., Xu, W. & Eckert, R. L. Loss of epidermal AP1 transcription factor function reduces filaggrin level, alters chemokine expression and produces an ichthyosis-related phenotype. *Cell Death Dis* **8,** e2840–e2840 (2017).
189. Peterson, J. *et al.* Activating a Reserve Neural Stem Cell Population In Vitro Enables Engraftment and Multipotency after Transplantation. *Stem Cell Reports* (2019). doi:10.1016/j.stemcr.2019.02.014
190. Shutes, A. *et al.* Specificity and mechanism of action of EHT 1864, a novel small molecule inhibitor of Rac family small GTPases. *J. Biol. Chem.* **282,** 35666–35678 (2007).
191. Schwob, J. E. *et al.* Stem and progenitor cells of the mammalian olfactory epithelium: Taking poietic license. *Journal of …* **525,** 1034–1054 (2017).
192. Hildebrand, M. S. *et al.* Survival of partially differentiated mouse embryonic stem cells in the scala media of the guinea pig cochlea. *J Assoc Res Otolaryngol* **6,** 341–354 (2005).
193. Taddei, I. *et al.* Beta1 integrin deletion from the basal compartment of the mammary epithelium affects stem cells. *Nat. Cell Biol.* **10,** 716–722 (2008).
194. Hellweg, C. E., Arenz, A., Bogner, S., Schmitz, C. & Baumstark-Khan, C. Activation of nuclear factor kappa B by different agents: influence of culture conditions in a cell-based assay. *Annals of the New York Academy of Sciences* **1091,** 191–204 (2006).
195. Nomura, N., Nomura, M., Mizuki, N. & Hamada, J.-I. Rac1 mediates phorbol 12-myristate 13-acetate-induced migration of glioblastoma cells via paxillin. *Oncol Rep* **20,** 705–711 (2008).

196. To, W. S. & Midwood, K. S. Plasma and cellular fibronectin: distinct and independent functions during tissue repair. *Fibrogenesis Tissue Repair* **4,** 21–17 (2011).
197. Rayagiri, S. S. *et al.* Basal lamina remodeling at the skeletal muscle stem cell niche mediates stem cell self-renewal. *Nat Commun* **9,** 1075–12 (2018).
198. Nakamura-Ishizu, A. *et al.* Extracellular matrix protein tenascin-C is required in the bone marrow microenvironment primed for hematopoietic regeneration. *Blood* **119,** 5429–5437 (2012).
199. Urciuolo, A. *et al.* Collagen VI regulates satellite cell self-renewal and muscle regeneration. *Nat Commun* **4,** 1964–13 (2013).
200. Sirko, S., Holst, von, A., Wizenmann, A., Götz, M. & Faissner, A. Chondroitin sulfate glycosaminoglycans control proliferation, radial glia cell differentiation and neurogenesis in neural stem/progenitor cells. *Development* **134,** 2727–2738 (2007).
201. Shen, Q. *et al.* Adult SVZ stem cells lie in a vascular niche: a quantitative analysis of niche cell-cell interactions. *Cell Stem Cell* **3,** 289–300 (2008).
202. Lee, S. T. *et al.* Engineering integrin signaling for promoting embryonic stem cell self-renewal in a precisely defined niche. *Biomaterials* **31,** 1219–1226 (2010).
203. Brizzi, M. F., Tarone, G. & Defilippi, P. Extracellular matrix, integrins, and growth factors as tailors of the stem cell niche. *Curr. Opin. Cell Biol.* **24,** 645–651 (2012).
204. Yu, W. *et al.* Beta1-integrin orients epithelial polarity via Rac1 and laminin. *Mol. Biol. Cell* **16,** 433–445 (2005).
205. Lawson, C. D. & Burridge, K. The on-off relationship of Rho and Rac during integrin-mediated adhesion and cell migration. *Small GTPases* **5,** e27958 (2014).
206. Koche, R. P. *et al.* Reprogramming factor expression initiates widespread targeted chromatin remodeling. *Cell Stem Cell* **8,** 96–105 (2011).
207. Gifford, C. A. *et al.* Transcriptional and epigenetic dynamics during specification of human embryonic stem cells. *Cell* **153,** 1149–1163 (2013).
208. Zhu, J. *et al.* Genome-wide chromatin state transitions associated with developmental and environmental cues. *Cell* **152,** 642–654 (2013).
209. McKinnell, I. W. *et al.* Pax7 activates myogenic genes by recruitment of a histone methyltransferase complex. *Nat. Cell Biol.* **10,** 77–84 (2008).
210. Sebastian, S. *et al.* MLL5, a trithorax homolog, indirectly regulates H3K4 methylation, represses cyclin A2 expression, and promotes myogenic differentiation. *Proc. Natl. Acad. Sci. U.S.A.* **106,** 4719–4724 (2009).
211. Naito, M. *et al.* Dnmt3a Regulates Proliferation of Muscle Satellite Cells via p57Kip2. *PLoS Genet.* **12,** e1006167 (2016).
212. Nguyen, B.-C. *et al.* Cross-regulation between Notch and p63 in keratinocyte commitment to differentiation. *Genes Dev.* **20,** 1028–1042 (2006).
213. Fortini, M. E. & Artavanis-Tsakonas, S. The suppressor of hairless protein participates in notch receptor signaling. *Cell* **79,** 273–282 (1994).
214. del Monte, G. *et al.* Differential Notch signaling in the epicardium is required for cardiac inflow development and coronary vessel morphogenesis. *Circ Res* **108,** 824–836 (2011).
215. Herzog, C. & Otto, T. Regeneration of olfactory receptor neurons following chemical lesion: time course and enhancement with growth factor administration. *Brain Res* **849,** 155–161 (1999).
216. Zhao, B. *et al.* Inactivation of YAP oncoprotein by the Hippo pathway is involved in cell contact inhibition and tissue growth control. *Genes Dev.* **21,** 2747–2761

(2007).
217. Mateus, R. *et al.* Control of tissue growth by Yap relies on cell density and F-actin in zebrafish fin regeneration. *Development* **142,** 2752–2763 (2015).
218. Xu, X. *et al.* YAP-TEAD up-regulates IRS2 expression to induce and deteriorate oesophageal cancer. *J Cell Mol Med* **25,** 2584–2595 (2021).
219. Sabra, H. *et al.* β1 integrin-dependent Rac/group I PAK signaling mediates YAP activation of Yes-associated protein 1 (YAP1) via NF2/merlin. *J. Biol. Chem.* **292,** 19179–19197 (2017).
220. Hui Mingalone, C. K. *et al.* Bioluminescence and second harmonic generation imaging reveal dynamic changes in the inflammatory and collagen landscape in early osteoarthritis. *Lab. Invest.* **98,** 656–669 (2018).
221. Grayson, L. S. *et al.* Quantitation of cytokine levels in skin graft donor site wound fluid. *Burns* **19,** 401–405 (1993).
222. McCarthy, D. W. *et al.* Production of heparin-binding epidermal growth factor-like growth factor (HB-EGF) at sites of thermal injury in pediatric patients. *J. Invest. Dermatol.* **106,** 49–56 (1996).
223. Ono, I., Gunji, H., Zhang, J. Z., Maruyama, K. & Kaneko, F. Studies on cytokines related to wound healing in donor site wound fluid. *J Dermatol Sci* **10,** 241–245 (1995).
224. Grotendorst, G. R., Soma, Y., Takehara, K. & Charette, M. EGF and TGF-alpha are potent chemoattractants for endothelial cells and EGF-like peptides are present at sites of tissue regeneration. *J Cell Physiol* **139,** 617–623 (1989).
225. Wenczak, B. A., Lynch, J. B. & Nanney, L. B. Epidermal growth factor receptor distribution in burn wounds. Implications for growth factor-mediated repair. *J. Clin. Invest.* **90,** 2392–2401 (1992).
226. Repertinger, S. K. *et al.* EGFR enhances early healing after cutaneous incisional wounding. *J. Invest. Dermatol.* **123,** 982–989 (2004).
227. Krishna, N. S., Little, S. S. & Getchell, T. V. Epidermal growth factor receptor mRNA and protein are expressed in progenitor cells of the olfactory epithelium. *J. Comp. Neurol.* **373,** 297–307 (1996).
228. Getchell, T. V., Narla, R. K., Little, S., Hyde, J. F. & Getchell, M. L. Horizontal basal cell proliferation in the olfactory epithelium of transforming growth factor-alpha transgenic mice. *Cell Tissue Res.* **299,** 185–192 (2000).
229. Ohta, Y. & Ichimura, K. Changes in epidermal growth factor receptors in olfactory epithelium associated with aging. *Ann. Otol. Rhinol. Laryngol.* **109,** 95–98 (2000).
230. Enwere, E. *et al.* Aging results in reduced epidermal growth factor receptor signaling, diminished olfactory neurogenesis, and deficits in fine olfactory discrimination. *J. Neurosci.* **24,** 8354–8365 (2004).
231. Zhu, G. *et al.* An EGFR/PI3K/AKT axis promotes accumulation of the Rac1-GEF Tiam1 that is critical in EGFR-driven tumorigenesis. *Oncogene* **34,** 5971–5982 (2015).
232. Wu, R., Coniglio, S. J., Chan, A., Symons, M. H. & Steinberg, B. M. Up-regulation of Rac1 by epidermal growth factor mediates COX-2 expression in recurrent respiratory papillomas. *Mol Med* **13,** 143–150 (2007).
233. Dise, R. S., Frey, M. R., Whitehead, R. H. & Polk, D. B. Epidermal growth factor stimulates Rac activation through Src and phosphatidylinositol 3-kinase to promote colonic epithelial cell migration. *Am J Physiol Gastrointest Liver Physiol* **294,** G276–85 (2008).
234. Sayyad, W. A., Fabris, P. & Torre, V. The Role of Rac1 in the Growth Cone Dynamics and Force Generation of DRG Neurons. *PLoS ONE* **11,** e0146842

(2016).
235. Johnston, S. A., Bramble, J. P., Yeung, C. L., Mendes, P. M. & Machesky, L. M. Arp2/3 complex activity in filopodia of spreading cells. *BMC Cell Biol* **9,** 65–17 (2008).
236. McCarty, O. J. T. *et al.* Rac1 is essential for platelet lamellipodia formation and aggregate stability under flow. *J. Biol. Chem.* **280,** 39474–39484 (2005).
237. Berlew, E. E., Kuznetsov, I. A., Yamada, K., Bugaj, L. J. & Chow, B. Y. Optogenetic Rac1 engineered from membrane lipid-binding RGS-LOV for inducible lamellipodia formation. *Photochem Photobiol Sci* **19,** 353–361 (2020).
238. Zhou, Q., Wang, Y., Peng, B., Liang, L. & Li, J. The roles of Notch1 expression in the migration of intrahepatic cholangiocarcinoma. *BMC Cancer* **13,** 244–10 (2013).
239. Ziouti, F. *et al.* NOTCH Signaling Is Activated through Mechanical Strain in Human Bone Marrow-Derived Mesenchymal Stromal Cells. *Stem Cells Int* **2019,** 5150634 (2019).
240. Dumont, C. *et al.* Rac GTPases play critical roles in early T-cell development. *Blood* **113,** 3990–3998 (2009).
241. Robles-Valero, J. *et al.* A Paradoxical Tumor-Suppressor Role for the Rac1 Exchange Factor Vav1 in T Cell Acute Lymphoblastic Leukemia. *Cancer Cell* **32,** 608–623.e9 (2017).
242. De Strooper, B., Iwatsubo, T. & Wolfe, M. S. Presenilins and γ-secretase: structure, function, and role in Alzheimer Disease. *Cold Spring Harb Perspect Med* **2,** a006304 (2012).